Investigation of *in vitro* diabetic inflammation and treatment with *Piper excelsum* tea extract

A thesis

Submitted in partial fulfilment

of the requirements for the degree

of

Master of Science (Research) in Molecular and Cellular Biology

at

The University of Waikato

by

Savannah Harvey

THE UNIVERSITY OF
WAIKATO
Te Whare Wānanga o Waikato

2021

Abstract

Induction of inflammation through hyperglycaemia and adiposity has been shown to contribute to the pathogenicity of type 2 diabetes (T2D). The pro-inflammatory cytokine, tumour necrosis factor α (TNF-α) was the first cytokine found to bridge the connection between the immune system and T2D. This was found due to its increased production in the disease state. TNF-α has specifically been linked to the onset of insulin resistance in T2D models. Evidence has shown that heat shock protein 60 (HSP60) may also play a role as a danger signal for the immune system as it can result in the induction of inflammation. Currently, there are no pharmaceutical options for T2D patients which target inflammation. Tea made from the leaves of kawakawa (*Piper excelsum)* has been used for many generations by Māori as a traditional rākau rongoā (traditional medicine) to treat a range of ailments including inflammation. The aim of this project was to investigate the modulation of inflammation using a commercially available kawakawa tea in human cancer cells *in vitro*.

This project involved measuring the growth rate, cytotoxicity, TNF-α production and HSP60 expression upon exposure to three treatments: high glucose, lipopolysaccharide (LPS) or kawakawa tea extract (KTE).

This study showed that a high concentration of KTE (1000 µg/mL) inhibited cell growth in both HEPG2 and HeLa cell lines. Cells treated with this concentration also showed typical morphological signs of apoptosis. Cytotoxicity testing confirmed that there was a significant (p <0.05) decrease in mitochondrial dehydrogenase activity for this treatment which confirmed the cells were likely dying through apoptosis. Over a course of 24-hours three LPS treatments were found to be cytotoxic. These were the 10 ng/mL, 10 µg/mL, and 100 µg/mL concentrations of LPS. After 48-hours all treatments apart from 100 µg/mL KTE treatment were also found to be cytotoxic. The cytotoxicity for these treatments was either due to a reduction in mitochondrial dehydrogenase activity (infers mitochondrial stress) or increased lactate dehydrogenase (LDH) release from cells (infers necrotic cell death). These cytotoxicity experiments allowed for identification of which concentrations should be selected or removed for future experiments.

Cytotoxicity levels were taken into consideration and experiments were run investigating the induction of TNF-α using enzyme-linked immunosorbent assays (ELISA). Issues

regarding negative readings from samples arose which resulted in protocol changes and extensive trouble shooting. It was found that extended exposure times were required to attenuate a positive result from the positive control, LPS.

HSP60 expression was also measured for human cells exposed to high glucose and KTE treatments. No change in HSP60 expression was detected. However, 24-hour LPS exposure resulted in a significant increase in HSP60 expression compared to the control for the 100 ng/mL LPS treatment. Two concentrations were investigated; 100 ng/mL LPS and 100 µg/mL LPS which resulted in 1.4- and 2.1-fold increases compared to the control, respectively.

Overall, no conclusion could be drawn regarding the modulation of inflammation by KTE. However, this study was able to identify the effect the tea has on human cancer cell growth and the nature of cytotoxicity the tea poses to the cells. It is recommended to continue this research exploring different kawakawa tea blends and using alternative *in vitro* cell lines and whole animal models.

Acknowledgements

I would like to firstly thank my fiancé Shaun Te Rire McNeil for the unwavering support you have given me throughout this project, the early morning starts, and late-night finishes were made so much easier with you by my side. I am so grateful for you and look forward to more years of research alongside each other.

I would then like to thank my supervisors. Thank you, Dr. Ryan Martinus for providing me with the opportunity to take on this project and for me teaching the valuable skills needed to become an independent researcher. I would also like to thank Dr. Linda Peters for the much-needed support on such short notice towards the end of this project and for putting the time in to help me with my thesis drafts.

I would like to thank Laura McColl for always being there to help. Your offers of support, last minute autoclaving and showing up in the lab very quickly after receiving an email with the subject "help" when I messed something up was very much appreciated.
Thank you as well Donisha Liyanagama for your support and help. It was very helpful having a lab mate who was always around to talk things over with and get support from when I was unsure. Thank you for always making time to help, it was much appreciated.

Next, I would like to thank Dr. Jonni Koia who helped me very early on in this project where she spent time teaching me to cell culture and helped increase my confidence working in a PC2 facility. Thank you to Cheryl Ward for helping me with the formatting of this thesis, a job I would not have been able to do on my own. Also, thank you to Prof. Merilyn Manley-Harris for offers of support towards the end of my project.

Thank you to the University of Waikato for providing me with the University of Waikato Research Masters Scholarship. This has helped relieve some financial stress and allow me to focus on my research.

I would also like to thank my dungeons and dragons' group for helping destress over this project by providing weekly escapism and laughs to combat the stress. Thanks, Cith, Durak, Luther and Raz.

Lastly, I would like to thank my family. Thank you to Mum for always being there for me when things got stressful and always having room at home for when I needed to escape for the weekend. Thanks, Dad for your support always being there to listen and encourage me when things where stressful. Thanks to Nicola, Whiti, Bev and the boys for always being there for me as well as my brother Levi.

Table of Contents

List of Figures

List of Tables

List of Equations

Abbreviations

Abbreviation	Meaning
ADP	Adenine Diphosphate
AGE	Advanced Glycated End Product
ATCC	American Tissue Culture Collection
ATP	Adenine Triphosphate
APC	Antigen Presenting Cell
BCA	Bicinchoninic Acid
BCR	B-cell Receptor
bFGF	Basic Fibroblast Growth Factor
BMI	Body Mass Index
BSA	Bovine Serum Albumin
CCT	Cytosolic Chaperonin-Containing t-complex Polypeptide 1
CD14	Cluster of Differentiation 14
DAG	Diacyl-glycerol
ELISA	Enzyme Linked Immunosorbent Assay
EMEM	Eagle's Minimum Essential Media
ERK	Extracellular-signal-regulated kinases
ETC	Electron Transport Chain
$FADH_2$	Flavin Adenine Dinucleotide
FBS	Fetal Bovine Serum
GAD	Glutamate Decarboxylase
GAPDH	Glyceraldehyde 3-phosphate Dehydrogenase

Abbreviation	Meaning
GFAT	Glutamine Fructose-6-phosphate Amidotransferase
GLUT	Glucose Transporter
GSH	Glutathione
HSP	Heat Shock Protein
IKK	IκB Kinase
IL-1β	Interleukin-1β
IL-6	Interleukin-6
INT	Tetrazolium Salt
IR	Insulin Receptor
IRS-1	Insulin Receptor Substrate-1
JAK	Janus Kinase
JNK	c-Jun N-terminal Kinases
KTE	Kawakawa Tea Extract
LBP	Lipopolysaccharide Binding Protein
LDH	Lactate Dehydrogenase
LOD	Limit of Detection
LPS	Lipopolysaccharide
MAPK	Mitogen-activated Protein Kinase
MAPKK	Mitogen-activated Protein Kinase Kinase
MAPKKK	Mitogen-activated Protein Kinase Kinase Kinase
MCP-1	Monocyte Chemoattractant Protein-1

Abbreviation	Meaning
MEM	Minimum Essential Media
MGO	Methylglyoxal
MODY	Maturity Onset Diabetes of the Young
MPER	Mammalian Protein Extraction Reagent
MTT	[3-(4,5-dimethylthiazol-2-yl)-2, -diphenyltetrazolium bromide]
NCM	Nitrocellulose Membrane
NF-κB	Nuclear factor-κB
NO	Nitic Oxide
NZ	New Zealand
PAMP	Pathogen Associated Molecular Pattern
PARP	Poly (ADP-ribose) polymerase
PBS	Phosphate Buffer Solution
PENSTRIP	Penicillin/streptomycin
PGE_2	Prostaglandin D_2
PKC	Protein Kinase C
PRR	Pattern Recognition Receptor
REDOX	Reduction-Oxidation
ROS	Reactive Oxidative Species
RT	Room Temperature
RT-qPCR	Real Time Quantitative Polymerase Chain Reaction
SEAP	Secreted alkaline phosphatase
SEM	Standard Error of the Mean

Abbreviation	Meaning
sTNFR	Soluble Tumour Necrosis Factor Receptor
T1D	Type 1 Diabetes
T2D	Type 2 Diabetes
TBS	Tris-buffered Saline
TBST	Tris-buffered Saline with Tween 20
TCA	Citric Acid Cycle
TCR	T-Cell Receptor
TLR	Toll-like Receptor
TNFR	Tumour Necrosis Factor Receptor
TNF-α	Tumour Necrosis Factor-α
Trif	TIR-domain containing adaptor inducing interferon -ß
WAT	White Adipose Tissue

Chapter 1

Literature Review

This chapter will provide an overview of the metabolic disorder Diabetes Mellitus and the impacts it has on the human body. A review of the induction of inflammation and heat shock protein 60 (HSP60) will also be covered. To conclude, the research aims of this project in context with the current literature will be outlined.

1.1 History of Diabetes Mellitus

Knowledge on diabetes has been accumulating for many centuries. The first documentation of diabetes was reported in the 5th century BC in writing from India, which described polyuria coupled with glucosuria [1]. The term diabetes was not coined until later by Demetrius of Apameia, in the 2nd century AD. This was derived from the Latin word meaning "siphon", due to the observable polyuria. The first accurate description of diabetes was by Aretaeus of Cappadocia which was also in the 2nd century AD. His description included details of "unquenchable thirst" and that the "kidneys and bladder never stop making water". This description was expanded upon by Galen between 129-200 AD. Galen conducted experiments on dogs showing that urine was produced in the kidneys, and, therefore, concluded that the presence of polyuria must indicate that diabetes is a kidney disease. During the 17th Century Thomas Willis expanded the term diabetes to diabetes mellitus (DM) to accurately describe the glycosuria. It was not until Oscar Minkowski and Joseph Mering (late 1800's- early 1900's) showed that removal of the pancreas in dogs results in the development of DM, which proved DM is a disease of the pancreas [1]. French lilac was used in Medieval Europe to treat DM; however, this did not aid insulin dependent individuals [2]. It was not until 1922 when Frederick Banting and Charles Best first purified insulin that treatment for insulin dependent individuals improved [3]. The discovery of purified insulin has saved many lives and paved the way for diabetes management.

1.2 Current Epidemiology

In the 1980's there was 108 million people recorded as living with DM across the globe [4]. As of 2019, that number has reached 463 million adults [5]. Thus, the number of affected individuals over 39 years has quadrupled. It is projected that this number has not finished rising and will likely reach 578 million by 2035 [5]. Type 1 diabetes (T1D) makes up 5-10% of total diabetes cases whilst T2D makes up the other 90-95% [6]. In New Zealand (NZ), as of 2019, there were 259,800 adults living with DM. It is expected that there is another 66,800 individuals living with undiagnosed diabetes [5]. Data collected over a range of studies has shown that the prevalence of diabetes across different ethnicities in NZ is not balanced [7]. This study analysed data sets collected between 2005 and 2015 to investigate any disparity between the ethnic groups in NZ. Overall, the study found that Pacific peoples tend to have the highest rates of DM, this is followed by Asian peoples, then Māori and finally by Europeans. The prevalence in Māori is twice as high as Europeans [7]. This study highlights the importance of the regulation of DM at both a national and global level.

1.3 Western Influence on T2D Epidemiology

Alongside the increasing number of people affected by DM is the increasing number of people who are affected by non-infectious degenerative diseases within Western civilisations [8]. These diseases are also referred to as civilisation diseases which include diabetes, obesity, and cardiovascular disease (CVD). With the widespread introduction of westernised diets and lifestyle there is a decrease in physical activity in combination with access to excess calorific nutrition. These factors can lead to obesity which is one of the largest risk factors for T2D. It is very important to identify that civilisation diseases are very rare in other non-westernised populations [8]. In relation to NZ, the prevalence of DM among Māori was very rare before introduction to westernized lifestyles [9]. This is interesting as this population is now disproportionately represented in the statistics for NZ. It has also been discussed that life-style changes for Māori, including eating traditional foods and consuming rākau rongoā (traditional medicine), could help prevent the growth of DM within the population [9]. Another strategy for at-risk communities is providing programmes which make medical treatment accessible and specific through having awareness and sensitivities for non-western cultures [7]. It has been shown that district health boards (DHB) in NZ that have tailored programmes for Māori and Pacific peoples that the prevalence of DM in these communities is lower than DHBs without these programmes [7]. It is essential that medical practitioners can provide care and create spaces that all ethnicities feel welcome and respected in.

1.4 Types of Diabetes

1.4.1 Diabetes Mellitus Definition

DM is defined as the overarching group of metabolic diseases that are a result of loss of hyperglycaemic control resulting in chronic hyperglycaemia [10].

1.4.2 Glucose Homeostasis in Healthy Individuals

In healthy individuals, blood sugar levels are maintained under tight homeostatic control with glucose concentration kept between 4-6 mM [11]. This level will naturally vary throughout the day, typically, spikes in glucose concentration are seen after a meal with decreases occurring during periods of fasting or sleep [11]. To prevent hyperglycaemia, insulin is secreted in response to glucose spikes, this homeostatic function results in the decrease of glucose levels within the blood [12].

When glucose in the bloodstream increases above the 4-6 mM threshold, insulin synthesis and secretion will begin [13]. Glucose will bind to glucose transporter type 2 (GLUT2) receptors on the cell membrane of pancreatic beta cells. This receptor allows entry of glucose into the cell. It then quickly undergoes the first steps of glucose metabolism, transforming glucose into glucose-6-phosphate. The addition of phosphate stops the glucose molecule from leaving the cell. The increase of glucose metabolism results in an increase of the ATP:ADP ratio. This change in ratio affects the concentration of K^+ inside the cell which in turn results in depolarisation of the cell membrane, subsequently causing Ca^{2+} voltage gated channels to open. This results in an influx of Ca^{2+} into the cell which is responsible for the secretion of insulin containing vesicles from the cell [13].

Once insulin is secreted from the pancreatic beta islet cells into the blood stream it binds to insulin receptors (IR) [14]. The main targets of insulin are the liver, skeletal muscle and adipose tissue [15]. When insulin binds to its receptor, the receptor undergoes a conformational change leading to a phosphorylation cascade [14]. This phosphorylation cascade results in the translocation of glucose transporter type 4 (GLUT4) receptors from within the cell to the membrane in skeletal muscle and adipose tissue [14]. GLUT4 receptors are insulin-dependent glucose receptors which are responsible for the uptake of glucose from the blood into cells. There are other types of GLUT receptors which are not insulin dependent present in other tissues [16]. These are detailed in **Table 1.1**.

Table 1.1 Overview of location and role of different glucose transporters (adapted from [16])

Glucose transporter type	Location	Role
GLUT 1	Central Nervous System	Catalyses the rate limiting step in glucose metabolism for cells in the central nervous system
GLUT 2	Pancreatic beta cells Kidney Liver	Responsible for glucose sensing
GLUT 3	Brain Lymphocytes Monocytes Platelets	Major neuronal glucose transporter
GLUT 4	Skeletal Muscle Adipose Tissue	Insulin dependent transport of glucose into the cell
GLUT 5	Intestinal epithelial cells	Has a high specificity for fructose and is responsible for absorption of dietary fructose

Insulin works to lower blood glucose levels by acting as a glucose-depositing hormone [17]. However, there are opposing homeostatic controls during periods of hypoglycaemia. When blood glucose levels are lower than 4-6 mM glucagon is secreted from pancreatic alpha cells [11]. Regulation of glucagon secretion by alpha cells is controlled by both intrinsic and paracrine function [18]. Paracrine regulation is suspected to take part in this regulation as alpha cells isolated from the pancreas can no longer secrete glucagon properly. However, there is also evidence for intrinsic regulation of glucagon secretion. In low glucose conditions there is excitation of the alpha cells which leads to the secretion of glucagon. This electrical stimulation is caused by action potentials through voltage gated Na^+ and Ca^{2+} channels [18]. Glucagon will enter the blood stream and stimulate gluconeogenesis in the liver which causes an increase in blood glucose levels [19]. The gluconeogenesis pathway can transform alpha-keto acids or lactate back into glucose through a nine-step pathway [19]. Dysregulation of this pathway results in blood glucose levels falling.

1.4.3 Type 1 Diabetes Pathogenicity

Generally, T1D is associated with immune mediated destruction of pancreatic beta islet cells. This destruction results in lowered beta cell mass and, therefore, less production of insulin [20]. Onset of this disease is most common in childhood, between ages 5-7. However, recent studies have shown that this may occur at any age [20]. The immune mediated destruction is typically associated with autoantibodies which target either the beta islet cells themselves, insulin, GAD or tyrosine phosphatases [6]. T1D is also a polygenic disorder, which means it is affected by several loci on genes. Specifically, the HLA region, which is located on human chromosome 6. Different haplotypes in this region are responsible for either protective or non-protective phenotypes.

The majority of T1D cases fall within the immune-mediated destruction category, however, there is heterogeneity for this form of diabetes. This gives rise to the idea that individuals with T1D may be placed into either type 1A (immune response resulting in diabetes) or type 1B (idiopathic). Type 1B individuals may become reliant on exogenous insulin but have no evidence of an auto immune response. It is also important to note, that these individuals do not display the same issues as T2D. The idiopathic form of T1D results in little to no insulin production rather than insulin resistance. Some of the individuals within this group may have a monogenic (rather than polygenic) form which is known as maturity onset diabetes of the young (MODY), which again, results in no autoimmune response but a reliance on exogenous insulin nonetheless [6].

1.4.4 Type 2 Diabetes Pathogenicity

T2D is associated with four phenotypes; obesity, decreased insulin secretion, increased glucose production and insulin resistance [21]. The onset of T2D heavily relies on both environmental and genetic factors and is a multifactorial disease [22]. Lifestyle factors which promote the onset of T2D are factors such as lack of exercise, lack of movement and consumption of alcohol [22]. These factors are typically associated with obesity. Although lifestyle factors play a role, having a high-risk factor is not always indicative that an individual will develop T2D.

There are currently large advances in genome wide association studies (GWAS) and screening for specific genes responsible to further understand the genetic factors. To date, there have been 176 GWAS studies for T2D with 4049 risk alleles identified [23]. If the

genetics for T2D can be elucidated it could be possible to identify individuals who are genetically predisposed before onset of the disease [22]. T2D pathogenicity progresses through the stressors put on the body by hyperglycaemia and obesity. These simultaneously stimulate impaired hormone signalling such as decreased insulin signalling but also perpetuates insulin resistance. This is shown diagrammatically in **Figure 1.1** [24].

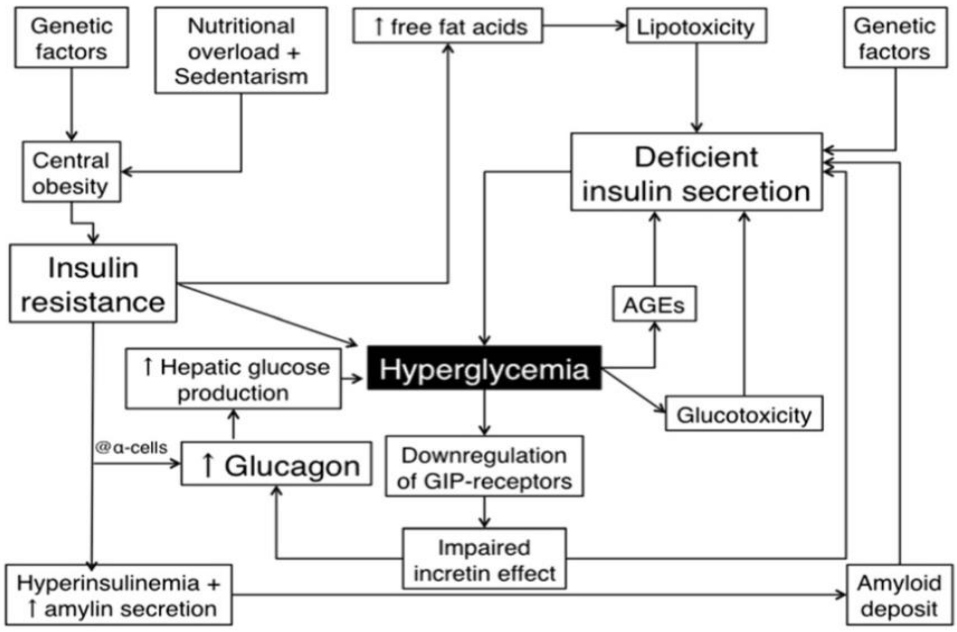

Figure 1.1 Diagram showing effect of excess nutrition and hyperglycaemia in the pathogenicity of T2D (image sourced from [24])

Research to understand the link between obesity and insulin resistance has shown that an increase in adipose tissue leads to insulin resistance [25]. Increased adipose levels in the pancreas causes an increase of fatty acids, leading to a suppression of insulin secretion in response to glucose [25].

Alongside low insulin secretion and signalling there is also over secretion of the peptide hormone, glucagon [24]. There is debate over what triggers the secretion of glucagon, however, it is known to be secreted during periods of hyperglycaemia in T2D. This adds to the high levels of glucose in the blood already by stimulating gluconeogenesis.

1.4.5 Obesity

Traditionally obesity has been considered the outcome of negative traits such as laziness and gluttony, however, this is not always the case. Obesity is defined as having excess body weight for height [26]. This is measured using the body mass index (BMI) which calculates the ratio between body weight and the square of height in meters (kg/m^2). Overweight is classified as having BMI > 25-30 kg/m^2 and clinically obese as BMI > 30 kg/m^2 [26]. With the widespread introduction of the Western diet there is now easy access to excessive calories. This, in combination with the biological predisposition that humans have to store energy for times of food shortage has led to increased numbers of people with obesity [27]. When an individual has excess energy, it is stored in the body in white adipose tissue (WAT) in the form of triglycerides [28]. This WAT can become highly vascularised and is known to secrete factors to maintain metabolic homeostasis. Hormones such as leptin are released by adipocytes and circulate in the body proportional to the amount of adipose tissue. Therefore, higher levels of leptin decrease hunger [29]. This relationship suggests that as the amount of adipose tissue increases, an individual's hunger should decrease, or that many obese individuals have a leptin deficiency. Often neither of these observations are made in obese individuals and instead hunger is not reduced due to leptin resistance [29]. Also secreted from adipocytes are pro-inflammatory cytokines such as TNF-α, interleukin 6 (IL-6) and monocyte chemoattractant protein 1 (MCP-1) [28]. MCP-1 is a monocyte attractant which means that adipose tissue becomes infiltrated with monocytes. The presence of these cells amplifies the secretion of these pro-inflammatory cytokines [28].

1.5 Complications of DM

DM results in both microvascular and macrovascular damage [30]. Micro vessels are responsible for the control of blood pressure and nutrient delivery to tissues based on metabolic need. Macro vessels, however, are responsible for the delivery of blood around the body on a much larger scale. DM associated damage to micro vessels occurs by increasing the vessel wall thickness. This leads to improper vessel function and can prelude other problems such as hypertension, hypoxia and delayed wound healing [30]. Damage to both types of blood vessel is due to the presence of hyperglycaemia and can also result in the onset of retinopathy, neuropathy, nephropathy, and CVD [31].

Hyperglycaemia is known to trigger increased levels of advanced glycated end products (AGEs), reactive oxidative species (ROS) and methylglyoxal (MGO) [31]. Increased AGEs are formed through a Maillard reaction, whereby, glucose reduces amino acids in proteins resulting in the formation of a Schiff base [32]. Proteins with Schiff bases will undergo irreversible dehydration and condensation reactions which produce AGEs. Due to the irreversible nature of the reactions, these proteins are permanently glycated [32]. Increased levels of ROS due to hyperglycaemia are produced by mitochondrial respiratory enzymes. Lastly, MGO is a reactive dicarbonyl compound which is produced during glycolysis [33]. The reactive nature of MGO means it can glycate DNA and proteins leading to the accumulation of more AGEs [33]. The increase in AGEs, ROS and MGO combined leads to further damage on the body by inducing oxidative stress, apoptosis, autophagy, necrosis and the increase in pro-inflammatory cytokine production [31]. These flow on effects are responsible for micro and macrovascular damage which in turn lead to retinopathy, neuropathy, nephropathy and CVD [30].

1.6 Role of Inflammation

Inflammation is a response that the body produces as a defence mechanism to harmful stimuli [34]. This response is used to start a chain of cellular reactions and interactions with the purpose of reducing the effect of the harmful stimuli on the body. However, if this response is too large (acute) or occurs over a long period of time (chronic) this is also damaging to the body. Typically, inflammation will cause redness, swelling and pain at the level of the tissue. However, at the cellular level this results in the translocation of immune system and the release of cytokines to the affected area. Although there are numerous causes of inflammation, it is important to note that there is a common mechanism amongst all of them. Inflammation begins with the recognition of harmful stimuli via cell surface pattern receptors. This is responsible for the activation of inflammatory pathways. The result of the inflammatory pathways is the production and release of inflammatory markers. These markers then attract immune cells to the affected area [34].

1.6.1 Role of Pattern Recognition Receptors

Pattern recognition receptors (PRRs) are important in every case of inflammation as they recognise motifs called pathogen associated molecular patterns (PAMPs) or damage associated molecular patterns (DAMPs) [34]. Within PRRs is a smaller family which are referred to as toll-like receptors (TLRs). Within the TLR family are ten different receptors found in humans, each of these receptors will detect a different PAMP or DAMP. TLR signalling occurs using two adaptor proteins, either the myeloid differentiation factor 88 (MyD88) or TIR-domain containing adaptor inducing interferon -ß (Trif) [35]. TLR3 is the only TLR which does not signal using the MyD88 adaptor protein. TLR4 and partially TLR2 also signal via a Trif dependent pathway [35]. This results in the induction of an inflammatory cascade which is triggered is depending on which TLR is activated [34].

1.6.2 Inflammatory Pathways of Interest

There are three pathways of specific interest for inflammation, especially in a diabetic context. These pathways are mitogen activated protein kinase (MAPK), nuclear factor-κB (NF-κB) and Janus kinase-signal transducer and activator of transcription (JAK-STAT) pathways. They are all activated when cytokines such as interleukin -1ß (IL-1ß), IL-6 and TNF-α interact with TLRs as well as by various PAMPS and DAMPS. These pathways involve the regulation of cellular processes such as apoptosis, survival, and proliferation as well as the regulation and induction of more cytokines.

1.6.2.1 Role of the MAPK Pathway

The role of the MAPK pathway is to regulate cellular processes such as differentiation, survival and apoptosis [36].

The MAPK pathway responds to stimuli such as heat shock, osmotic stress, and inflammatory cytokines. Once activated this pathway undergoes a chain of phosphorylation events starting with a MAPK kinase kinase (MAPKKK) phosphorylating a MAPK kinase (MAPKK) which lastly, phosphorylates a MAP kinase (MAPK). There are various different types of MAPKKK, MAPKK and MAPK which are utilised to distinguish which cellular process will be regulated due to the presence of different stimuli [36]. The different types of these kinases include extracellular-signal-regulated kinases (ERKs) and c-Jun N-terminal kinases (JNKs) [34]. ERKs are typically employed when activation is triggered by mitogens and differentiation signals. JNKs are instead used when the activation is triggered by inflammatory stimuli and stress [34].

1.6.2.2 Role of the JAK-STAT Pathway

The JAK-STAT pathway is involved in the stimulation of cellular proliferation, migration, differentiation as well as apoptosis [37].

This pathway is complex, involving a number of different factors such as cytokines, interferons, and hormones [34]. However, this pathway is very useful as it is able to translate a diverse range of intracellular signals directly into a transcriptional response [34]. Associated with each JAK-STAT receptor are two JAK tyrosine kinases [37]. When a factor binds to the receptor there is a multimerization between the two JAK tyrosine kinases as they are brought close together allowing for trans-phosphorylation to occur. This then begins a phosphorylation cascade in which STAT ends up being phosphorylated.

The C-terminus on STAT proteins are highly conserved and are the site of phosphorylation in this case. This allows STAT proteins to dimerise and subsequently translocate to the nucleus to activate or repress target genes [37].

1.6.2.3 Role of the NF-κB Pathway

This pathway results in the activation of transcription factor NF-κB which is involved with regulation of inflammatory genes in innate immune cells as well as regulation of differentiation and activation of T-cells [38].

NF-κB can be activated through either the canonical or non-canonical pathways. These pathways have very similar outcomes although they respond to different stimuli and have slightly different reaction schemes. The canonical pathway can respond to a range of stimuli through a range of different receptors (PRRs, tumour necrosis receptor (TNFR), B and T-cell receptors (BCR) (TCR)). When a stimulus binds to one of these receptors there is phosphorylation of the multi-subunit IκB kinase (IKK) complex. This complex is responsible for the subsequent phosphorylation of the IκBα complex which results in its degradation in the proteasome. This results in translocation of NF-κB (or other similar members in its family) to the nucleus to work as transcription factors. The non-canonical pathway is very similar to this but it does not respond to a wide range of stimuli and it does not involve the degradation if the IκBα complex, instead it employs the use of the P100 protein instead [38].

1.6.3 Relationship Between Inflammation and Obesity

As mentioned in **Chapter 1.4.5** adipocytes have the ability to secrete pro-inflammatory cytokines alongside macrophages, these are cytokines such as, IL-ß, IL-6 and TNF-α. [28]. Adipocytes also secrete MCP-1 which encourages macrophage invasion of adipose tissue [28]. Of these cytokines, TNF-α was the first cytokine to be linked between inflammation and insulin resistance [39].

Interestingly, adipocytes will secrete pro-inflammatory cytokines in obese individuals and anti-inflammatory cytokines in lean individuals [40]. Factors such as changes to the number of adipocytes, the phenotype of the adipocyte and the number of structural, vascular, and immune cells in the adipose tissue determines whether the cytokines secreted are pro or anti-inflammatory. These factors are mainly modulated by the composition of cells in the adipose tissue. Adipocytes make up the majority of adipose

tissue, but there are also pre-adipocytes, lymphocytes, macrophages, and vascular cells present as well. Dysregulation of these cells is known to influence the pathogenicity of T2D. For example, the number of macrophages present is proportional to the level of adiposity, if there are more macrophages present there are more pro-inflammatory cytokines being secreted into the bloodstream. Adipose tissue which becomes metabolically dysfunctional also produces excess matrix components, this disrupts adipose expansion and can lead to the secretion of pro-inflammatory cytokines. Another interesting factor is that macrophage phenotypes differ between lean and obese individuals. Macrophages in obese individuals present a M1 phenotype which causes the cell to secrete pro-inflammatory cytokines and recruit T-helper cells whilst lean subjects have macrophages presenting a M2 phenotype which protect against insulin resistance induced through obesity [40].

Although TNF-α was the first molecular link to be identified between obesity and inflammation, there are a number of other pro-inflammatory cytokines which are up-regulated as well.

1.6.3.1 Leptin as a Pro-inflammatory Cytokine

Leptin is secreted from adipocytes in an endocrine manner and normally functions to regulate hunger [40]. However, it is also related to the pathogenicity of T2D as leptin production is proportional to the amount of adiposity. If an individual is producing a lot of leptin over time, leptin resistance can occur. It has also been stated that leptin increases the production of TNF-α and IL-6 through by activating the JAK-STAT pathway in macrophages which labels leptin as a pro-inflammatory cytokine [40].

1.6.3.2 TNF-α as a Pro-inflammatory Cytokine

It was identified that TNF-α was upregulated in obese mice and that long-term treatment of adipocytes lead to down-regulation of GLUT4 receptors [39]. This down-regulation is due to the inhibitory phosphorylation that occurs on the serine residues of insulin receptor substrate 1 (IRS-1) [41]. During insulin signalling, insulin binds to IR causing a phosphorylation cascade in which IRS are phosphorylated. Inhibitory phosphorylation of IRS-1 results in no translocation of GLUT4 receptors [41]. Following the initial identification of TNF-α up-regulation in mice, a positive correlation between obesity and TNF-α levels was identified in humans and that TNF-α levels decrease with weight loss [42].

1.6.3.3 IL-6 as a Pro-inflammatory Cytokine

In a clinical environment it has been shown in humans that IL-6 is upregulated in obese individuals and that it is down regulated when the level of adiposity decreases [40]. There is debate regarding the role of IL-6 in insulin resistance. However, data shows that it can lead to insulin resistance in hepatocytes by modulating the expression of SOCS3 in the liver [43].

1.6.4 Inflammatory Pathways Induced by Hyperglycaemia.

Alongside obesity induced inflammation contributing to the pathogenicity of T2D, there is also hyperglycaemia induced inflammation. It is accepted that there are four main pathways in which hyperglycaemia induces inflammation [44]. However, more recent studies have shown that these pathways all converge on an increase in ROS levels which then leads to an increase in inflammation [45]. The four mechanisms which contribute to increased ROS levels are the polyol pathway flux, production of AGEs, protein kinase C (PKC) activation and the hexosamine pathway [46].

1.6.4.1 Polyol Pathway Flux

The polyol pathway is responsible for the conversion of glucose into fructose [47]. This pathway is only used during periods of hyperglycaemia and leads to diabetic complications due to the products produced. Diabetic complications are seen in the retina and endothelial cells where this pathway is present. This is a two-step pathway which firstly reduces glucose to sorbitol through aldose reductase, this step consumes NADPH, transferring it to NADH. The second step is carried out by sorbitol dehydrogenase, which converts sorbitol to fructose. Firstly, the consumption of NADPH can contribute to increasing levels of ROS. NADPH works as co-factor in the regeneration of glutathione (GSH), which in turn scavenges ROS. The increase of ROS is the main contributor to the induction of inflammation but the other products in this pathway also play a role. During the induction of this pathway there is also an increase of sorbitol in the cell. Sorbitol is an alcohol, and its accumulation can lead to osmotic pressure put on the cell membrane which leads to osmotic stress. Fructose can also contribute to inflammation by being phosphorylated to fructose-3-phosphate. This can be broken down to 3-deoxyglucosone which is glycosylating in nature, and thus, contributes to the generation of AGEs [47].

1.6.4.2 Production of AGE Precursors

It appears that the production of AGE precursors induce damage and inflammation through three mechanisms [46].

The first being the glycosylation of intracellular endothelial proteins, especially proteins involved in transcription. It was hypothesised and proven by Ida Giardino, Diane Edelstein and Michael Brownlee that during periods of hyperglycaemia there is an increase in the amount of glucose-6-phosphate, glyceraldehyde-3-phosphate and fructose in cells [48]. All three of these sugars are known to glycosylate much faster than glucose which has the slowest rate of glycosylation of naturally produced sugars. This study used basic fibroblast growth factor (bFGF) which is an intracellular protein that cannot be secreted as a model. Significant glycosylation of this protein by these sugars was found. Glycosylation of intracellular proteins can lead to cellular damage [48].

The second mechanism causes cellular damage by inducing cellular dysfunction [46]. The secreted AGE precursors interact and modify extracellular matrix factors, this results in impaired cellular signalling which results in cellular dysfunction.

The last mechanism results in the induction of inflammation. The AGE precursors which are secreted from the cell can also interact with circulating proteins in the blood. Modifying these proteins allows them to interact with AGE receptors on other cells. Docking to an AGE receptor results in the induction of ROS which further leads on to the induction of the NF-κB pathway [46].

1.6.4.3 Activation of PKC

Increased levels of glucose causes in intracellular hyperglycaemia which subsequently results in increased production of diacyl-glycerol (DAG), this then activates PKC [46]. *De novo* DAG synthesis can be produced through multiple pathways in response to high glucose [49]. PKC up and down-regulates a number of pathways and factors resulting in abnormal blood flow, angiogenesis, capillary and vascular occlusion, induction of pro-inflammatory gene expression and increased levels of ROS [46].

1.6.4.4 Hexosamine Pathway Flux

During hyperglycaemia, as seen in the activation of PKC, more glucose is transported inside of the cell [46]. Most intracellular glucose is metabolised through glycolysis which results in the formation of glucose-6-phosphate and eventually fructose-6-phoshate. At this stage some fructose-6-phosphate is diverted from glycolysis to glutamine:fructose-6-phosphate amidotransferase (GFAT). This results in the conversion of fructose-6-phosphate to glucosamine-6-phosphate. After subsequent reactions this is converted to *N*-acetyl-glucosamine. This molecule then has the ability to modify serine and threonine residues on transcription factors which can result in pathogenic gene transcription. For example, it is known that *N*-acetyl-glucosamine has modified a transcription factor called SP1. This transcription factor is responsible for the transcription of transforming growth factor – β1 and plasminogen inhibitor-1. However, when it is modified by *N*-acetyl-glucosamine it can overexpresses these genes, having a detrimental effect on blood vessels, thus, contributing to CVD which is associated with DM [46].

1.6.4.5 Common pathway for induction of inflammation

Each of the four pathways discussed individually contribute to the pathogenicity and inflammation seen in DM, but they are also connected through a common pathway. This pathway is the overproduction of ROS [44]. The overgeneration of ROS through the cellular respiration pathway allows for excessive products to be diverted to the previously described damaging pathways in hyperglycaemia [44].

Under normal physiological circumstances glucose is taken into the cell through GLUT receptors. From here it is oxidised through glycolysis in the cytosol resulting in the formation of pyruvate. [50]. Pyruvate is then transported into the mitochondria where it is converted into acetyl-CoA. Acetyl-CoA is utilised by the citric acid cycle (TCA) to produce NADH and flavin adenine dinucleotide ($FADH_2$). These two molecules are used as electron donors in the mitochondrial electron transport chain (ETC). The ETC is made up of four complexes which are embedded in the mitochondrial inner membrane. The purpose of this chain is to establish a proton gradient by using reduction-oxidation (REDOX) potentials. This is achieved by NADH and $FADH_2$ donating electrons to complex I and complex II, respectively. Following this, the electrons are passed along the complexes using electron carriers. Complex I and complex III are responsible for pumping protons into the intermembrane space of the mitochondria. The proton gradient

is dissipated by ATP synthase to form ATP. The entire process from transport of glucose into the cell to the synthesis of ATP is cellular respiration [50].

However, in hyperglycaemic conditions there is more glucose available to be metabolised [44]. The production of ROS is proportional to the amount of NADH and $FADH_2$ produced [51]. Excessive production of electron donors such as NADH and $FADH_2$ in combination with a high proton gradient and low levels co-enzyme Q (electron carrier from complex I to complex III) results in electrons donated to complex I being unusable. This results in elevated production of ROS [51].

Each of the four pathways previously described are influenced by the overuse of the cellular respiration pathway. This is shown in **Figure 1.2**. The polyol pathway is activated when there is excess glucose in the cell, instead of being completely metabolised by glycolysis, the polyol pathway is utilised [43]. The hexosamine pathway is activated when higher levels of fructose-6-phosphate are present due to higher usage of glycolysis. Both the PKC and AGE pathways are stimulated by the higher levels of glyceraldehyde – 3-phosphate produced during glycolysis [43].

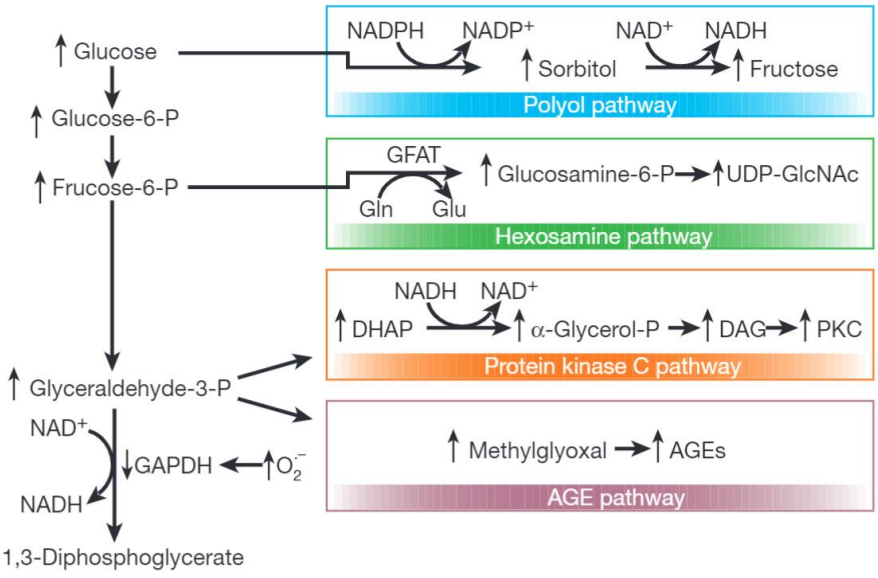

Figure 1.2 Diagram showing how the polyol, hexosamine PKC and AGE pathways are interlinked through glycolysis in cellular respiration. Image sourced from (42)

1.7 Heat Shock Proteins

Heat shock proteins (HSP) are induced in response to stress and have two main functions; (1) to work as a molecular chaperones which mediate protein folding and (2) protein degradation [52]. HSPs were first discovered by the Italian geneticist Ferrucccio Ritossa during the 1960's as an accident [53]. Ritossa was originally studying different nucleic acids that were synthesised in puffs found in the salivary glands of the fruit fly, *Drosophila melanogaster*. One night there was an accidental increase of the temperature in the incubator in which the *Drosophila* were kept. This resulted in the formation of new puffing patterns and the identification of HSPs, where their name originated from. Ritossa was also responsible for identifying that treatment with dinitrophenol and salicylate (which are ATP synthase uncouplers) also promotes the induction of HSPs [53]. Now it is known that prior exposure to sublethal heat changes results in improved HSP response. Interestingly, this prior exposure can also offer cross-tolerance for up-regulation of HSPs in response to other stressors as well [54]. There are a range of HSPs which have molecular weights ranging between 10-150 kDa. Thus, the molecular weight is how different HSPs are identified, such as HSP60 and HSP70. HSPs can also be grouped into families (**Table 1.1)**

Table 1.2 Summary of HSP families including the members and function of each family. Adapted from [55]

HSP family	**Function**
HSP40	Co-chaperone for HSP70, orients substrates for HSP70.
HSP60	Carries out ATP-dependant refolding of denatured proteins and aids in the folding of nascent proteins.
HSP70	Prevents aggregation of proteins and is also involved in protein trafficking and regulation of HSP responses.
HSP90	Displays a generalised chaperone role and has functions in signal transduction pathways.
HSP100	Responsible for the disassembly of protein oligomers and protein aggregates.
Small HSP (sHSP)	Carries out ATP-independent chaperone functions and binds non-native proteins

1.7.1 HSP60 Family

The HSP60 family is a chaperonin family. The most well studied members of this family are GroEL and GroES which are found in *Escherichia coli* whilst the equivalent proteins in humans are HSP60 and HSP10 respectively [55]. HSP10 does not fall within the HSP60 family but is a vital co chaperone for HSP60. HSP60 consists of two heptamer rings which stack together to form barrel-like structure whereas HSP10 is a 7-mer ring [55]. Together HSP60 and HSP10 form a barrel-like oligomeric structure to carry out protein folding and proteolytic degradation of denatured or misfolded proteins [56; 57]. Each of the two heptamer rings making up HSP60 has 14 subunits with each subunit being made up of the apical, intermediate, and equatorial domains. The apical domain is responsible for binding to denatured proteins through hydrophobic interactions. The equatorial domain binds ATP which is responsible for conformational changes in the protein. The intermediate domain works as a hinge between the apical and equatorial domains allowing for conformational changes to occur which subsequently change the substrate binding surface in the apical domain. The change in the apical domain allows for the release of proteins by switching the domain from a hydrophobic state to a hydrophilic one. The structure of HSP60 is demonstrated diagrammatically in **Figure 1.3.**

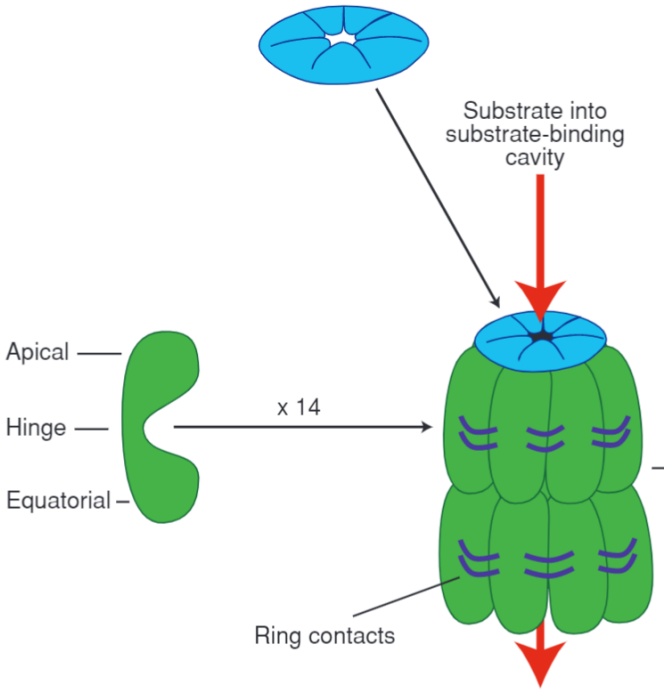

Figure 1.3 Diagram showing HSP60 heptamer rings, subunits and apical, intermediate and equatorial domains of the subunits (reproduced from [55]).

Humans have both HSP60 and chaperone containing TCP-1 (CCT) expressed throughout the body [56]. HSP60 is located in the mitochondria, primarily in the matrix and outer mitochondrial membrane, although it can be found outside of these locations. CCT on the other hand is found outside of the mitochondria, in the cytosol of the cell [57]. The protein structure for CCT differs to that of HSP60, instead of being a tetradecamer the protein consists of eight subunits. CCT also does not have a co-chaperone, instead it has a cap system built into the protein.

HSP60 is constitutively expressed under normal physiological conditions but if the mitochondria is subject to stress it is quickly upregulated [57].

1.7.2 Localisation of HSP60 in the Mammalian Cell

HSP60 is synthesised with 573 amino acids which includes a 26 amino acid N-terminus signal that allows for transport into the matrix of the mitochondria. The N-terminus is cleaved upon entry allowing for the formation of mature HSP60 [58]. In the mitochondria HSP60 is known to have several biological roles [59]. Primarily it is responsible for the refolding of nascent proteins and aids with the degradation of aggregated proteins. However, there is other evidence showing that it may play a role in apoptosis and cell survival depending on cellular conditions. When driving apoptosis, it is known to interact with other mitochondrial proteins such as p53 and mitochondrial HSP70. HSP60 is also stated to interfere with the functions of some endogenous and exogenous proteins [59]. It has been shown that over expression of HSP60 in the mitochondria can infer a protection against apoptosis when there are low levels of cytochrome c and caspase-3 activity but increased levels of ATP and mitochondrial complexes III and IV [60]. Cytochrome C and caspase-3 are both important proteins in the apoptotic pathway.

Immunogold labelling and electron microscopy of HSP60 identified there can also be localisation of HSP60 to the surface of the cell [61]. However, when the levels of surface HSP60 are increased this infers a danger signal for the cell [59]. These increased levels of HSP60 attract immune cells to the area which results in activation and maturation of dendritic cells alongside the generation of T-cells. Increased surface HSP60 is also of interest in oncology as it has found to associate within proteins involved with aiding the adhesion of metastasized breast cancer cells to secondary locations such as the lymph nodes [59].

Further work was achieved using gold immunolabelling electron microscopy to investigate the extracellular distribution of HSP60 [62]. One group found significant levels of HSP60 secreted in growth hormone and pancreatic zymogen granules. These HSP60 containing granules were found to be localised to the pancreas and the pituitary [62]. Another group lead by Jo Lewthwaite found that HSP60 could be secreted from the cell via exosomes by lymphoma cells [63]. Using electron microscopy, the secreted exosomes could be identified and through the employment of western blotting they were able to identify that these exosomes contained HSP60 [63]. Interestingly, the extracellular HSP60 found did not contain the N-terminal sequence which localises the protein to the mitochondria [59]. This suggests that the HSP60 is imported to the mitochondrial before extracellular secretion [59]. Further work has also shown that HSP60 exists in circulation, not only in extracellular compartments [64]. Extracellular HSP60 has been shown to work as a pro-inflammatory agent through binding to TLRs. This binding can stimulate the maturation of dendritic cells which results in the activation of inflammatory pathways. Alongside this it has also been shown to induce inflammatory cytokines such as TNF-α through the interaction and presenting of antigens to immune cells [59].

1.7.3 HSP60 Induction of Diabetes Related Inflammation

Elevated levels of HSP60 have been associated with T2D. Studies conducted with healthy individuals and individuals with T2D have shown that levels of HSP60 are four-fold higher in the serum of individuals with T2D than healthy individuals. Extracellular HSP60 has been implicated with the induction of inflammatory pathways resulting in the induction of inflammatory cytokines such as TNF-α [35]. It has been shown to do this through the activation of TLR4. As discussed in **Chapter 1.6.1**, TLR4 is MyD88 dependent and can lead to the activation of the NF-κB pathway. In cardiomyocytes which have been subjected to reduced blood flow (ischemia), HSP60 was up regulated in response and secreted from the cell. From here HSP60 can interact with TLR4 on the surfaces of other cells. When it binds to TLR4 it can induce the NF-κB pathway resulting in the induction of pro-inflammatory cytokines, or it can activate the JNK and NF-κB pathways in unison to upregulate TLR2 and TLR4 [35].

1.8 Current and Potential Future Treatments for T2D

There are several drug targets for management for T2D. However, although there is a plethora of drugs available, there is no to cure the disease, only management of the symptoms to prevent further deterioration of the body [65]. The different classes of drugs include biguanides, sulfonylureas, meglitinides and thiazolidinediones as well as lifestyle changes which are commonly prescribed to patients. As discussed throughout this chapter, inflammation is strongly linked to the pathogenicity of T2D which means investigation into anti-inflammatory treatments could be a promising new target for T2D medication [65].

1.8.1 Biguanides

Biguanides are a class of drug which improve sensitivity to insulin and decrease glucose production in the liver [2]. Within the biguanide class is a very commonly prescribed drug, metformin. Metformin ($C_4H_{11}N_5$) is orally administered and has been shown to significantly lower patient's blood glucose levels, without posing them at risk of developing hypoglycaemia. Similar biguanides to metformin have been used since medieval Europe, however, adjustments to these structures produced metformin which is much safer than the precursors. Despite the safety and long-term use of metformin there is still no elucidated mechanism of action for this drug [2].

1.8.2 Sulfonylureas and Meglitinides

The use of sulfonylureas and meglitinides began in 1937 and 1997, respectively [66]. Sulfonylureas and meglitinides are classes of drugs that work through the same mechanism to increase the levels of insulin secreted from pancreatic beta cells [67]. They bind to the potassium channels on beta cells which are sensitive to the intracellular ATP:ADP ratio. Binding to these channels causes depolarisation, mimicking what happens when increased levels of glucose enter the cell, resulting in the secretion of insulin. Unlike metformin, these drugs do place patients at risk of developing hypoglycaemia. Sulfonylureas have also been shown to increase the risk of CVD as myocardial potassium channels can also be targeted with these drugs [67].

1.8.3 Thiazolidinediones

Thiazolidinediones have been used since 1996 [66] to lower blood glucose levels whilst still preserving pancreatic beta cell function [67]. This class of drug works by increasing insulin sensitivity by targeting the muscle tissue, adipose tissue, and the liver to increase the uptake of glucose and decrease glucose production. This is very similar to metformin; however, this class of drug are more expensive and also carry side effects. Thiazolidinediones are associated with weight gain due to fluid retention and heart failure which is why metformin is typically chosen instead [67].

1.8.4 Lifestyle Changes

Lifestyle changes are one of the most effective treatments that T2D patients can undergo. Although treatment with pharmaceuticals is an option to prevent the worsening of the disease state it is important that lifestyle risk factors are minimised and are no longer contributing to hyperglycaemia [67].

1.8.4.1 Diet

Eating a well-balanced healthy diet will aid in decreasing adiposity, but it will also ensure that the body has the right nutrients it needs. Decreasing caloric intake, balancing micronutrient intake, eating enough fibre and decreasing fat, alcohol and sodium intake to reasonable levels will help with glycaemic control and will also lower the risk of secondary diseases such as CVD [67].

1.8.4.2 Exercise

Introducing a regular exercise regimen also has a range of benefits for T2D patients. These can include weight loss, control of cardiovascular risk factors, improved cardiorespiratory fitness and improved peripheral neuropathy [67]. Alongside this there is evidence that exercising after a meal can result in improved glucose uptake although the individual is experiencing insulin resistance. During exercise it is important for muscle cells to have adequate access to glucose for fuel [68]. It has been shown that contraction of muscles can induce GLUT4 translocation to the cell surface for glucose uptake in the absence of insulin. This indicates that exercising after meals could help maintain hyperglycaemic control [68].

1.8.5 Kawakawa Tea as an Anti-inflammatory Treatment

Kawakawa is an endemic plant to NZ, it is a small tree at least 5 m tall which produces characteristic heart shaped leaves and yellow berries as shown in **Figure 1.4** [9].

Figure 1.4 Kawakawa plant and characteristic kawakawa heart shaped leaves. Photo taken by Savannah Harvey.

Historically kawakawa has been used as rākau rongoā (traditional medicine) by Māori to treat ailments such as kidney and bladder problems as well as cuts and bruises, amongst other problems [9]. There are also reports of other species within the *Piper* genus being used as traditional medicine for very similar ailments around the world [69]. Many *Piper* species were utilised in African medicine [69]. There are also reports that *P. fimbriulatum* which is found in Panama, has been used as traditional medicine throughout South America to treat inflammation (amongst other ailments) [70]. Chemical analysis of kawakawa leaves has shown the main compounds they contain are phenylpropanoids, lignans and amides [71]. Of particular interest are the lignans, diayangambin, elemicin, myristicin and vitexin glycoside [71]. Elemicin has been shown to work as an antimicrobial agent against *Campylobacter jejuni* and has also demonstrated anti-allergic effects [72] [73]. Diayangambin, myristicin and vitexin glycoside have all shown anti-inflammatory effects. The range of anti-inflammatory molecules within kawakawa leaves suggests that there is potential for its use in the treatment of DM. Previous work carried

out by MSc student Huawen Xu investigated the anti-inflammatory effect of kawakawa leaf extracts on four *in vitro* cell lines (HEK-BLUE™ 2, HEK-BLUE™ 4, NOD 2 WT and NOD G908R) as a therapy for Crohn's disease [74]. They found that secreted human placental alkaline phosphatase (SEAP) production was significantly lowered in cells treated with kawakawa leaf extract. SEAP is produced as a reporter gene for NF-κB, therefore, reduction in SEAP production indicates a reduction in NF-κB production which subsequently shows a reduction in inflammation [74].

1.8.5.1 Diayangambin

Diayangambin is the main lignan found in kawakawa, it has been shown to exhibit immunosuppressive and anti-inflammatory properties [70]. Investigation of the biological activity of diayangambin has shown that it can decrease the normal up-regulation seen of prostaglandin D_2 (PGE_2) from macrophages when they are in an inflammatory state. Administration of isolated diayangambin resulted in a decrease in PGE_2 in macrophages subjected to LPS to induce inflammation [70]. PGE_2 is up-regulated during inflammation [75]. The anti-inflammatory effect of diayangambin was also investigated *in vivo* using carrageenan-induced paw oedema mouse models [70]. When diayangambin was administered there was significant inhibition of the oedema formation after the onset of inflammation [70].

1.8.5.2 Myristicin

Myristicin is found in kawakawa but it also the main component found in nutmeg [76]. Myristicin is known to have hallucinogenic effects which can be fatal if the dose ingested is too high. However, nutmeg has also been used in Indonesia as a traditional medicine to treat ailments such as stomach cramps, diarrhoea and rheumatism, all of which are similar ailments kawakawa is used to treat [76]. Myristicin has also demonstrated anti-cholinergic, antibacterial, hepatoprotective, and anti-inflammatory effects [77]. The anti-inflammatory effects have shown inhibition of pro-inflammatory cytokines, nitic oxide (NO) and chemokines [77].

1.8.5.3 Vitexin Glycoside

Vitexin is a flavonoid and has been found to inhibit inflammatory pain in mice [78]. There is also evidence that this molecule works as an antioxidant and anticancer agent. It has been shown to suppress tumour growth through the induction of apoptosis in both human choriocarcinoma and oral cancer. Antioxidant effects of vitexin glycoside are due to its ability to scavenge cations and anionic free radicals. As for anti-inflammatory effects it

has been shown to inhibit the production of pro-inflammatory cytokines such as TNF-α and IL-6 [78].

1.9 Aims and Objectives

Inflammation is known to be linked to the pathogenicity of T2D through both hyperglycaemia and adipose related mechanisms. Current pharmaceuticals used in treatment of this disease do not cure or prevent the disease state. They are used to prevent further DM associated complications. This is why this project aims to investigate the anti-inflammatory properties of kawakawa present in a commercially available tea. Publications before this study have investigated the biological activity of singular components such as diayangambin and myristicin from kawakawa leaves but this study will aim to look at the anti-inflammatory effect of kawakawa as a whole tea. This will be representative of how it is typically consumed.

To achieve this, concentrations of KTE need to be selected that are not cytotoxic. To do this, dose response curves and cytotoxicity assays assessing apoptotic and necrotic cell death will be carried out to ensure that non-cytotoxic concentrations are selected.

As discussed throughout **Chapter 1,** HSP60 plays a role in the induction of pro-inflammatory cytokines, therefore, western blot experiments will be conducted to study the levels of HSP60 in response to kawakawa treated cells in a hyperglycaemic state.

As well as HSP60 studies, investigation of TNF-α expression after cells had been treated with KTE will be conducted to infer whether modulation of inflammation was occurring.

Investigating both HSP60 and TNF-α will allow for insight into the anti-inflammatory effects of KTE and will provide a start point for the elucidation of pathways involved in this anti-inflammatory effect.

Chapter 2

Materials and Methods

This chapter aims to cover general methods which have been used throughout the project. Specific methods for individual experiments will be discussed in the methods section of the proceeding chapters. All experiments were carried out in the E3.11 or E3.13 laboratories at the University of Waikato (UoW). The E3.11 laboratory functions under PC1 conditions and E3.13 functions under PC2. These facilities were used in conjunction with aseptic techniques and cleaning with 70% ethanol prior to any cell work to minimise the risk of microbial contamination. The freeze dried commercial kawakawa tea was kindly received from Donisha Liyanagama UoW.

2.1 Preparation of Common Solutions

Table 2.1 Compositions of common solutions. All solutions were stored at room temperature unless specified.

Solution	Composition
Complete MEM media	45 mL MEM media (Gibco, Catalogue no. 11095080). 5 mL fetal bovine serum (FBS). Store at 4^{o}C.
1 M Glucose	9 g Glucose. Dissolve in 50 mL ddH_2O. Filter using a 0.2 µm filter. Store at 4^{o}C.
Complete 50 mM Glucose media	42.7 mL MEM media. 5 mL FBS. 2.3 mL 1 M Glucose. Store at 4^{o}C.
1 X Phosphate buffered saline (PBS)	0.2 g KCl. 0.24 g KH_2PO_4. 8 g NaCl. 1.44 g Na_2HPO_4. Dissolve in 800 mL ddH_2O. pH to 7 and make up to 1 L. Autoclave to sterilise. Store at 4^{o}C
Reconstituted lipopolysaccharide (LPS)	5 mg LPS. 5 mL sterile PBS. Store at -18^{o}C. Store in glass.

Solution	Composition
Reconstituted kawakawa tea extract (KTE)	50 mg freeze dried KTE (Kawakawa tea pure, Oku NZ Native Herbal Products). Dissolve in 5 mL of 1X PBS. Filter using a 0.2 µm filter. Store at 4^{o}C. Use before the colour changes from green to brown or store at -18^{o}C.
ELISA buffer	10 mL ELISA buffer concentrate 10X. 90 mL MQH_2O. Store at 4^{o}C
ELISA wash buffer	1.25 mL Wash buffer concentrate 400 X 0.25 mL Polysorbate. 500 mL ddH_2O. Store at 4^{o}C.
TNF-α AChE-Fab' conjugate	100 dtn TNF-α AchE-Fab' Conjugate vial. Reconstitute in 10 mL of ELISA buffer. Store at 4^{o}C
Ellman's reagent	100 dtn Ellman's reagent vial. Reconstitute in 20 mL of MQH_2O.
10% SDS	5 g SDS. Dissolve in 50 mL of ddH_2O.
5 X Running buffer	72 g Glycine. 15 g Tris. 50 mL 10% SDS. 950 mL ddH_2O.
10 X Tris buffered saline (TBS)	43.83 g NaCl. 6.05 g Tris. Dissolve in 400 mL ddH_2O. Bring pH to 7.7, make up to 500 mL. Store at 4^{o}C.
TBS-Tween (TBST)	100 mL 10 x TBS. 0.5 mL Tween 20. 899.5 mL ddH_2O.
10% skim milk in TBST	10 g Skim milk powder (Pams). 100 mL TBST. Store at 4^{o}C. Use within 1-2 weeks.
Ponceau S stain	0.5 g Ponceau S 5 mL Glacial acetic acid Bring to 500 mL using MQ H_2O

Solution	Composition
Protein loading buffer	0.04 g BPB 4 mL Glycerol 280 µL 2-mercaptoethanol 2 mL Tris (pH 6.8, 1M) 0.8 g SDS Make up to 10 mL using MQ H2O
1:1000 Primary polyclonal rabbit HSP60 antibody	10 µL Primary polyclonal rabbit HSP60 antibody (Abcam, catalogue no. Ab46798). Make up to 10 mL in 5% skim milk TBST.
1:1000 Secondary peroxidase conjugated goat anti-rabbit IgG antibody	10 µL Secondary peroxidase conjugated goat anti-rabbit IgG antibody (Life technologies, catalogue no. G-21234). Make up to 10 mL in 5% skim milk TBST.
DAB solution	DAB tablet (Sigma Aldrich, catalogue no. D5905-50TAB) 20 mL TBS 2 µL 30% H_2O_2

2.2 Culturing HEPG2 and HeLa Cell lines

2.2.1 Thawing Cells

Commercial HEPG2 (ATCC® HB-8065™) and HeLa (ATCC® CCL-2™) cells were obtained from the American Type Culture Collection (ATCC). These cells (1 mL) were rapidly thawed by immersing in a water bath at 37°C and were then added to 37°C pre-warmed complete MEM media (3 mL) in a sterile 15 mL falcon tube. The cells were centrifuged (Megafuge 1.0) at 300 rpm for 5 minutes at room temperature (RT). The supernatant was removed, and the cell pellet was resuspended in complete media (5 mL) before being transferred to a treated T25 flask (CellStar). The cells were kept in a humidified incubator (HERA Cell 240) at 37°C with 5% CO_2 (standard incubator conditions).

2.2.2 Growing Cells

Cells were grown in standard incubator conditions and underwent a media change every two days or as needed (indicated by a media colour change from pink to orange). This was achieved by removing the media from the cells and replacing it with complete 37°C MEM media (5 mL). Two flasks of HEPG2 cells were kept at any time, one was subjected to normal glucose conditions (4 mM) and one to high glucose conditions (50 mM). This allowed for the establishment of a model which has been exposed to long-term high glucose conditions. HeLa cells were only grown under normal glucose conditions. Cells were viewed every two days using an inverted microscope (Nikon type 120) to check the confluency and for the presence of contamination. When required 1% penicillin/streptomycin (PENSTRIP) (Gibco) was added to the media to prevent contamination. Cells were grown until they reached 80% confluency. Once at 80% confluency they were passaged, harvested for experiments or frozen. All experiments were carried out within 10 passages.

2.2.3 Passaging Cells

To passage cells, the media was removed and discarded. Cells were washed with pre-warmed 0.25% trypsin-EDTA (trypsin, 2 mL) or phosphate buffer solution (PBS) and were then incubated with an aliquot of trypsin (2 mL). Cells were incubated until they were floating in suspension and no longer adhered to the flask surface. Once this occurred, pre-warmed complete media (2 mL) was added to neutralise the trypsin. Aliquots of the

cell suspension (4X 1 mL) would be transferred to new flasks with the addition of complete media (4 mL) to each new flask to allow for further cell culturing.

2.2.4 Freezing Cells

Cells were frozen to accumulate stocks. The cells would undergo the same trypsinisation process as when they are passaged (described in **Chapter 2.2.3**). However, rather than adding aliquots of cell suspension to T25 flasks the aliquots (1 mL) were placed into 2 mL cryotubes. DMSO (10%) was also added to the cryotube to protect the cells during freezing. The cells were placed into a cool cell and kept in the freezer at -80^{o}C. After 24-hours the cells were moved to long-term storage in the freezer.

2.3 Cell Counting Using the Trypan Blue Exclusion Method

Cells were counted by mixing cell suspension (10 µL) with trypan blue (10 µL) on parafilm so that a homogenous bubble of the mixture was achieved. This mixture (10 µL) was loaded onto a haemocytometer and the resulting cells were using counted an inverted microscope. Any cells stained blue were not counted as this indicates a loss of integrity of the cell membrane, thus, allowing entry of the trypan blue into the cell. Non-blue cells present in the outer four corners of the haemocytometer were counted and averaged together. The number of cells per mL were calculated using **Equation 2.1**:

$$Averaged\ cell\ count\ number\ \times\ 2 \times 10^4 = Cells/mL$$

Equation 2.1– Calculation of cells/mL from a haemocytometer cell count

2.4 Dose-response curve

A dose-response curve was carried out to observe the growth of HEPG2 and HeLa cells under different conditions for a 6-7-day period.

2.4.1 Seeding cells for exposure to treatments

Cells were harvested from 80% confluent T25 flasks. Media was removed from the flask and the cells were washed with PBS (2 mL). The cells were incubated at 37ºC with an aliquot of trypsin (2 mL) until they detached from the flask. Pre-warmed complete media (2 mL) was added to flask to neutralise the trypsin. The cell suspension was transferred to a falcon tube (15 mL) so that it could be pumped using a micropipette (1000 µL) to break up any clumps of cells. Next, cell counting was performed as described in **Chapter 2.3**. To determine the desired number of cells to be added to a 96-well plate. **Equation 2.2** was applied.

1. $cells/mL \div 1000 \ = cells/\mu L$
2. $(desired\ cell\ number) \div$ cells/µL = aliquot of suspension required

Equation 2.2 Calculation of aliquot required to seed desired cell density for 96-well plate.

This calculated volume of cell suspension was added to the clear, sterile, flat bottom 96-well plate and complete media with treatments was added to make a final volume of 100 µL.

2.4.2 Cell conditions and cell counting

The cells were grown in complete media supplemented with different treatments in a sterile 96-well plate. The media was renewed after three days. When cells were counted the media was removed, they were washed using PBS (30 µL) and incubated with trypsin (30 µL) under standard incubator conditions until the cells were no longer adherent to the plate (checked using an inverted microscope). Once no longer adherent, complete media (70 µL) was added to neutralise the trypsin. The cell suspension was counted as described in **Chapter 2.3**. This was repeated every 24-hours until the end of the 6-7-day period.

2.5 Cytotoxicity Assays

2.5.1 MTT Assay

The Roche Cell Proliferation Kit I (MTT) was used as per the manufacturer's instructions. After the 24-hour and 48-hour exposure periods, MTT (10 µL) was added to each well. The sterile, treated, flat-bottom, 96-well plate was incubated in standard incubator conditions for 4 hours. Solubilising solution (100 µL) was added to each well and was left to incubate in standard incubator conditions overnight. Finally, the plate was read at 490 nm using a plate reader (800^{TS} Biotek). The optimal wavelength recommended by the manufacturer is between 550-600 nm. However, 490 nm was selected as this is the next most suitable wavelength for this assay with the technology available.

$$Mitochondrial\ Dehydrogenase\ Activity\ (\%) = \frac{Sample\ Absorbance - Blank}{Control\ Absorbance - Blank} \times 100$$

Equation 2.3. Calculation of mitochondrial dehydrogenase activity using MTT absorbance values.

2.5.2 LDH Assay

The CyQUANT LDH Cytotoxicity Assay kit was used as per the manufacturer's instructions to detect the presence of lactate dehydrogenase (LDH) in the complete culture medium. After the treatment exposure period, lysis buffer (10 µL) was added to cells which had been grown under normal conditions in complete media. The sterile, treated flat-bottom 96-well plate was incubated in standard incubator conditions for 45 minutes. Following incubation, the complete media from each well was removed (50 µL) and added to a new sterile 96-well plate. Reaction mixture was made by diluting the Assay Buffer vial from the kit in ddH_2O (11.4 mL). The reaction mixture (50 µL) was added to each well and the plate was protected from light and left to develop for 30 minutes on a shaking platform (Gyro-Rocker® STR9) at 30 rev/min. After development, the stop solution (50 µL) was added and mixed into each well. The absorbance was read at 490 nm and 680 nm using a plate reader (800^{TS} Biotek). The 630 nm wavelength was subtracted from the 490 nm wavelength for each measurement before inputting the absorbances into **Equation 2.4.**

$$\%\ Cytotoxicity = \left[\frac{Sample\ Absorbance - Blank\ Absorbance}{Maximum\ LDH\ absorbance - Blank\ Absorbance}\right]$$

Equation 2.4 Calculation of cytotoxicity using LDH absorbance values.

2.6 Quantification of TNF-α Response

Cells were seeded into sterile, treated, flat-bottom, 96-well or 6-well plates following the same procedure described in **Chapter 2.4.1.** The seeding of the sterile 6-well plate differs slightly as 3 x 10^6 cells/mL were seeded per well rather than 2 x 10^5 cells/mL. The total complete media volume increased to 2 mL in a 6-well plate compared to 100 µL in a 96-well plate. HeLa cells were grown for 24-hours before treatment and HEPG2 cells were grown for 48-hours before the addition of treatment. Once treatment was added the cells would be incubated in standard incubator conditions for the desired exposure period.

2.6.1 Collection of Media and Cells for Enzyme-Linked Immunosorbent Assay (ELISA)

After exposure to treatment the conditioned media was removed from the cells transferred to a new, sterile, treated, 96-well plate using a micropipette. This plate was centrifuged (MultifugeX3R) at 1200 rpm for 10 minutes at RT. Next, the media was transferred to a new 96-well plate to ensure that any cell debris had been removed from the media. This plate was stored at -20^{o}C. The left-over cells were harvested using the same protocol outlined in **Chapter 2.4.2.** That protocol was adjusted when using 6-well plates. Instead, cells were washed with PBS (500 µL) followed by incubation with trypsin (500 µL). Once the cells were no longer adherent and were floating in suspension, pre-warmed complete media was added (1.5 mL). Once in suspension the cells were transferred to a new 96-well plate with DMSO (10%) added to the media to allow for freezing of the cells at -20^{o}C.

2.6.2 Measurement of TNF-α in Conditioned Media by ELISA

An ELISA kit was purchased from Cayman Chemical. Standards were made by serially diluting the 5 ng/mL stock with complete MEM media (250, 125, 62.5, 31.3, 15.6, 7.8, 3.9, 0 pg/mL). Standards (100 µL), samples (100 µL) and blanks (100 µL) (complete MEM media) were all added to the plate in duplicate. To each well except the blanks, TNF-α (human) AchE-Fab' conjugate (100 µL) was added. The plate was incubated at 4^{o}C overnight. After incubation, the wells were emptied and washed five times with ELISA wash buffer using a plate washer (50^{TS} Biotek). After washing, Ellman's reagent (200 µL) was added to each well and the plate was left to develop on a shaking platform for 60-120 minutes at 30 rev/min in the dark. Finally, the plate was read at 405 nm using a plate reader.

2.6.3 Extraction of Protein from Frozen Cells in a 96-well Plate

For protein extraction, the cells were treated as suspension-based cells as they were not adhered to the 96-well plate when they were frozen. The cells were transferred to 1 mL microcentrifuge tubes and centrifuged at 2500 x g for 10 minutes at RT. The supernatant was removed, and the cell pellet was resuspended in PBS (100 µL). The cells were centrifuged again at 2,500 x g for 10 minutes at RT. The supernatant was removed again, and Mammalian Protein Extraction Reagent (MPER) (120 µL) was added. The tubes were shaken on a shaking platform at 30 rev/min for ten minutes and were centrifuged at 14,000 x g for ten minutes at RT before transferring the supernatant to a new 1 mL microcentrifuge tube. Protein estimation was carried out using the method described in **Chapter 2.7.2.**

2.7 Quantification of HSP60 Expression

2.7.1 Protein Extraction – Adherent cells

In this case the protocol differs to **Chapter 2.6.3** as the cells are adherent. To begin, the cell media was removed from cells grown in T75 flasks, followed by washing the cells with PBS. Next, MPER (600 µL) was added to the flask. The flask is shaken on a shaking platform at 60 rev/min until the cells were lysed and no longer adherent to the flask (checked using an inverted microscope). The lysate was collected in a 1 mL microcentrifuge tube and centrifuged at 14,000 g for 10 minutes at RT. The supernatant was transferred to a new 1 mL microcentrifuge tube.

2.7.2 Estimation of Protein Concentration

The concentration of total protein was estimated using a BCA protein assay kit (Pierce). The procedure was carried out as per the manufacturers protocol. This involved preparing a standard curve by serially diluting bovine serum albumin (BSA) with PBS (concentrations included 200, 40, 20, 10, 5, 2.5, 1, 0.5, 0 µg/mL). A working reagent was also prepared by adding 25 parts of reagent MA, 24 parts of reagent MB and 1 part reagent MC together. Following this, the standards (120 µL), lysate (120 µL) and blanks (120 µL) were added to a 96-well plate. Although a PBS blank is included in the standard curve (0 µg/mL BSA) a MPER blank was also added to the plate so that the samples which were lysed in MPER can also be accurately blanked. Working reagent (120 µL) was added to each well. The plate was sealed using masking tape and left to incubate in standard incubator conditions for 2 hours. After incubation, the plate was left to cool to RT before reading the absorbance at 630 nm using a plate reader (800^{TS} Biotek)

2.7.3 Protein Separation and Transfer

2.7.3.1 Sample Preparation

Using lysate collected following the methods described in **Chapter 2.7.1** and using the protein estimation data collected in **Chapter 2.7.2,** samples were prepared with equal protein mass (5-10 µg) made up to 20 µL using PBS and protein loading buffer (5 µL). The samples were placed in a thermomixer at 95^{o}C for five minutes to denature the protein.

2.7.3.2 PAGE Gel Electrophoresis

The Electrophoresis chamber was assembled and an 8-16% Mini-PROTEAN® precast protein polyacrylamide gel (Bio-Rad) was loaded into the chamber. The upper and lower reservoirs of the electrophoresis chamber were filled with 5X running buffer. The samples containing equal masses of protein were loaded onto a precast gel alongside a protein ladder (See-blue Pre-stained ®, 5 µL). The gel was electrophoresed at 200 V until the loading dye was near the bottom of the gel.

2.7.3.3 Semi-dry Transfer

The electrophoresed proteins were transferred to a nitrocellulose membrane (NCM, 0.2 µm) using a western blotting transfer system (eBLOT). Firstly, the NCM was incubated in equilibration buffer for 1 minute at RT. Following this an anode was placed on the bottom of the western blotting transfer instrument and the pre-soaked NCM was layered on top. Air bubbles were removed, and the electrophoresed gel was placed on top. Again, air bubbles were removed before placing the cathode pad on top. The transfer system was run for 7 minutes. Once this was complete the NCM was removed from the stack and was rinsed with distilled water, followed by Ponceau S staining to ensure that successful transfer had occurred. Finally, the NCM was rinsed again with distilled water.

2.7.4 Western Blot

The NCM was blocked in 10% skim milk in TBST (10 mL) for 30 minutes on a shaking platform at 30 rev/min. Following this the membrane was washed three times with TBST (10 mL) for 5 minutes on a shaking platform at 30 rev/min. After washing, the membrane was incubated with primary polyclonal rabbit HSP60 antibody 1:1000 in 5% skim milk with TBST (10 mL) overnight at 4^{o}C. After the incubation, the NCM was washed three times with TBST (10 mL) for 5 minutes on a shaking platform at 30 rev/min. Following this the NCM was soaked in peroxidase conjugated goat anti-rabbit IgG 1:1000 in 5% skim milk in TBST (10 mL) for 30 minutes. After this period, the NCM was again washed three times in TBST (10 mL) for 5 minutes on a shaking platform at 30 rev/min. Lastly the membrane was soaked in DAB solution until bands on the NCM became visible. The western blot was imaged using an OPPO Reno2 cell phone as the gel imager was not functioning. Differences in pixel intensity were analysed using ImageJ software.

2.8 Statistics

All statistical analysis and construction of graphs were carried out using Microsoft Excel. Statistical significance was calculated using two-tailed student's *t*-tests. The accepted significance level was $p < 0.05$.

Chapter 3
Effects of Glucose and Tea Extract on Mammalian Cell Growth

3.1 Introduction

Kawakawa has been used as a rākau rongoā (traditional medicine) by Māori for many generations [9]. Their mātauranga (knowledge) has shown that kawakawa, when consumed as a tea, is safe and effective for a range of ailments including inflammatory problems [9]. Further scientific work has shown that *in vivo* up to 4 cups of tea per day is safe for consumption (the maximum cups of tea per day may be higher, however, this was the upper limit for testing in the experiment) [71]. When using cellular models, it is important that correct concentrations are selected so that the biological effects and potentially dangerous doses of the tea can be identified.

Dose-response curves are an effective way of measuring cellular growth over time. Measuring the cellular density every 24-hours will allow for the construction of a plot showing the phases of growth the cells enter for the duration of the experiment. Comparing treated cells with a control grown under standard conditions allows for identification of changes to growth rate by the treatments. Dose-response curves have been carried out in the past for kawakawa tea treated human *in vitro* cervical cancer (HeLa) and monocytic leukaemia (THP-1) cells [79], however, that experiment did not have repeat experiments (n=1). This experiment aims to test higher concentrations of the extract for a longer period of time on liver cancer (HEPG2) and HeLa cells with repeat experiments.

This set of experiments aimed to identify the effect of different KTE and glucose concentrations on the growth of HEPG2 and HeLa cells. These experiments also aimed to identify the different growth phases for these cell lines. This was achieved by calculating the cell density for each of these treatments every 24-hours for 6-7 days and using this data to compare relative growth rates for the treatments during the exponential growth phase.

3.2 Methods

Stock solutions of glucose (1M) and KTE (10 mg/mL, 1 mg/mL, 0.1 mg/mL, and 0.01 mg/mL) were prepared in 1X PBS (pH 7.4) and were sterilised using a 0.2 µm filter. The HEPG2 or HeLa cells were seeded into clear, sterile, 96-well plates as described in **Chapter 2.4**. The treatments were added to the media to give the following final concentrations: 50 mM glucose, 1 µg/mL KTE, 10 µg/mL KTE, 100 µg/mL KTE and 1000 µg/mL KTE. The treatment control consisted of cells grown in complete media only. Cell density was measured every 24-hours using the trypan blue exclusion method as described in **Chapter 2.4.** In addition, cell morphology was observed under an inverted microscope (Nikon type 120). Cell media was changed on day 3. The experimental samples were run in triplicate with each treatment set up in duplicate. Images of HeLa cells were captured on day 1, day 2 and day 7 using a microscope camera (OMAX, A35180U3). Unfortunately, the camera was unavailable during the HEPG2 experiment.

3.3 Results

3.3.1 Effect of KTE and Glucose Treatment on HEPG2 Cell Growth

HEPG2 cells treated with 1000 µg/mL KTE showed reduced growth compared to the control for the entire 6-day culture period. The 100 µg/mL KTE treatment showed varied growth rates, however, by the end of the culture period it was also showing a decreased growth rate compared to the control. The control growth reported here deviates from data presented in other studies [80; 81], it does not show defined growth phases unlike previous data which suggests that there should be a well-defined exponential growth phase between days 2-4 [80; 81]. The 1 µg/mL and 10 µg/mL KTE treatments had varied growth rates for the first two days but showed very similar growth rates to the control for the last three days. The exception is the last count for the 1 µg/mL treatment which was much higher than the control, however, a very large error bar was noted. These trends are demonstrated in **Figure 3.1**.

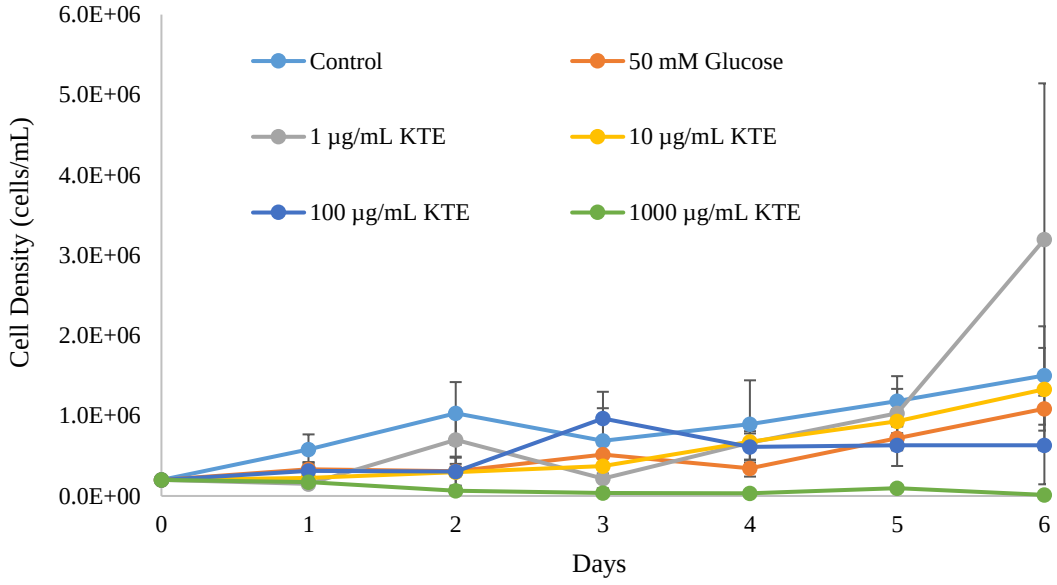

Figure 3.1. HEPG2 Cell Growth in glucose (mM) or KTE (µg/mL). Error bars showing ±S.E.M, *n*=3 in duplicate.

In order to quantitatively compare the growth rate across the different treatments in comparison to the control the growth rates for each treatment were plotted for days 3-5 (shown in **Figure 3.2**). Over these days cells should have entered the exponential growth phase. For each treatment, the line of best fit was used to determine the gradient for the growth rate. This allowed for calculation of relative growth rates between the treatments compared to the control which are demonstrated in **Table 3.1** and **Figure 3.3**

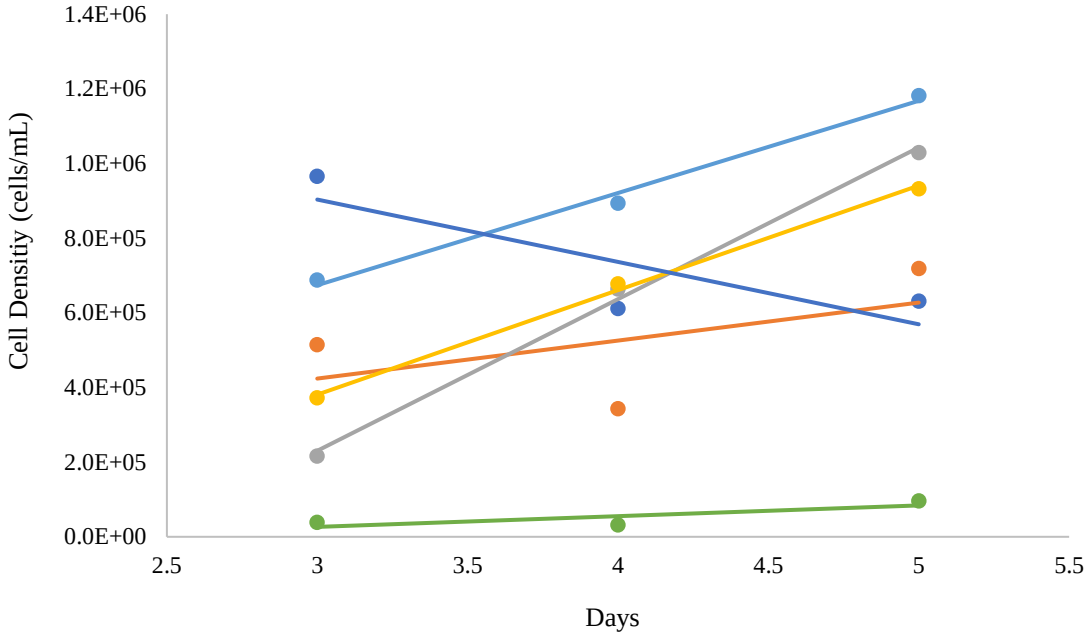

Figure 3.2. Comparison of growth rates for exponential phase of growth between days 3-5 for determination of growth rate gradient for HEPG2 cells

Table 3.1. Relative growth rate for HEPG2 cells for each treatment in comparison to the control

Treatment	Relative Growth Rate
Control	1.00
50 mM Glucose	0.41
1 µg/mL KTE	1.64
10 µg/mL KTE	1.13
100 µg/mL KTE	-0.68
1000 µg/mL KTE	0.12

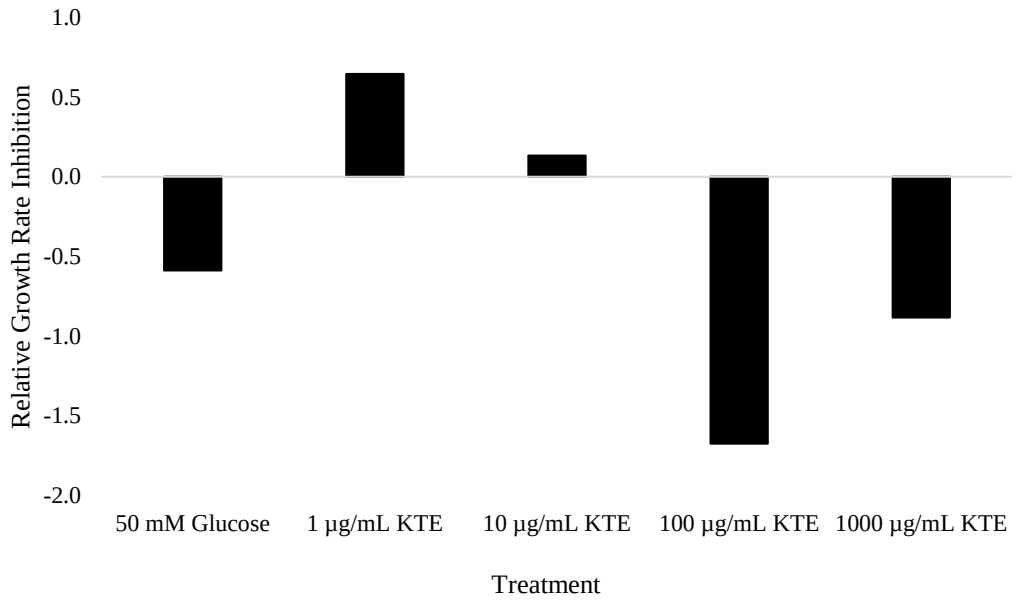

Figure 3.3. Growth inhibition rate of HeLa cells for each treatment in comparison to the control.

Comparisons of growth rate inhibition for cells exposed to different treatments during the exponential growth phase are shown in Figure **3.3.** Exposure to 50 mM glucose and the higher concentrations of KTE (100 µg/mL and 1000 µg/mL) inhibits the growth rate of the cells compared to the control. The two lower concentrations of KTE (1 µg/mL and 10 µg/mL) both increased the growth rate for the cells exposed during the exponential growth phase compared to the control.

3.3.2 Effect of KTE and Glucose Treatment on HeLa Cell Growth

The effect of KTE and glucose was also tested using the HeLa cell line. A similar trend can be seen in the HeLa cells as the HEPG2 cells which is that treatment with 1000 µg/mL KTE inhibits cell growth. In the HeLa cell line, there is a more defined exponential growth period between days 1-3 for all treatments except the 1000 µg/mL KTE treatment, as shown in **Figure 3.4**.

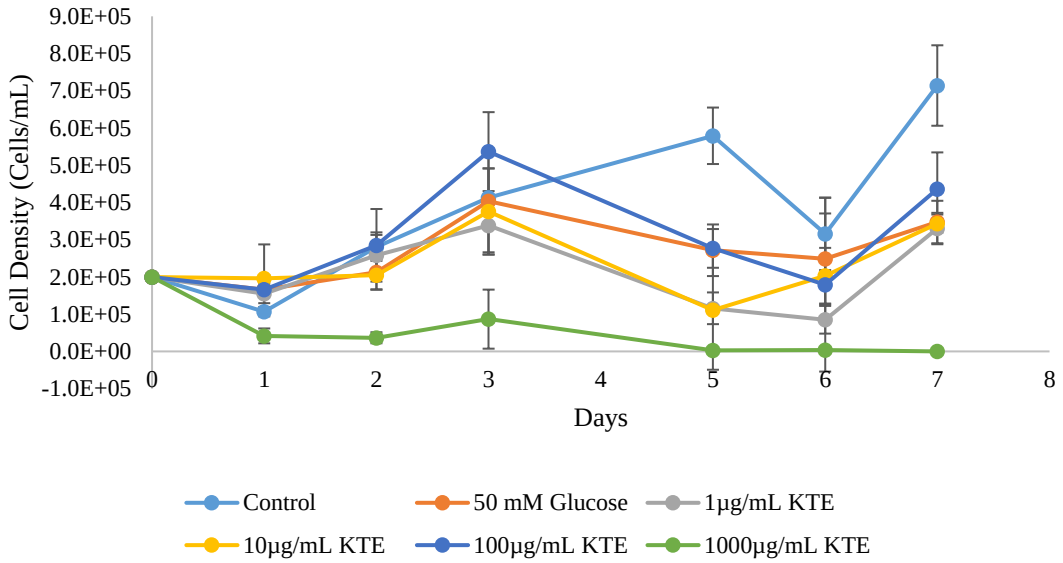

Figure 3.4. Growth Curve for HeLa cells exposed to different KTE or glucose concentrations. Error bars showing ±S.E.M, *n*=3 in duplicate**.**

Shown in **Figure 3.5** are the changes in cell density during the exponential growth period for each of the treatments. Lines of best fit were used to compare the growth rates to the control between days 1-3 as outlined in **Table 3.2** and **Figure 3.5**.

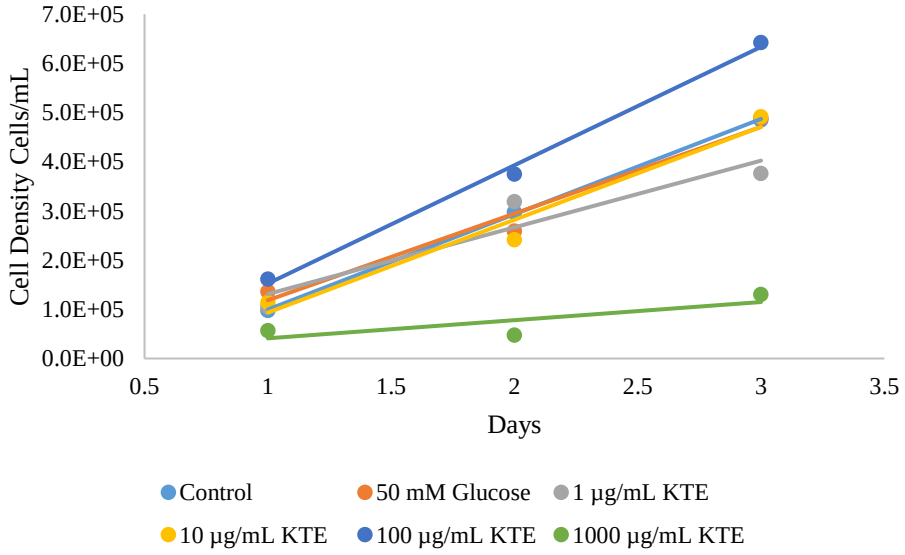

Figure 3.5. Comparison of growth rates for exponential phase of growth between days 1-3 for determination of growth rate gradient for HeLa cells

Table 3.2. Relative growth rate for HeLa cells for each treatment in comparison to the control

Treatment	Relative Growth Rate
Control	1.00
50 mM Glucose	0.77
1 µg/mL KTE	0.60
10 µg/mL KTE	0.58
100 µg/mL KTE	1.21
1000 µg/mL KTE	0.15

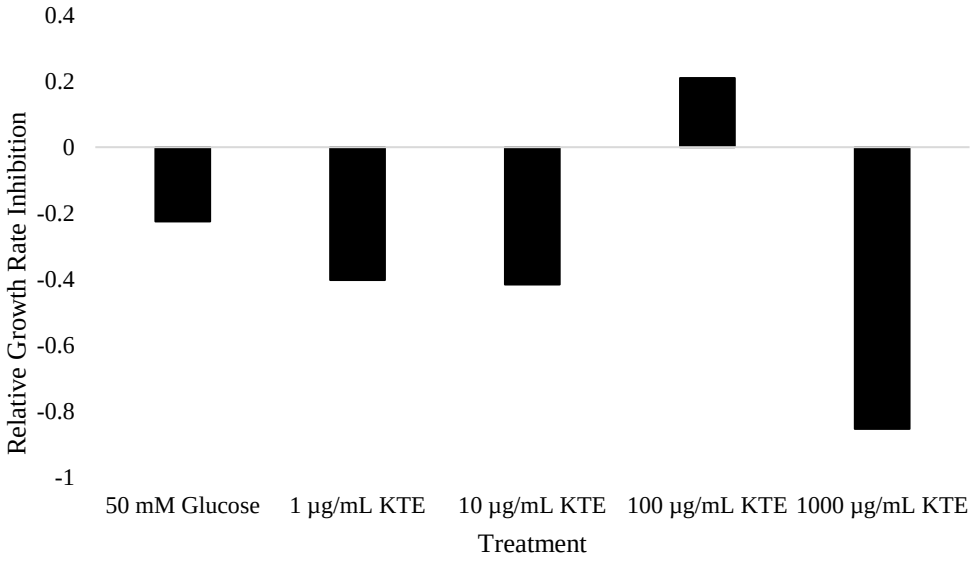

Figure 3.6. Growth inhibition rate of HeLa cells for each treatment in comparison to the control.

Comparisons of the growth rate for cells exposed to different treatments during the exponential growth phase in **Figure 3.6** shows that exposure to 50 mM glucose and all KTE treatments except 100 µg/mL slow the growth rate of the cells compared to the control. The 100 µg/mL KTE treatment instead increased the growth rate compared to the control.

Shown in **Figure 3.7** are images of cell morphology for each treatment on days 1,2 and 7 for the HeLa growth curve. This figure demonstrates that there are no major changes in morphology except for the 1000 µg/mL KTE treatment. There is a largely reduced cell number with the cells growing in an isolated manner rather than in colonies. Images of

HEPG2 cells have not been included due to the camera used for imaging only becoming available after the HEPG2 experiment had been carried out. A scale bar has not been provided for the images of the HeLa cells as this was not available at the time of image capture.

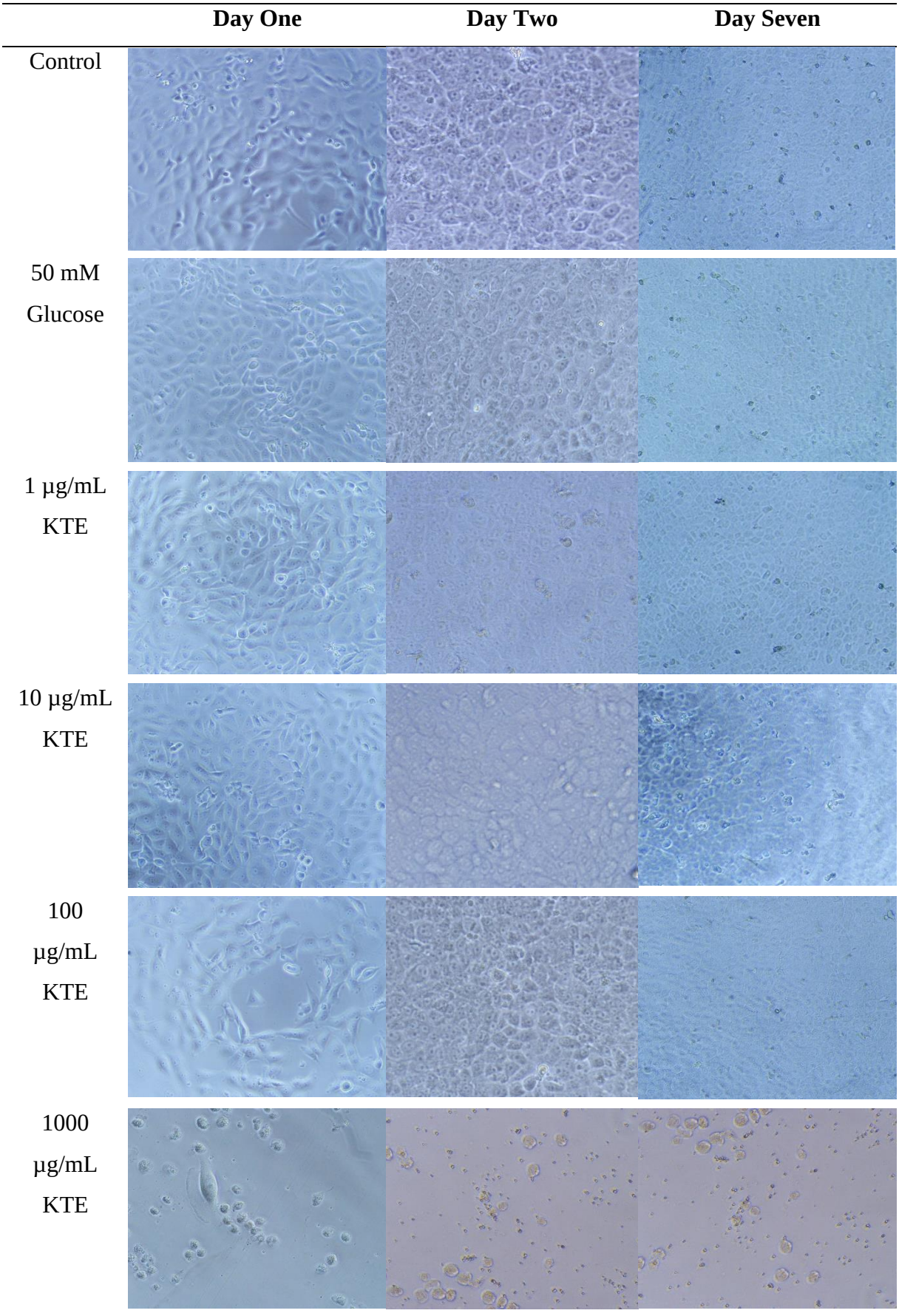

Figure 3.7. Photos of live HeLa cells for each glucose and KTE treatment on days 1, 2 and 7

3.4 Discussion

The overall purpose of these experiments was to identify the growth phases and growth rates of HEPG2 and HeLa cells in response to different glucose and KTE treatments. This was carried out by measuring cell density every 24-hours for 6-7 days.

3.4.1 Discussion of HEPG2 results

Cell growth curves for HEPG2 cells using the trypan blue exclusion method do not appear to be available in the literature. However, there is data investigating HEPG2 cell growth over periods of 6 – 7 days using different methods [80; 81]. One study measured HEPG2 growth under normal conditions using a cell counter every 24-hours [81]. Cell counters give readings in absorbance which should be proportional to the cell density. This study found that the cells went through a lag phase between days 1-2 and then entered exponential growth between days 2 – 4 [81]. This differs when compared to a second study that measured growth via a MTT assay [80]. A MTT assay is a colorimetric assay which measures mitochondrial dehydrogenase activity, which again, should be proportional to viable cell density. This study found that the cells went through a lag phase for the first two days and then entered exponential growth between days 3-6 [80]. The output for these two studies is different to this study. When analysing the HEPG2 growth curve from this study there is no clear lag or exponential phase. The only clear trend from this curve is that the cells treated with 1000 µg/mL KTE are inhibited. Because of this growth rate comparisons have been conducted between days 3-5 as this is when the cells would typically be in exponential growth.

It is important to identify that the cell density results seem erratic compared to the trends for similar data collected in the literature, it is also important to identify that some of the points in **Figure 3.1** have very large errors.

An explanation for this is that HEPG2 cells tend to grow in clumps rather than in a monolayer. This causes problems when using the trypan blue exclusion method as a clump could contain hundreds of cells that are impossible to separate and count by eye. The impact of the clumps does not just affect counting them, but it also makes seeding plates with a specific number of cells highly inaccurate as the cells are not evenly distributed in a solution. The erratic counts for this experiment will be a culmination of error during seeding and the inability to read or obtain accurate counts for each given well.

Another source of error for this experiment is that HEPG2 cells are adherent cells and must be removed from the plate using trypsin. The issue with this step in the protocol is that it is very difficult to tell whether all the cells have been removed from the bottom of the plate if they have not this will affect the cell density. To check for detachment the plate would be visualised under the microscope after ten minutes of exposure to trypsin. After this time, it was often found that agitation was required to remove the cells from plate either by gently shaking the plate or by pumping the trypsin in each well using a micropipette. These fixes aid in removing the cells from the bottom of the plate but increase clumping. As stated by ATCC, trypsinisation for periods longer than 5-15 minutes should be avoided as cell viability may be affected [82]. Therefore, to ensure that over trypsinisation was not affecting the results agitation would be used. However, it was also stated by ATCC for HEPG2 cells is that agitation should be avoided as this increases clumping (Hep G2 [HEPG2] (ATCC® HB8065™)). It is likely that as these cells have been passaged over time clonal selection has resulted in cells with stronger cell-matrix adhesions which makes the trypsin less effective at detaching the cells from the plate.

The results from this experiment do not show very clear growth phases unlike previous studies which employed different cell counting methods. The growth rates for the cells between days 3-5 show that the lower concentrations of KTE (1 µg/mL and 10 µg/mL) show a greater growth rate than the control. The two higher concentrations of KTE both show large growth rate inhibition. Interestingly, the 100 µg/mL treatment showed the highest inhibition which can be attributed to the undefined growth phases due to inaccurate counting. It can be seen in **Figure 3.1** that during days 3-5 the cell growth for this treatment is in decline rather than in exponential growth in these cells. The error due to clumping makes it difficult to interpret these results and also makes it very difficult to draw any conclusions from this experiment. However, the data has been included here for comparison against the HeLa cell line which is another adherent cell line that is not affected by clumping to the same extent.

A way in which this experiment could have been improved upon for the HEPG2 cells is through the use of a cell counter. The cells must be counted to seed the plate for the experiment which means that the use of an MTT assay would still have error from seeding although the daily readings would contribute less error. The issue of clumping has been source of error and had significant effects on later experiments which will be discussed further in the following chapters. For future work, reviving frozen HEPG2 cells stored in

liquid nitrogen rather than at -80^{o}C would be ideal. The use of Eagle's Minimum Essential Media (EMEM) rather than Minimum Essential Media (MEM) as recommended by ATCC may also be helpful. The main difference between the media is that EMEM has additional components such as Earle's Balanced Salt Solution, L-glutamine (2 mM), sodium pyruvate (1 mM), sodium bicarbonate (1500 mg/L) and non-essential amino acids alongside the components found in MEM.

3.4.2 Discussion of HeLa results

The results shown in **Figure 3.4** show well defined growth phases and demonstrate the effect of each treatment on cell growth more clearly than the HEPG2 cells shown in **Figure 3.1**. Between day 0 and day 1 there is a lag phase which is very quickly followed by exponential growth between days 1-3. This is very quickly followed by a decline in cell number for all treatments except the control by day 5, then between days 5-7 the cell number increases again. In comparison to previous experiments less time is spent in each growth phase. However, because the cells enter exponential growth after day 1 it is likely that they are growing to confluency very quickly. Once the cells become overconfluent it is normal the cell number to decrease due to lack of space.

Also shown in **Figure 3.4** is that all treatments except for the 1000 µg/mL KTE grew well and showed well defined growth phases. However, by analysing the relative growth rate for each of the treatments in comparison to the control in **Table 3.2**, there is no apparent trend between KTE concentration and growth rate. The 10 µg/mL KTE treatment increased the growth rate of cells above the control, however, the other KTE treatments inhibited growth by varying amounts, as shown in **Figure 3.6.** It is interesting that the lowest concentration (1 µg/mL) of KTE showed higher inhibition of growth than both the 10 µg/mL and 100 µg/mL treatments. This is in disagreement with the previous MSc study by Julia Newland [79]. However, it is also interesting to acknowledge that their study compared the growth of cells treated with KTE that had been made by boiling kawakawa leaves at different temperatures (RT and 60^{O}C). The dose response curves differed for these different temperatures, indicating that the temperature of extraction had differing compositions of KTE [79]. In this study the KTE sourced had been made by boiling the tea for ten minutes before being freeze dried. The difference in temperature, tea and time of extraction could explain the varying results between this study and

Newland's study. However, comparisons between the datasets are difficult to make due to Newland's experiments not having independent repeats.

Although the growth rate for each of the treatments apart from the 10 µg/mL KTE are slower than the control, only the 1000 µg/mL KTE treatment completely inhibited growth. Photographs were captured for the HeLa cells shown in **Table 3.3**, these photographs confirm that the majority of cells for the 1000 µg/mL treatment had died rather than just having their growth inhibited. Close analysis of the photographs for this treatment shows that by day 1 the cells contained many granules which only increased as treatment exposure time increased. The granular shapes within the cell are typically an indication that the cell is undergoing apoptosis [83]. Alongside this the photographs on day 2 and day 7 both show small cell fragments in the well which is also likely due to the cell being killed by apoptosis [83].

To further investigate the apoptotic nature of the 1000 µg/mL KTE treatment and check the cytotoxicity of the other KTE concentrations alongside LPS treatment MTT and LDH assays were carried out.

Chapter 4
Cytotoxicity of Tea Extract, Glucose and Lipopolysaccharide on HeLa cells

4.1 Introduction

The MTT assay is widely used and considered to be a versatile cell viability assay [84]. It involves adding a water-soluble reagent, 3-(4,5-dimethylthiazol-2-yl)-2, -diphenyltetrazolium bromide (MTT) to live cells where it is converted to the chromatophore formazan by mitochondrial reductase. The formazan can then be solubilised to allow for measurement of the optical density. Any mitochondrial stress will reduce the conversion rate of MTT to formazan which allows for measurement of stress without complete cell death occurring. Thus, the more formazan that is present after MTT addition, the less mitochondrial stress the cells are under [84].

In comparison, the LDH assay measures the presence of lactate dehydrogenase (LDH) in the media. LDH is a cytosolic enzyme which is released into the cell when the plasma membrane is compromised, this is typically indicative of necrotic cell death. This assay works through a coupled enzymatic reaction, LDH present in the media will convert lactate to pyruvate. This reaction simultaneously reduces NAD^+ to NADH. This reduction to NADH is then utilised by the reagents of this assay. To the assay medium tetrazolium salt (INT) is added which is reduced to formazan by the NADH produced from the LDH catalysed reaction. This coupled reaction converting INT to formazan is proportional to the amount of LDH present in the medium [85].

Previous MTT and LDH assays have been carried out using KTE on HeLa cells. However, differences in the cells due to clonal selection, the use of different concentrations of KTE, and the lack of repeat experiments in the previous study, means this experiment will add to the previously collected data [79]. Due to accuracy issues with seeding HEPG2 cells and issues that occurred in other experiments (discussed in later chapters) only the HeLa cells were used for these cytotoxicity experiments.

The purpose of these experiments is to identify whether the concentrations of KTE selected for inflammatory studies are cytotoxic to HeLa cells. Also, this LPS has been

included in these assays as it will be used in later experiments as a positive control, therefore, a non-cytotoxic concentration should be selected.

4.2 Methods

4.2.1 MTT Assay

HeLa cells were seeded into a 96-well plate as discussed in **Chapter 2.4**. Cells were left to grow through the lag phase (24-hours) which was determined in **Chapter 3** before 50 mM glucose, KTE concentrations 1 µg/mL, 10 µg/mL, 100 µg/mL and 1000 µg/mL and LPS concentrations 1 ng/mL, 10 ng/mL, 1 µg/mL and 10 µg/mL were added to cells alongside control cells which were grown in complete media only. Each treatment was added in triplicate for each time point. The cells were exposed to the treatment for 24 and 48-hours before the MTT assay was run as described in **Chapter 2.5.1**. This experiment was carried out with triplicate repeats.

4.2.2 LDH Assay

HeLa cells were seeded into a 96-well plate and grown through their lag phase. After 24-hours, the cells were exposed to glucose, LPS and KTE, as previously stated above in **Chapter 4.2.1**, alongside cells grown in normal conditions (MEM media). Four wells with cells grown under normal conditions were set up, two for the control and two for the maximum LDH release wells. The cells were exposed to the treatment for 24 and 48-hours, the LDH assay was run as described in **Chapter 2.5.2.** Each treatment for each time point was set up in duplicate for conservation of reagents, with triplicate repeats of the experiment.

4.3 Results

4.3.1 MTT Assay of Glucose and KTE and LPS on HeLa Cells

No glucose or KTE treatments showed statistically significant (p >0.05) changes in mitochondrial dehydrogenase activity compared to the control within 24-hours.

After 48-hours the 50 mM glucose, 1 µg/mL, 10 µg/mL, and 1000 µg/mL KTE treatments showed significantly reduced mitochondrial dehydrogenase activity (p<0.05) compared to the control. This is indicative of mitochondrial stress being induced by these treatments. Treatment with 50 mM glucose showed 87.7±0.57%, 1 µg/mL showed 79.1±5.6%, 10 µg/mL KTE showed 80.2±6.3%, and 1000 µg/mL KTE showed 52.1±10.8% mitochondrial dehydrogenase activity. This means that the mitochondrial dehydrogenase activity decreased compared to the control by 12.26±0.57%, 20.9±5.6%, 19.8±6.3% and 47.9±10.8 % respectively after 48-hour exposure to treatment.

There are also statistically significant decreases between the 24-hour and 48-hour exposure periods for each of the treatments. These results are all demonstrated in **Figure 4.1.**

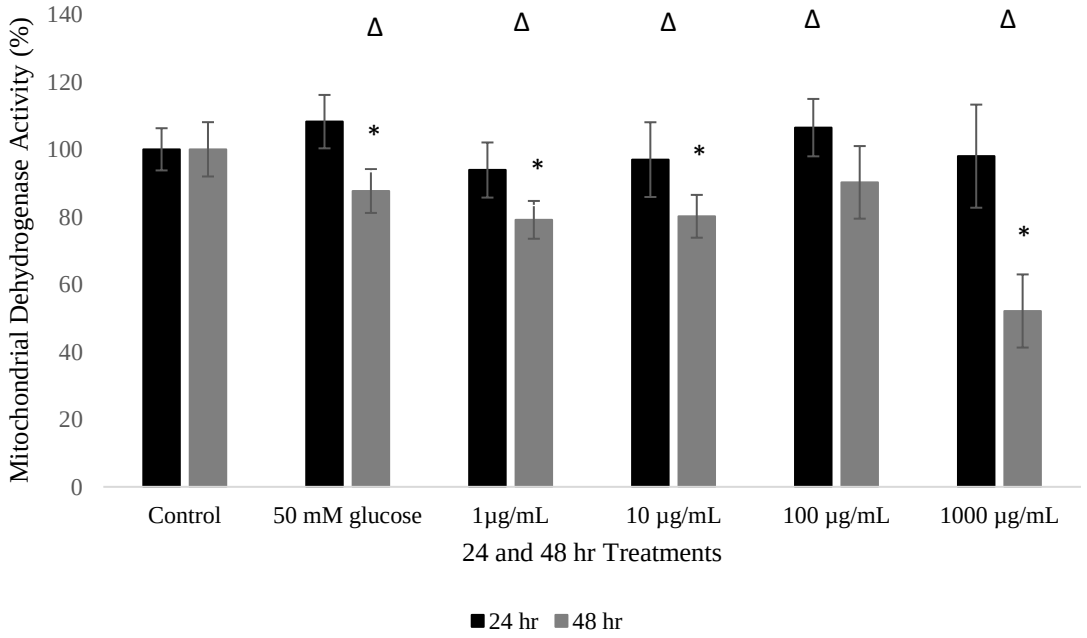

Figure 4.1. Cytotoxicity percentage for HeLa cells in response to different LPS concentrations after 24 hr and 48 hr exposure. Error bars showing ± S.E.M. * indicates a statistically significant difference between treatment and control, Δ indicates a statistically difference between 24-hr and 48 hr treatment p <0.05, n=3 in triplicate.

4.3.1.1 LPS MTT Assays

One LPS treatment showed significantly (p >0.05) decreased mitochondrial dehydrogenase activity within the 24-hour exposure period compared to the control. This is the 100 µg/mL treatment with a decrease of 6.06±1.06%. It is likely this treatment is significant due to its low error compared to the other treatments. After 48-hours all LPS treatments showed significantly decreased mitochondrial dehydrogenase activity. The 10 ng/mL, 100 ng/mL, 10 µg/mL, and 100 µg/mL treatments decreased by 27.97±6.40%, 28.61±6.7%, 23.61±7.37% and 28.11±9.85 respectively after 48-hours. There are also significant decreases in mitochondrial dehydrogenase activities between the 24 and 48-hour exposure periods (p <0.05) for all LPS concentrations except for the 100 µg/mL treatment. These results are all demonstrated in **Figure 4.2**.

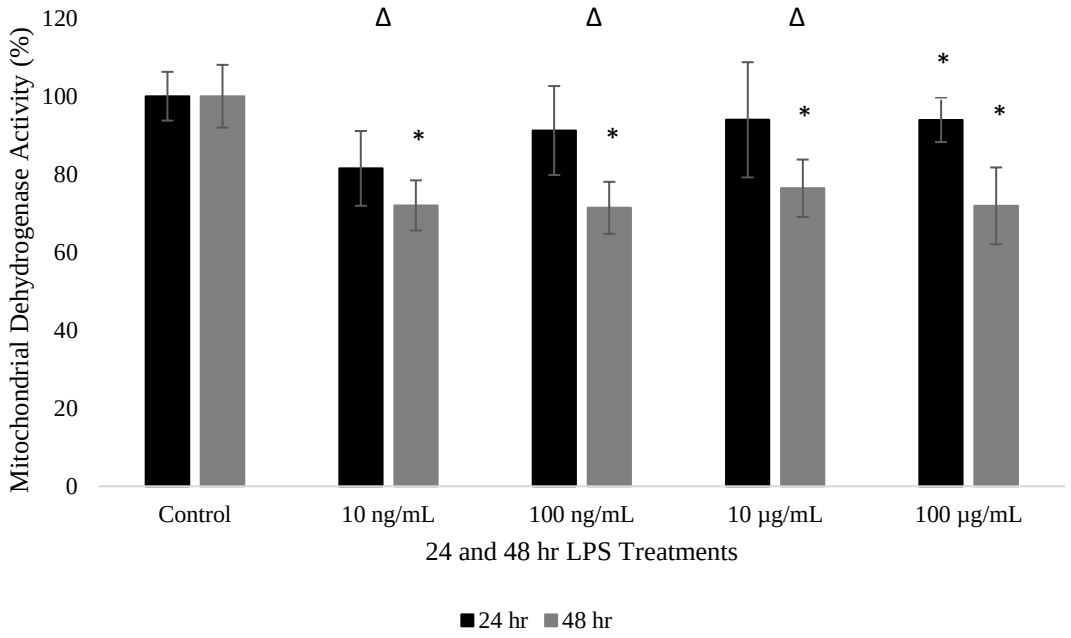

Figure 4.2. Cytotoxicity percentage for HeLa cells in response to different LPS concentrations after 24 hr and 48 hr exposure. Error bars showing ± S.E.M, n=3 in triplicate. * indicates a statistically significant difference between treatment and control, Δ indicates a statistically difference between 24-hr and 48 hr treatment p <0.05, n=3 in triplicate.

4.3.2 LDH Assay Results of Glucose, KTE and LPS on Hela Cells

Figure 4.3 demonstrates the cytotoxicity for HeLa cells based on the amount of LDH present in the complete media after treatment with different glucose and KTE concentrations. After the full 48-hour exposure period no treatments show a statistically significant difference (p >0.05) from the control. It is worth noting that the trends shown in this data indicate large differences, however, due to the degrees of freedom for this

experiment and the error between replicates no comment on the statistical significance can be made. One repeat from this data set had to be discounted due to contamination of the blank, which lowered the degrees of freedom for this experiment, subsequently making determination of the data's significance impossible. Unfortunately, no further repeats could not be carried out due to limited lab resources.

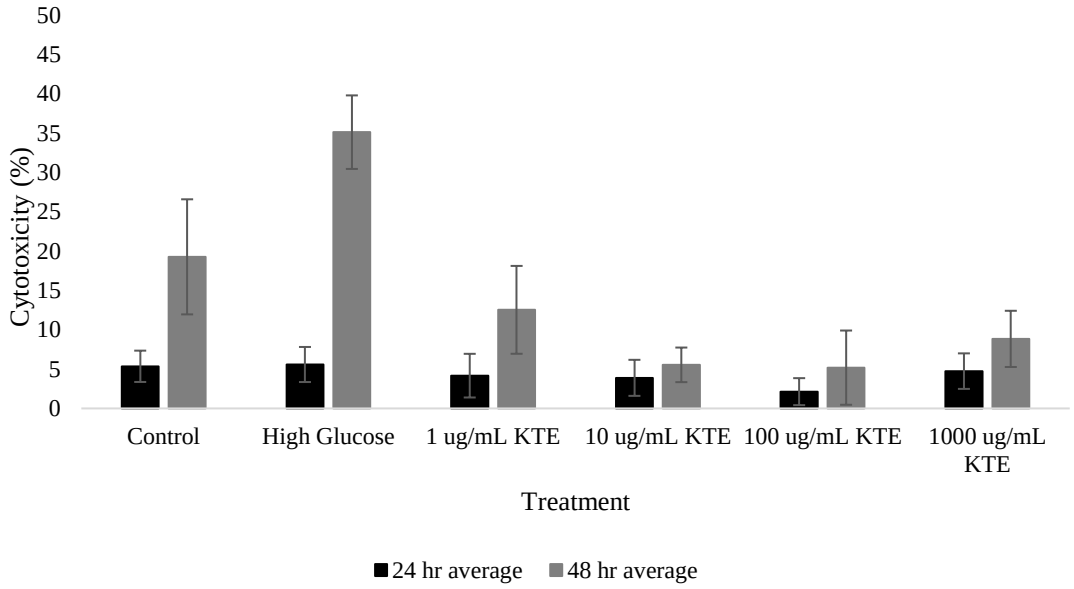

Figure 4.3. Cytotoxicity percentage for HeLa cells in response to different glucose and KTE concentrations after 24-hr and 48 hr exposure. Error bars showing ± S.E.M. * indicates a statistically significant difference between treatment and control, p <0.05, n=2 in duplicate.

4.3.2.1 LPS LDH Results

The cytotoxicity for HeLa cells based on the amount of LDH present in the complete media after treatment with different LPS concentrations for 24 and 48-hours is shown in **Figure 4.4**. After 24-hours of exposure two treatments showed significant (p <0.05) decreases in cytotoxicity compared to the control. The 10 ng/mL and 10 µg/mL treatments showed decreases of 4.25±0.05% and 5.11±1.97%, respectively. However, after 48-hours only the 100 µg/mL LPS treatment showed a significant decrease in cytotoxicity compared with the control with a decrease of 14.79±0.63%. The significant decrease seen in this treatment is likely due to the very low error between replicates. Very similar values are seen for the other non-significant treatments. However, there is a larger error for these data points which makes it difficult to determine whether they are accurate or not through

statistical significance testing. It would be beneficial in the future for more repeats to be taken to minimise error, increase accuracy and increase the degrees of freedom.

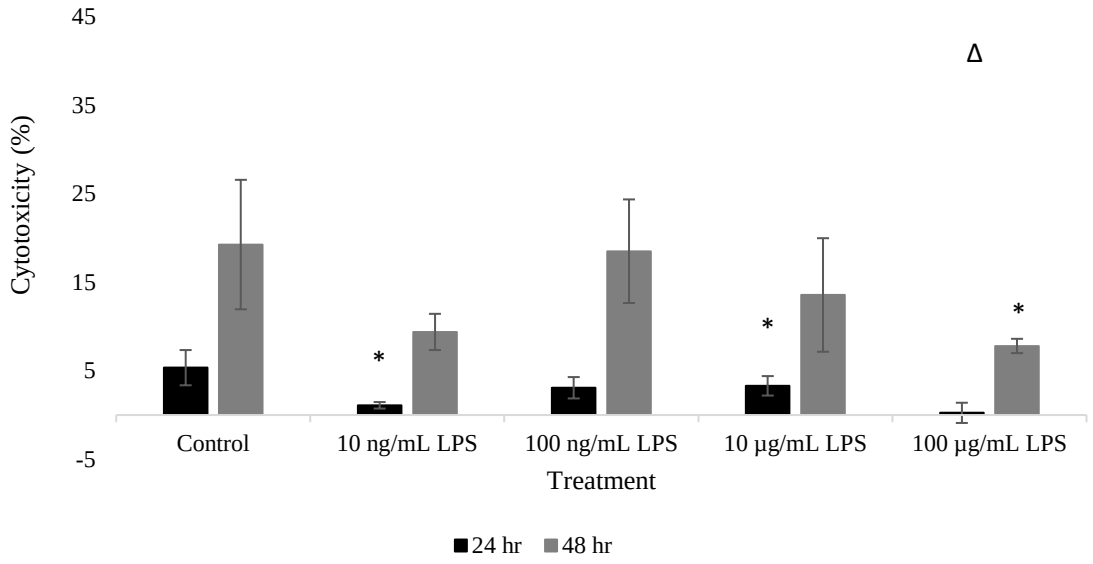

Figure 4.4. Cytotoxicity percentage for HeLa cells in response to different LPS concentrations after 24-hr and 48 hr exposure. Error bars showing ± S.E.M. * indicates a statistically significant difference between treatment and control, Δ indicates a statistically difference between 24-hr and 48 hr treatment $p < 0.05$, $n=2$ in duplicate.

The overall cytotoxicity for each treatment after 48-hours of exposure is detailed in **Table 4.1** for both the MTT and LDH assays.

Table 4.1. Summary of cytotoxicity for each treatment after 48-hr exposure as determined by MTT and LDH assays. Data extrapolated from Figures 4.1, 4.2, 4.3, and 4.4.

48-hr Treatment	Concentration (µg/mL)	Decreased Mitochondrial Dehydrogenase		Increased LDH Release into Complete Media		Decreased LDH Release into Complete Media
Control		**P-Value**	**Significant**	**P-Value**	**Significant**	**Significant**
50 mM Glucose		0.002152	Yes	0.172839	No	No
KTE	1	0.001483	Yes	0.253931	No	No
	10	0.000985	Yes	0.043281	No	Yes
	100	0.093809	Yes	0.114533	No	No
	1000	0.022016	Yes	0.06673	No	No
LPS	0.01	0.005231	Yes	0.07563	No	No
	0.1	0.003693	Yes	0.096898	No	No
	10	0.002504	Yes	0.304258	No	No
	100	0.032323	Yes	0.013645	No	Yes

* These treatments significantly decreased LDH release into complete media.

4.4 Discussion

The aim of these experiments was to identify whether certain concentrations of KTE, LPS and glucose were cytotoxic to HeLa cells. MTT and LDH assays were selected to test cytotoxicity as they give insight into whether cytotoxicity occurs due to mitochondrial stress or necrotic damage. Analysis of this data in conjunction with the trends found in **Chapter 3** allowed for an accurate analysis of the effect these treatments had on growth and why differences in growth rate may be observed.

4.4.1 MTT Assay Results for KTE Treatments

The MTT assay showed that over a 24-hour period there was no significant decrease in mitochondrial dehydrogenase activity for the any of the glucose or KTE treatments. Interestingly, after 48-hours, all KTE concentrations except the 100 µg/mL concentration significantly (p <0.05) decreased mitochondrial dehydrogenase activity. It was expected that there would be a significant (p <0.05) decrease in activity for the cells treated with the 1000 µg/mL KTE treatment as the growth rate of the cells shown in **Chapter 3** was largely inhibited from 24-hours onwards. Also shown in **Chapter 3**, specifically in **Figure 3.7** are images of cell morphology over different time points. The 1000 µg/mL treated cells began to show signs of apoptosis as early as 24-hours after exposure. Typical warning signs of apoptosis can be seen under light microscopy [86]. The cells will begin to separate and remove attachments from surroundings cells and the extracellular matrix. Alongside this, it is common to see small protrusions coming from the membrane of the cell and the accumulation of apoptotic bodies within the cell. Apoptotic bodies are vesicles which are bound to the membrane containing cellular components. Rather than the cell wall lysing and spilling cellular components around surrounding cells, apoptosis collects the cellular components and releases them inside vesicles [86]. After 24-hours the images in **Figure 3.7** show accumulation of these membrane bound vesicles within the cell. It is also clear that the cells are not connected to one another as seen in the control cells. This indicates that they are severing their attachments to the surrounding cells and the extracellular matrix. It is surprising that a non-significant result for a decrease in mitochondrial dehydrogenase activity was obtained after 24-hours for the 1000 µg/mL treated cells, however, it is likely that the cells required a longer exposure time to produce a significant response. After 48-hours it is clear in **Figure 3.7** that apoptosis is occurring with fewer cells visible than after 24-hours and there is also a high number of small

vesicles present in the well. It is at the 48-hour time point that the decrease in mitochondrial dehydrogenase activity is apparent which was expected.

It was expected that cytotoxicity would decrease proportionally with decreasing KTE concentration, however this was not the case. Although it is unusual that the 1 µg/mL and 10 µg/mL show decreased mitochondrial dehydrogenase activity but not the 100 µg/mL treatment, this does agree with the results obtained by Newland, 2016 [79].

As mentioned in **Chapter 3** the extraction time and temperature of the KTE has an impact on growth rate. However, although the extraction conditions differ a similar trend is seen between the results of this experiment and the results of Newlands experiment investigating the mitochondrial dehydrogenase activity of HeLa cells treated with KTE extracted at 60 ^{o}C. There is a difference in some of the concentrations tested, however, in Newlands experiment the 100 µg/mL KTE treatment had higher mitochondrial dehydrogenase activity than the lower concentrations. This result, however, does not agree with the relative growth compared to the control which is observed in **Chapter 3** which may indicate that there is an error with the assay method.

There is evidence in the literature that some plant extracts may be able to reduce MTT without the presence of cells [87]. A study treated complete media with herbal extracts and MTT and found that the tetrazolium salt was reduced in the absence of cells [87]. This shows that some plant extracts may interfere with this assay and result in false positive readings. However, if this were an issue with this experiment it is expected that there would be a larger difference between the 1 µg/mL, 10 µg/mL, and 100 µg/mL concentrations. To remove doubt surrounding the interference of KTE with the MTT further experiments could have blank wells for each concentration of KTE so that any reduction of MTT by KTE can be subtracted from the treated cells to give the amount of MTT being reduced by the cells alone.

4.4.2 LDH Assay Results for KTE Treatments

It was expected that there would be low LDH presence in the media treated with KTE due to the decreased mitochondrial dehydrogenase activity seen for these treatments in the MTT assay. It is unlikely that the cell would be going through necrotic cell death if there was a decrease in activity for mitochondrial dehydrogenase. The decrease in

mitochondrial dehydrogenase activity alone does not directly infer that the cell is going through apoptosis. But with the evidence of morphological changes shown in **Figure 3.7** there is indications that with a high enough concentration of KTE, apoptosis will occur. After 48-hours of exposure there was no significant change in cellular cytotoxicity shown by the LDH assay for any of the treatments.

4.4.3 MTT Assay Results for LPS Treatments

One treatment of LPS showed a significant decrease in mitochondrial dehydrogenase activity within the 24-hour exposure period, this treatment was the 100 µg/mL LPS treatment. After 48-hours all treatments showed a significantly decreased mitochondrial dehydrogenase activity. The 10 ng/mL, 100 ng/mL, 10 µg/mL, and 100 µg/mL treatments decreased by 27.97±6.40%, 28.61±6.7%, 23.61±7.37% and 28.11±9.85% respectively. In the literature there are a range of papers discussing the cytotoxicity of LPS on various cell lines. It is known that LPS is a component of gram-negative bacteria, is a virulent, and interacts with TLRs on the cell surface causing inflammation [88]. In some cell lines it is apparent that this induction of inflammation can lead to apoptotic cell death. For example, PC12 cells were exposed to concentrations of LPS ranging between 10 µg/mL – 200 µg/mL for 72 hours and a significant decrease in mitochondrial dehydrogenase activity was seen. Alongside this western blotting showed that there was also up-regulation of pro-apoptotic protein BAX [88]. However, PC12 cells are derived from a non-cancerous adrenal gland tumour in rats which differs to HeLa cells which are HPV positive cervical cancer cells [89].

There is also literature on the cytotoxicity of LPS in HeLa cells [90; 91], evidence from these studies directly disagrees with PC12 cell data. Rather than inducing apoptosis, LPS provides protection from apoptosis and increases the proliferation in these cancer cells [91]. When LPS binds the TLR4 on the cell surface of HeLa cells, the receptor is upregulated within minutes so that more LPS can bind to the cell. Following this is the activation of NF-κB which activates inflammatory proteins but simultaneously works as an activator for anti-apoptotic genes. In that study it was seen that 24-hour exposure of HeLa cells to 100 ng/mL, 1 µg/mL and 10 µg/mL LPS significantly increased cell viability [91].

It is interesting to note the difference in phenotype seen in cancerous cells compared to non-cancerous after exposure to LPS. The results of this study agree with the experiment run using the PC12 cells although it should more closely resemble the results seen in the experiment employing the use of HeLa cells. There are some differences between the previous HeLa experiment and this one. The incubation time in the previous experiment was only 24-hours. If the results for the 24-hour exposure of this experiment are considered here, they are not entirely dissimilar. There was no significant increase in cell viability but there was also no significant decrease at this stage. It would have been interesting to see in the previous experiment what happened to the cell viability if a longer exposure period were used.

So, although it was expected that HeLa cells would show an increase in mitochondrial dehydrogenase activity in response to LPS treatment, a decrease has been identified instead. This is taken into consideration for following experiments by ensuring where possible, exposure times of HeLa cells to LPS have been kept to 24-hours.

4.4.4 LDH Assay Results for LPS Treatments

The LDH results for the LPS treatments agree with the MTT results. This means that there was no significant increase in LDH presence for these treatments compared to the control. It is interesting to note that within the first 24-hours of exposure there was a significant decrease in LDH present in the media for the 10 ng/mL and 10 µg/mL treatments. After 48-hours only the 100 µg/mL treatment showed a significant decrease in cytotoxicity compared to the control. Although the percentage of LDH increased after 48-hours of exposure, the cytotoxicity was still lower than the control. This indicates that some concentrations of LPS are protecting the cells from necrosis under normal conditions over different time periods. Further experimentation testing the effectiveness of these concentrations with different concentrations of known lysis agents would see to what extent they prevent necrosis.

4.4.5 MTT and LDH Results for 50 mM Glucose Treatment

The results from this study show that there was only a significant change in mitochondrial dehydrogenase activity for the 50 mM glucose treatment after 48-hours. Although a non-significant increase in LDH was obtained, it is likely that an increase would be seen if more repeats were carried out. During the experiment, one repeat was discounted due to

contamination of the blank which decreased the degrees of freedom and, therefore, the statistical power. Although the values between repeats varied largely, within each repeat experiment this treatment reliably showed the highest absorbance after 48-hours. Therefore, discussion regarding necrosis in high glucose treatments has still been discussed here.

Many studies have been dedicated to investigating hyperglycaemia induced apoptosis in the literature [92; 93]. However, it has also been discussed in the literature that rather than cell death occurring through either apoptosis or necrosis, that cell death between these two exists on a continuum [94]. One lab has investigated both the induction of apoptosis and necrosis in epithelial cells after exposure to hyperglycaemia [92]. They have indicated that short term exposure results in the induction of necrosis whereas long term exposure allows for the induction of apoptosis [92].

When the cell is exposed to high glucose conditions there are four pathways which are linked through the induction of ROS which are responsible for hyperglycaemia related cell damage, as described in **Chapter 1.6.4**. These pathways are the activation of the polyol pathway, the production AGE's, PKC activation, and the hexosamine pathway. The induction of these pathways also result in the up-regulation of poly(ADP-ribose) polymerase (PARP) [92]. High levels of PARP can subsequently lead to the inactivation of glyceraldehyde-3-phosphate (GAPDH). GAPDH is essential in glycolysis which means that its deactivation can result in disruption of glucose metabolism. This itself results in the release of pro-apoptotic proteins.

A study was conducted investigating necrotic cell death of epithelial cells exposed to 25 mM glucose between 3 - 24-hours [92]. The study discussed that under hyperglycaemic conditions there is an increase in intracellular Ca^{2+}. This increase in intracellular Ca^{2+} can lead to the induction of calpain. Calpain is a cysteine protease, which like caspases, are involved in apoptosis. Calpain is known to play roles in both the apoptotic and necrotic cell death pathways. This necrotic cell death study exposed epithelial cells in 25 mM glucose and treated some cells with calpain inhibitors, PARP inhibitors or ROS scavengers. It was found that PARP inhibition did not completely stop necrotic cell death which was measured using and LDH assay. ROS scavenging reduced some of the early onset cytotoxicity. However, inhibition of calpain completely stopped the necrotic cell death. The study also found that there was significant LDH release after just 3-hours. It

is also known that PARP overactivation does not occur until at least 24-hours after exposure, in HeLa cells this does not occur until after 36 hours of exposure. This indicates that this early onset necrotic cell death is PARP independent. In this case it is likely that calpain is the main contributor to this cytotoxicity but also the higher levels of ROS due to hyperglycaemia may contribute to the early onset of necrotic cell death [92].

The results of this study agree with the necrotic cell death investigation in the literature [92]. However, the group which published this research also discussed that in their previous experiments they had seen significant apoptotic cell death in epithelial cells after 24-hours [92; 93]. The evidence from this study shows a significant decrease in mitochondrial dehydrogenase activity at both the 24-hour and 48-hour time points. It is also stated in the literature, cervical epithelial cells take 36 hours of high glucose exposure to begin overexpressing PARP [92]. This indicates that if a longer exposure period were used a larger decrease in mitochondrial dehydrogenase activity may have been seen.

Chapter 5
Optimisation of TNF-α ELISA and Measurement of TNF-α Induction.

5.1 Introduction

Enzyme linked immunosorbent assays (ELISA) employ the use of antibodies to selectively detect the cytokines or antigens of interest by working as an antibody sandwich [95]. The sandwich is composed of an antibody attached to the bottom of a plate responsible for antigen capture and immune specificity, with the secondary antibody which is responsible for detection. Since their introduction in the 1970's ELISA have become the standard method for detection of cytokines due to their highly quantitative ability. However, there are weaknesses regarding ELISA performance. This is largely due to the quality of the manufactured kit and/or the operator's skill and experience with the method [95].

Previously it has been found that 25 mM glucose exposure over a 24-hour period resulted in a significant increase in TNF-α production for HEPG2 cells [96]. A similar trend was observed when HEPG2 cells were exposed to 1 µg/mL LPS for 12 hours [97]. In addition, using the same concentration of LPS (1 µg/mL) over a 24-hour period also showed a significant increase in TNF-α production in HeLa cells [98].

Originally, the aim for this set of experiments was to induce production of TNF-α into the cell media in HEPG2 cells through exposure to LPS and high glucose treatments. Following this it would be investigated whether the induction of TNF-α could be modulated by adding KTE to these treatments. It was hypothesised that there would be increased TNF-α production in the LPS and high glucose treatments and decreased TNF-α production in the KTE treated cells. However, a series of troubleshooting steps was required to obtain results in the positive control. Without a working positive control, results for the other treatments were unusable.

5.2 Methods

The methods for this set of experiments were optimised and changed over time, therefore, the initial methods and the subsequent changes to these protocols have been discussed in this chapter.

5.2.1 Data Generation for TNF-α Response Normalisation

Quantification of total protein compared to a known cell number was generated so that the TNF-α response in the media of each well tested could be normalised to the number of cells present in each well to decrease error occurring during plate seeding. This was carried out for both the HEPG2 and HeLa cell lines.

Cells were removed from the T25 flask as described in **Chapter 2.4.1.** However, rather than seeding the cells into a plate, aliquots were calculated so that five known cell densities could be transferred to 1 mL microcentrifuge tubes. The desired cell numbers were 2000, 10000, 20000, 30000 and 50000. Each cell number was added to two 1 mL microcentrifuge tubes so that the total protein content could be analysed in duplicate. Following this the protocol for protein extraction of suspension cells as described in **Chapter 2.6.3** was followed.

The protein estimation procedure described in **Chapter 2.7.2** was followed to allow for calculation of total protein content for each given cell number. This experiment was repeated in triplicate.

5.2.2 Measuring the Stability of TNF-α ELISA Standards

A TNF-α ELISA kit was purchased from Cayman Chemical, USA and was used as per the manufacturer's recommendations. However, one of the recommendations was that the standard was reconstituted in complete media if this matched the matrix of the samples. In this case there was no stability data from the manufacturer regarding how long the standard would remain stable if it were made up in complete medium rather than ELISA buffer. Cayman Chemical was contacted, and it was recommended that the standards were tested over time to investigate whether a decrease in linearity of the standard curve was observed. A correlation coefficient close to one ($R^2 = 1$) is considered sufficient evidence to conclude that the calibration curve is linear, denoting a positive correlation between

the x and y axis' [99]. Dilutions of the TNF-α protein (250, 125, 62.5, 31.3, 15.6, 7.8, 3.9 and 0 pg/mL) were run using the ELISA protocol described in **Chapter 2.6.2**. The linearity of the curve was tested using Microsoft Excel on day 1 and day 14 after reconstitution of the standard.

5.2.3 Optimisation of ELISA Method

5.2.3.1 HEPG2 Method 1 Using the Original Laboratory Protocol

A previous method from our laboratory was followed for the first attempt at this experiment. This general protocol for seeding the cells and detecting TNF-α followed the methods described in **Chapter 2.6.1** and **Chapter 2.6.2**. However, this protocol stated that 2,000 cells per well should be seeded into the 96-well plate and that the HEPG2 cells should be left to grow through their lag phase without treatment for 48-hours. Cells grown under normal conditions were seeded for all treatments except for the long-term high glucose model which remained in high glucose media for the full 48-hour growth period. After the 48-hour growth period the complete media was removed from the cells and treatments to a final volume of 100 µL in complete media were added. The treatments included a control (only grown in complete media), 10 ng/mL LPS, 100 ng/mL LPS and 50 mM glucose (for cells undergoing short-term glucose exposure). These treatments were added in triplicate and had both 24-hour and 48-hour exposure periods. This experiment was not repeated.

5.2.3.2 HEPG2 Method 2 – Changing the Cell Concentration

It was noticed that the seeding density specified in **Chapter 5.2.3.1** was not the optimal seeding density for a 96-well plate. This method followed the same protocol as described in **Chapter 5.2.3.1**; except, 20,000 cells were seeded per well. The treatments used for this method did not include the short-term exposure to glucose. Therefore, the treatments used for this experiment were a control (grown only in complete media), 10 ng/mL LPS, 100 ng/mL LPS and long term 50 mM glucose exposure. Each treatment was added in duplicate, and the experiment was repeated in triplicate. Total protein was extracted as described in **Chapter 2.6.3.**

5.2.3.3 HeLa Method 3

Next, it was decided that the HeLa cell line would be tested using this method to investigate whether a positive TNF-α response could be obtained for the high glucose and LPS treatments. Following the work achieved in **Chapter 4** the highest non-cytotoxic concentration of LPS and three non-cytotoxic concentrations of KTE were selected (from within a 24-hour exposure). Due to the change of cell line a long-term high glucose model was no longer available. Therefore, the treatments selected were, a control (only grown in complete media), 1, 10, 100 µg/mL KTE, 100 µg/mL LPS and 50 mM glucose. All treatments were made up to a final volume of 100 µL. Cells were exposed to treatments for 24-hours. Each treatment was added in duplicate, and the experiment was repeated in triplicate. Total protein was extracted as described in **Chapter 2.6.3**. This experiment was repeated in triplicate.

5.2.3.4 HeLa Method 4

There was no induction of TNF-α observed in the high glucose and LPS treatments (**Chapter 5.2.3.3).** Thus, three changes were implemented: removal of the KTE treatments, an increase in exposure time and the utilisation of metformin. The method for the 6-well plate in **Chapter 2.6** was followed. Following the 24-hour growth period allowing the HeLa cells to grow through their lag phase treatments were added. The treatments included a control (only grown in complete media), 500 µg/mL metformin and 100 µg/mL LPS. Cells were exposed to these treatments for five days. Each treatment was added in duplicate, and the experiment was repeated in triplicate. Protein was extracted as outlined in **Chapter 2.6.3.** This experiment was repeated in triplicate.

5.3 Results

5.3.1 ELISA Standard Stability

The linearity of the slopes for TNF-α standard curves were compared over 14 days (**Figure 5.1)** A significant decrease in linearity of the slope would suggest that the standard was no longer stable and had begun to expire. No significant decrease in linearity was seen over 14 days.

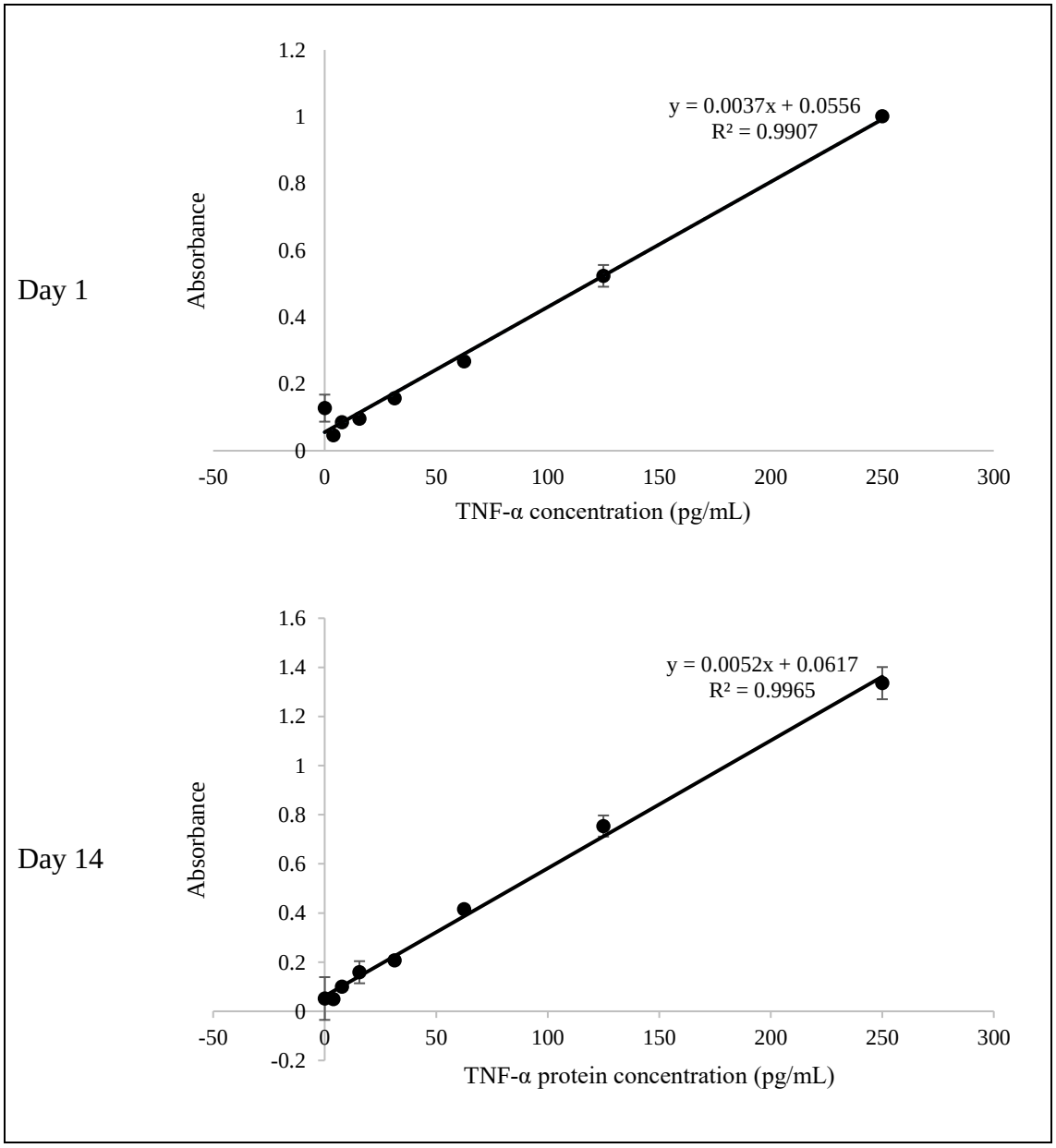

Figure 5.1. Comparison of standard curves made by diluting TNF-α protein in complete MEM media on after 1 and 14 days from preparation.

5.3.2 HEPG2 TNF-α Response to LPS and High Glucose

Three treatments came out with extracellular TNF-α concentrations less than 0 pg/mL indicating that the concentration of the protein is lower than the limit of detection (L.O.D, 3.9 pg/mM). However, positive TNF-α concentrations were seen for the 48-hour exposure of both LPS treatments and the long term 50 mM glucose treatment.

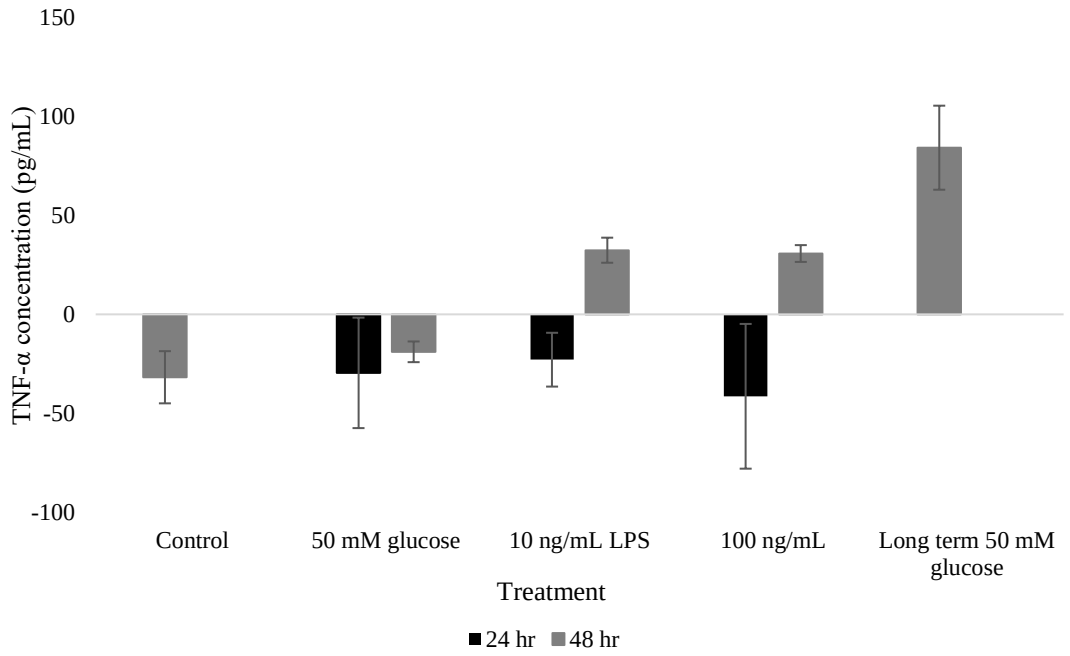

Figure 5.2. Non-normalised TNF-α protein concentration in response to high glucose and two LPS treatments in HEPG2 cells. Error bars showing S.E.M, *n*=1 in triplicate.

Next, changes to protocol described in **Chapter 5.2.4.1** were trialled but the same negative concentrations for TNF-α protein were yielded after both 24-hour and 48-hour exposure periods for all treatments. Negative results were also obtained for the total protein in each well from which treatment was collected (data not shown). Thus, increasing the number of cells seeded to 20,000 from 2,000 did not result in TNF-α protein detection using ELISA.

5.3.3 HeLa TNF-α Response to LPS, High Glucose and KTE.

Different treatments were then trialled in this experiment for only a 24-hour exposure, however, again there were no positive results seen in the LPS or 50 mM treatments. Having negative values in the positive control treatments means it is difficult to interpret the data from the control and KTE treatments (data not shown). Therefore, it was decided to increase the exposure time of the HeLa cells to only treatments which should induce a TNF-α response. It had been determined previously within the laboratory (unpublished data) that exposure to metformin (500 µg/mL) over a five-day period yielded positive TNF-α results. The results shown in **Figure 5.3** demonstrate the response that was shown from this change.

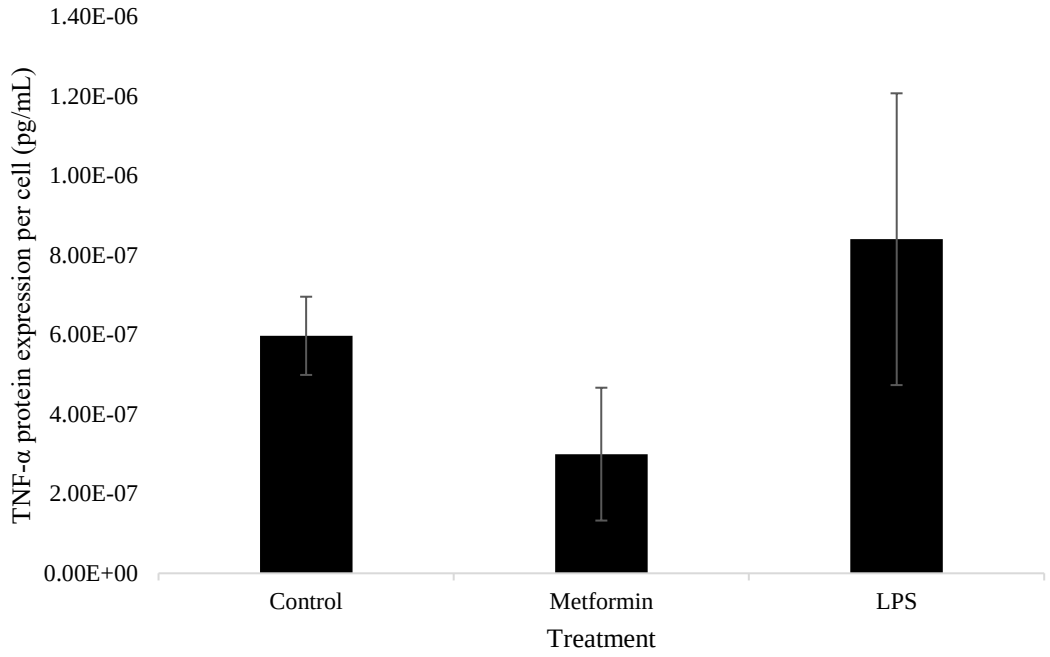

Figure 5.3. Normalised TNF-α Protein Concentration for HeLa cells exposed to Metformin and LPS concentrations for 5 days. Error bars showing S.E.M. *n*=3 in duplicate.

Figure 5.3 demonstrates a positive TNF-α response for each treatment which meant that the response could be normalised to the total number of cells present in each well. These results show that after a five-day exposure to each treatment the control, metformin and LPS treated cells produce $5.97x10^{-7}$ pg/mL±$9.84x10^{-8}$ pg/mL, $3.0x10^{-7}$± $1.67x10^{-7}$ pg/mL and $8.4x10^{-7}$±$3.67x10^{-7}$ pg/mL TNF-α per cell. Due to the error between replicates for this experiment the differences in TNF-α concentration between treatments was non-significant (p >0.05).

5.4 Discussion

Prior to analysing TNF-α protein expression *in vitro*, stability testing of the ELISA standard made up in complete media, rather than ELISA buffer was carried out as there was no data suggesting how long it is stable for.

The standard was tested over two weeks. This length of time was selected as other components of the kit begin to expire two weeks after reconstitution. As shown in **Figure 5.1,** there was no significant decline in linearity of the slope within this time period which indicates that the standard stays stable during this period of time.

When unexpected results with high variability between replicates were returned after running Method 1 for the HEPG2 cells a closer analysis of the prescribed protocol was performed. This brought to attention that the number of cells seeded per well was factor of ten lower than the recommended seeding density. Therefore, repeat experiments using Method 2 for the HEPG2 cells were conducted. It was originally thought that the error in the results was due to a low seeding density and that the clumping from the HEPG2 cells would increase the error largely at a lower seeding density. It was also decided that total protein from each well should be collected and compared to total protein for known cell numbers so that a number of cells for each well after the removal of treatment could be inferred. This way the TNF-α response could be normalised to the number of cells per well to reduce variation caused by seeding density error.

However, the results from Method 2 did not show positive results for both TNF-α and total protein. Firstly, the negative TNF-α concentrations do not indicate non-sensical values for the protein concentrations. Although the standard curves display good linearity (R^2>0.98) there is still some variation in the slope which means that the intercept does not go perfectly through 0. The low absorbance values for the samples result in TNF-α protein calculations which are smaller than this intercept value leading to negative results. This indicates that the protein concentration is not negative or necessarily zero, but that it is likely lower than the L.O.D for the assay.

It was observed that there was excessive clumping in the HEPG2 cells which makes them firstly, very difficult to count, and secondly, very inaccurate to seed due to non-equal distribution of cells throughout the cell suspension. Therefore, it is recommended that future experiments employ the use of an automated cell counter to help reduce this error. However, it is unlikely that the total protein was less than the L.O.D which is 0.5 µg/mL,

as the total protein of known cell numbers smaller than the seeding density were analysed and still showed a positive total protein result. The seeded HEPG2 cells had also been observed under the inverted microscope which showed that the wells were near confluent when treatments were added. Instead, it is likely that when the cells were transferred from the 96-well plate they were treated in, to a fresh plate to be frozen, that there was accidental loss of cells. This loss of cells could be due to error in the trypsinization process as it is difficult to remove every cell from the plate. Another source of error could be loss of the cell pellet that is formed during the lysing of cells which is carried out for the BSA assay. Due to the number of cells in the well being low, it is very difficult to see the cell pellet throughout the lysis process which means it is difficult to tell if the pellet has accidentally been disturbed or lost. Throughout repetitions of the known-cell number curve formation this also happened to some of the smaller seeding density samples.

Following more inconsistent results, it was decided that this experiment would be repeated in the HeLa cell line to check whether the issues seen were HEPG2 specific. The cytotoxicity assay data was taken into consideration when selecting which concentration of LPS to use and what exposure time to use as there was no previous laboratory protocol for this cell line. It was important to check that the concentrations used in the HEPG2 cells were not cytotoxic to the HeLa cells, but it was also decided to see whether higher concentrations could be used increase the chance of a positive TNF-α response. Due to limited resources, it was decided to use the highest possible LPS concentration in a 24-hour exposure alongside KTE concentrations and a 50 mM glucose treatment. From the cytotoxicity assays it was known that these concentrations were not cytotoxic within the 24-exposure time period aside from the 50 mM glucose treatment. However, even though the cell line does not clump and, therefore, has a more accurate seeding density, negative TNF-α concentrations were obtained again for all treatments.

This set of negative TNF-α concentration results raised suspicion regarding whether the LPS being used for treatments was working or had all the constituents needed to bind to TLR4 and induce TNF-α.

LPS is an endotoxin which found on the outer membrane of gram-negative bacteria [100]. This endotoxin has the ability to induce inflammation, sepsis, and septic shock in humans and it is known that LPS binds to TLR4 to initiate the signal transduction pathways needed for these responses. However, LPS cannot bind TLR4 on its own and relies on the

presence of LPS binding protein (LBP) and cluster of differentiation 14 (CD14) to bind to this receptor. LBP is synthesised by both hepatocytes and intestinal epithelial cells and is typically found in serum at a concentration of 5-10 µg/mL; however, this concentration can increase up to 200 µg/mL after 24-hours of acute inflammation. LBP is found in the serum of many mammals including FBS [101]. CD14 has both soluble and membrane bound forms [100]. Previous research has shown that the removal of LBP by using LBP negative serum or no serum at all prevents LPS binding to monocytes and stops downstream effects of this binding. LBP has been shown to bind to a range of chemotypes of LPS including lipid A which is regarded as the endotoxic section of LPS. LBP is thought to intercalate within the cell membrane where it binds LPS. It has been suggested that micro-domains of LBP and CD14 or TLR4 exist in the membrane as LBP is unable to transduce signalling upon LPS binding, therefore it is likely that it works as a shuttle protein.

LBP is present in serum but may be inactivated after heat treatment [100], therefore, it was theorised that the FBS in this study may not contain LBP and, therefore, efficient signalling may not be attenuated. However, in the case of the HEPG2 cells, which are hepatocytes, it is likely that LBP would be present regardless of whether it is in the FBS as hepatocytes synthesise LBP. As for the HeLa cells, it was found that the FBS used is not heat treated, therefore, the LPS should have all the components needed for correct binding to the cell. It is also known that TLR4 is overexpressed in HPV positive cervical cells, which indicates that lowered LPS signalling is not due to a low presence of TLR4 [102]. There is also evidence showing that treatment of HEPG2 cells with LPS results in up-regulation of TLR4 on the cell surface [103].

This indicates that the LPS activity may not be optimal or there is another interfering factor which has not been considered. Precautions were taken to ensure the LPS was stored correctly such as storing in a glass vial to prevent LPS adsorption to the container and storage at - 18ºC. It was also noted that the LPS used in this experiment had not expired.

The final ELISA experiment investigated whether an increase in exposure time to the LPS would result in the induction of a TNF-α response. Metformin was also used in this experiment as a positive control as positive TNF-α concentrations had been obtained by the laboratory previously (unpublished data). This would ideally show whether there was

an issue with the LPS or with the assay procedure. Exposing HeLa cells to LPS and metformin treatments for five days resulted in a positive TNF-α concentration response for the LPS and metformin treatments, however, there was a lower TNF-α concentration than the control for the metformin treatment. Unfortunately, due to the high error between replicates for this experiment, the difference in TNF-α induction between the treatments and the control were not statistically significant (p >0.05).

An interfering factor which could provide an explanation for the results seen are soluble TNF-α receptors (sTNFR) [104]. These soluble receptors are extracellular components of membrane bound TNF-α receptors which are present in serum, urine, and plasma. Because the soluble receptors consist of the extracellular section of the membrane bound TNF-α receptor, they have the ability to bind TNF-α external to the cell. This results in modulation of TNF-α activity by either stabilising the TNF-α which preserves its activity or inhibiting its ability to bind to cells and elicit an inflammatory response. These soluble receptors have been identified as a potential source of interference for immunological studies of TNF-α. If the antibody used to capture TNF-α in the ELISA is capturing the protein at the receptor binding site, then the assay will be competing with the sTNFR which will lower the detectable concentrations of TNF-α. There is evidence in the literature that increasing the time of exposure can allow enough time for TNF-α:sTNFR complexes to disassociate which, thereby, increases the detection rate of TNF-α by ELISA [104]. Interestingly, when the exposure period was increased in the HeLa Method 4 a positive TNF-α concentration was obtained for the LPS treatment.

The total protein for the HeLa Method 2 experiment was measured without freezing the cells first. This decreased the error seen in the previous experiments and resulted in accurate total protein concentrations for each of the wells in relation to the previously constructed curve of known HeLa cell numbers against total protein concentration (**Appendix**). If this were carried out in conjunction with cell counting by an automated cell counter the error would be largely decreased.

It is recommended for future research to investigate the presence of sTNFR in the condition media. If their presence could be proven, then the use of a different capture antibody would be extremely useful for removing interference. Alternatively, a different detection method such as RT-qPCR or mass spectrometry which bypasses the point of interference altogether would also be a powerful tool.

Chapter 6

Analysis of HSP60 Induction by Glucose, Tea Extract and Lipopolysaccharide.

6.1 Introduction

For the proceeding experiments, intracellular HSP60 was measured using western blotting as elevated HSP60 levels are associated with the induction of T2D [35]. As discussed in **Chapter 1.7.3** the levels of HSP60 in the serum of a T2D patient are four-fold higher than a healthy individual. HSP60 has also been associated with the induction of TNF-α through the MyD88 dependent TLR4 signalling pathway which subsequently activates the NF-κB inflammatory pathway [105]. The increased levels of HSP60 which leads to the induction of pro-inflammatory cytokines through the NF-κB pathway expresses the protein's role as a danger signal for the innate immune system [106].

Western blotting is another immunological detection method for determining the presence of a specific protein. Rather than working as an antibody sandwich like the ELISA as discussed in **Chapter 5.1** the total cellular protein is separated and transferred onto a membrane before having a detection antibody washed across the protein. This primary antibody should attach to the target protein before a secondary antibody is washed across for detection.

Previous work has been carried out investigating the induction of HSP60 in response to high glucose (100 μM) in HeLa cells with a statistically significant increase in HSP60 protein expression after 3 and 7 day exposure [107] . This set of experiments aimed to investigate induction of HSP60 in 50 mM glucose conditions as a model for the hyperglycaemia seen in DM. Following this, KTE concentrations were added to the 50 mM glucose media to analyse whether modulation of HSP60 expression would occur. It was also of interest whether there would be an induction of HSP60 when the cells were exposed to LPS. Due to the issues described in **Chapter 5** regarding the use of HEPG2 cells it was decided that HeLa cells alone would be used for analysis in these sets of experiments.

6.2 Methods

6.2.1 HSP60 Modulation by KTE

Five T75 flasks of HeLa cells were grown until they reached 80% confluency in complete media. At this stage, each flask had the media removed and the following treatments were added in one flask each: complete media (control), 50 mM glucose, 1 µg/mL KTE, 10 µg/mL KTE and 100 µg/mL KTE. Each of the KTE concentrations was made up in 50 mM complete media. The cells were exposed to these treatments for 24-hours before the media was removed, and the total protein of the cells was harvested using the method described in **Chapter 2.7.1.** Following this, the total protein concentration was estimated using the method described in **Chapter 2.7.2.** For each repeat experiment the flask which contained the lowest total protein concentration determined the maximum amount of protein between 5-10 µg which could be used in a 15 µL aliquot. Once this calculation was carried out all samples were prepared as described in **Chapter 2.7.3.1**. Electrophoresis was used to separate the proteins in the sample as described in **Chapter 2.7.3.2** and semi-dry transfer of the proteins from the SDS-PAGE gel was also carried out as described in **Chapter 2.7.3.3.** Finally, the western blot procedure described in **Chapter 2.7.4** was used to visualise the HSP60 bands from each treatment. This experiment was repeated in triplicate.

6.2.2 HSP60 Modulation by LPS

The methodology as described above in **Chapter 6.2.1** was applied to determine HSP60 modulation by LPS. In this set of experiments, the following treatments were used: complete media (control), 100 ng/mL LPS and 100 µg/mL LPS. This experiment was also repeated in triplicate.

6.3 Results

6.3.1 HSP60 Modulation by KTE

Once the separated total protein had been transferred from the SDS-PAGE gel to the NCM, the membrane was stained using Ponceau S to confirm protein transfer and that equal concentration loading had been achieved (**Appendix**). The bands for each sample stained with Ponceau S should have the same intensity if the total protein has been loaded equally. Ponceau S showed equal loading and the protein size range transferred was 14-198 kDa (**Appendix**).

Following the Ponceau S staining the NCM was blocked and then incubated firstly with the primary antibody. Following washing, the NCM was incubated with the secondary antibody. The HSP60 bands were visualised using DAB solution and the bands could be compared after imaging using ImageJ software. The bands shown in **Figure 6.1** came out at a different size than expected. In **Figure 6.1** it is clear that they are situated close to the 49 kDa marker on the protein ladder when it is expected that they would be very near the 62 kDa mark. The relative differences of each band to the control were averaged across three repeat experiments and unfortunately, due to the error between repeats, there is no significant difference in HSP60 induction between any of the treatments and the control. The relative HSP60 expressions for each of the treatments compared to the control is shown in **Figure 6.2**.

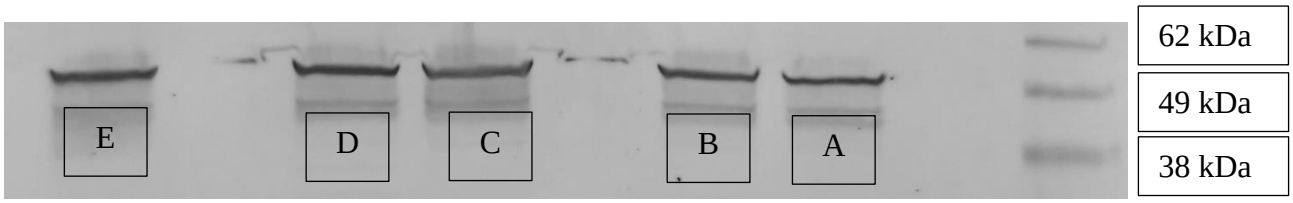

Figure 6.1. HSP60 expression for four treatments after 24-hour exposure. A = Control, B = 50 mM Glucose, C =1 µg/mL KTE, D= 10 µg/mL KTE, E = 100 µg/mL KTE.

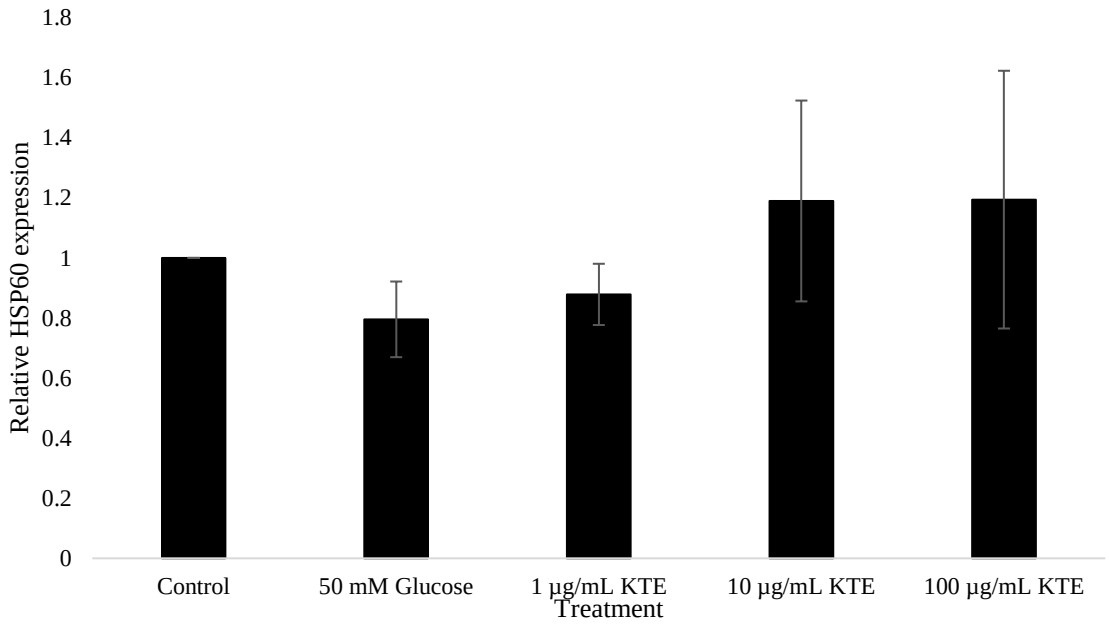

Figure 6.2. Relative HSP60 expression for HeLa cells exposed to varying concentrations of glucose and tea extract for 24 hours. Error bars showing S.E.M, *n*=3.

6.3.2 HSP60 Modulation by LPS

After the separated total protein had been transferred onto the NCM, the membrane was stained using Ponceau S (**Appendix**) which showed equal loading and that the protein size range transferred was 14-198 kDa. A western blot was then carried out using HSP60 antibody (**Figure 6.3)**. The relative differences of each band intensity to the control were averaged across three repeat experiments and HSP60 expression was shown to increase with increasing LPS concentration. The 100 ng/mL LPS treatment showed a significant 1.4-fold increase in HSP60 expression compared to the control and the 100 µg/mL LPS treatment showed a non-significant 2.1-fold increase. The relative HSP60 expressions for each of the treatments compared to the control is shown in **Figure 6.4**.

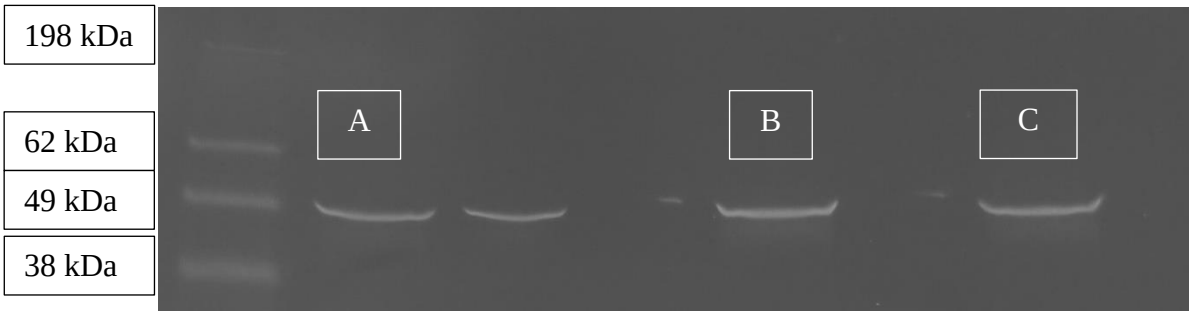

Figure 6.3. HSP60 expression for treatments. A = Control, B =100 ng/mL LPS, C =100 µg/mL LPS, unlabelled band was incorrectly loaded and has been discounted from these results.

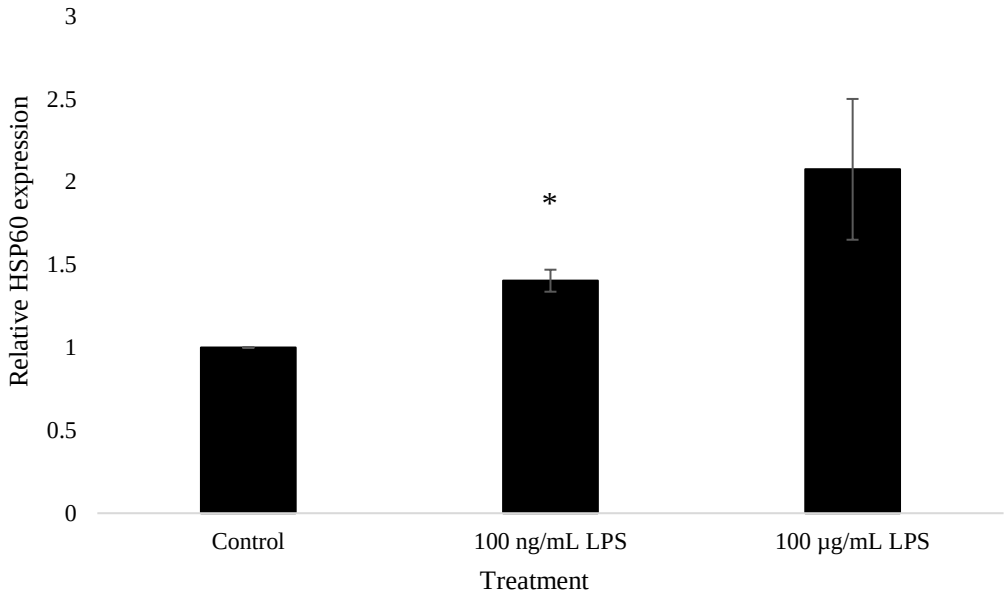

Figure 6.4. Relative HSP60 expression for HeLa cells exposed to varying LPS concentrations for 24 hours. Error bars showing S.E.M, *n*=3. * indicates a statistically significant difference from the control at the 95% confidence level (p <0.05).

6.4 Discussion

HSP60 is primarily a mitochondrial protein which is responsible for the refolding of nascent proteins and aiding in the degradation of aggregated proteins. There is also evidence that HSP60 plays a role in apoptosis, whereby, it interacts with other mitochondrial proteins such as P53 and HSP70. Alongside HSP60's intracellular functions, the protein may be packaged into exosomes and excreted into the extracellular space where it has been shown to interact with other cells, inducing inflammatory responses. There is evidence that serum levels of HSP60 can increase four-fold in patients with T2D compared with healthy individuals.

In regard to the results, for all experiments, the bands of HSP60 were visualised next to the 49 kDa marker on the protein ladder rather than close to the 62 kDa marker as expected. However, there is evidence in the literature that pre-stained molecular weight markers such as the one used in these experiments can give inaccurate molecular weights when used in gel electrophoresis and western blotting [108]. This was determined in the literature by comparing different protein ladders on the same Criterion TGX gel which showed each ladder giving different molecular weights at different positions on the gel. It was recommended that two different protein standards should be used initially when running gel electrophoresis or western blots to ensure that the molecular weight reference for both ladders is accurate and reliable [108].

Another potential explanation for the bands appearing at the wrong molecular weight is that the antibody is binding non-specifically. The manufacturer of the protein shows that when used with HeLa cell generated HSP60 the protein band should come out at 60 kDa [109]. It is recommended to test the specificity of the HSP60 antibody against recombinant purified HSP60 protein or HSP60 antigen and other non-related pure proteins such as BSA to demonstrate the antibody specificity.

It is unlikely that the samples have undergone proteolysis as they were not subject to more than one freeze thaw if any during these experiments. It is also unlikely that HSP60 has undergone post translational modification which would change its molecular weight as there are no alternative splice forms for the protein. This indicates that the issue likely lies with the protein ladder or the primary antibody. In the future the SeeBlue™ Pre-stained Protein Standard should be run alongside a western protein standard such as MagicMark™ XP Western Protein Standard to ensure that there is agreement between

the two ladders. If there is agreement this would indicate the problem is with the antibody which indicates that a new antibody should be purchased.

After these recommendations had been made our laboratory ran tests which showed that the ladder did indeed run incorrectly when compared against ladders from Biorad and Genscript (data not shown). It was shown that the HSP60 antibody is binding specifically to HSP60 as it was shown to bind recombinant HSP60 protein at 60 kDa but not BSA protein (data not shown).

As for comparing the band intensities, it was difficult to interpret the results testing HSP60 expression in cells exposed to 50 mM glucose conditions and varying concentrations of KTE. The main issue was that the large differences in HSP60 expression for the same treatments between repeats. This resulted in large errors and made it impossible to tell if there was a statistically significant difference between the expression of HSP60 for the treatments compared to the control. Following this, without the TNF-α concentration values for these samples it is difficult to tell whether any modulation in HSP60 expression would be affecting the induction of inflammatory cytokines. Future work repeating this experiment to minimise error between repeats would be beneficial, in this case it could not be carried out due to limited resources. Analysing the intracellular HSP60 protein alone also does not fill in the entire picture regarding modulation of inflammation as it cannot be inferred those intracellular levels of HSP60 will have any indication of extracellular expression. Therefore, future work should also test the complete media for each treatment for HSP60 using an HSP60 ELISA. However, if a decrease in HSP60 had been seen for the KTE concentrations compared to the 50 mM glucose treatment this would indicate at the intracellular level that the KTE is providing protection from hyperglycaemia as a cell stressor. Induction of intracellular HSP60 can range from a number of stressors, including oxidative stress [54]. As discussed in **Chapter 1.6.4** hyperglycaemic conditions trigger four damaging pathways, all of which converge on the induction of ROS [44]. It has been shown that the upregulated levels of ROS significantly increase damage on the body including oxidative stress, apoptosis, autophagy, necrosis and the up-regulation of pro-inflammatory cytokines [31]. If the HSP60 expression were decreased in the KTE treatments compared to the 50 mM treatment this would indicate that the cell is not likely to undergo apoptosis or necrosis. As shown in **Chapter 4.3.2.1** the 50 mM glucose treatment resulted in a significant increase of cytotoxicity due to mitochondrial stress. Therefore, this would indicate that

KTE displays a protective role for cells exposed to hyperglycaemic conditions. Following this it would be important to check the condition media to ensure that HSP60 is not actively being exported out of the cell. If this were not the case this may also be an indication that the KTE treatments are exhibiting an anti-inflammatory effect through the inhibition of HSP60 induction in hyperglycaemic condition. However, to be able to draw this conclusion it would also be very important to see a decrease in inflammatory cytokines such as TNF-α.

This study has been unable to make inferences regarding the modulation of HSP60 expression in high glucose conditions or whether this response can be modulated by KTE. However, inferences can be made from this data as to why problems with the method arose and prevented the results from being interpretable.

In **Chapter 5.4** it was discussed that a long exposure of five days was required for the LPS treatment to induce a TNF-α response that was above the L.O.D for the commercially purchased ELISA kit. Reasoning for this response was that there may be sTNFRs present in the conditioned media which will result in complexes forming with any extracellular TNF-α and subsequently interfering with the readings. However, the results from those experiments could not rule out that the LPS was not functioning efficiently in the first place. The results from HSP60 induction indicates that the LPS is functioning under smaller exposure periods. Within 24 hours of exposure a 1.4-fold and 2.1-fold increase was seen in HSP60 expression for treatment with 100 ng/mL and 100 µg/mL LPS respectively. The induction of HSP60 intracellularly indicates that the LPS treatment is resulting in cellular stress. In the interpretation of these results, it is important to note that a non-significant result was obtained for the 100 µg/mL treatment. Two of the three repeats for this experiment closely agreed showing that the 100 µg/mL treatment resulted in a higher HSP60 response, however, disagreement with the third repeat has increased the error, thus decreasing its statistical significance. Running a Q-test has shown that this disagreeing point is not an outlier, however, further repeats would increase the statistical power and help narrow done the absolute value for this point.

There is evidence in the literature that HSP60 functions as a danger signal to the immune system [106]. Habich *et al,* demonstrated that HSP60 can work as a chaperone which activates the immune system after a bacterial infection. Their study showed that triggering of the immune system is reliant on HSP60 being bound to LPS. At the time of the study

there was debate in the literature as to whether this activation of the immune system was actually due to the HSP60:LPS complex or whether it was due to unbound LPS in the system. The study by Habich *et al* showed that specific macrophage activation was carried out only by the HSP60:LPS complex. The findings of that study also determined that HSP60 works in a similar manner as an antigen presenting cell (APC). It is likely that HSP60 binds LPS and presents it to TLR4 on cell surfaces aiding binding in a similar manner to LBP and CD14. This indicated that HSP60 improves the immune system efficiency in the presence of bacterial infection [106]. Therefore, LPS should elucidate an HSP60 response under a short exposure time if it is working at its normal standard.

The significance of the results from this study in conjunction with the role of HSP60 binding LPS shows that LPS was functioning as intended. This indicates that the issues seen with gaining a positive TNF-α response from the ELISA testing is not due to poorly functioning LPS. Instead, this indicates that it is likely TNF-α detection is being interfered with by sTNFRs. The need for a longer exposure time to read a change in TNF-α but only a 24-hour exposure time needed to see modulation of intracellular HSP60 using the same LPS indicates a fault with the ELISA testing.

Lastly, in the future it would be ideal if experiments were able to employ the use of a housekeeping antibody such as GAPDH or actin. Other experiments such as HSP60 ELISA of the conditioned media and repeat experiments such as the KTE and high glucose western blot experiment could also be carried out. These further experiments would help narrow down the cellular process occurring with treatment of KTE and any anti-inflammatory properties it may be exhibiting.

Chapter 7
Final Summary and Future Directions

This project originally aimed to investigate the modulation of diabetic inflammation in *in vitro* human cell lines by using tea extract. HEPG2 cells were initially the cellular model of choice as they are cancerous hepatocytes which are immortal and from a relevant organ for studying diabetes. Initially, a dose-response curve was carried out so that cell growth stages and any changes in growth rate by KTE could be identified. However, at this stage there were problems regarding clumping of the HEPG2 cells. Initial fixes such as attempting to displace the cells using a micropipette and leaving the trypsin to work as long as possible without risking cell viability were trialled. These fixes, however, did not stop the formation of HEPG2 cell clumps which were far too large to count. This meant that there were no well-defined cell growth stages in the control or any of the KTE treatments. Although the cell growth stages were not clear in these cells it was clear that treatment with 1000 µg/mL KTE caused significant cell death. In the future it would be beneficial to firstly confirm the cells are HEPG2 cells using genetic short tandem repeat (STR) markers. Alongside this, PCR should be carried out to check that mycoplasma is absent. If it is identified that the cells are not HEPG2 or that there is mycoplasma present, a new cell line should be ordered. If the clumping is still persistent then the cells could be grown in flasks containing collagen. When they are harvested, they can be pipetted up and down using a mixing cannula connected to a 10 mL syringe. Collagen allows the cells to grow on a 3D matrix which is more representative to how they would grow *in vivo* [110]. The mixing cannula will allow for aspiration of the cells which may break the clumps apart in a gentler manner than using a micropipette. Also, making sure to harvest the cells at a lower confluency would decrease the time allowed for 3D cluster formations to grow. Lastly, the use of an automated cell counter would increase the accuracy in seeding experiments and would reduce the effect on accuracy that HEPG2 clumping has.

Following the growth curves, TNF-α ELISAs were carried out with HEPG2 cells. Cells were subjected to high glucose and LPS to check that there was an increase in TNF-α in the positive control and high glucose treatment before further testing was carried out. Firstly, stability testing of the TNF-α ELISA standards was carried out to ensure that there

was no decline in linearity when the standards are made up in complete media instead of ELISA buffer. When the first set of samples from the HEPG2 cells were run it was found that there was a large error between duplicates. This resulted in the identification of a problem in the protocol which was that the seeding density of cells into the 96-well plate was 2,000 cells per well instead of 20,000 cells per well. This adjustment to the protocol was made but unfortunately the change did not improve the results.

It was at this stage that it was decided that protein estimation of the cells in each well would be carried out so that the TNF-α response could be normalised to those levels. After carrying out protein estimation on the cells, negative protein results were obtained. This indicated that there were no cells present in the wells or that there was an issue during the protocol such as loss of the cell pellet. These findings again highlighted the issue that the clumping of the HEPG2 cells was significant and that it was, indeed, very difficult to accurately seed cells into the 96-well plates. Therefore, it was decided that experimentation would move into the HeLa cell line as it is a robust cell line which grows quickly. This change checked to see if the issues with the ELISA were HEPG2 specific. The use of the HeLa cell line meant that preliminary testing needed to be carried out before running the TNF-α ELISA to check that the concentrations and conditions used for the HEPG2 cells were suitable for the HeLa cells.

The HeLa growth curve, MTT and LDH assays were carried out before ELISA work commenced allowing for cytotoxicity of these treatments to be considered. The HeLa growth curve showed well-defined cell growth stages and clumping of the cells was minimal. This 1000 µg/mL KTE treatment agreed with the trend seen in the HEPG2 growth curve. Significant cell death was seen in the cells exposed to 1000 µg/mL KTE. Therefore, it was important to determine whether the cytotoxic effect the KTE was having was necrotic or apoptotic in nature.

Carrying out the cytotoxicity testing highlighted that three concentrations of LPS showed cytotoxicity of some kind within 24-hours of exposure. These were the 10 ng/mL, 10 µg/mL, and 100 µg/mL treatments. After 48 hours all glucose, KTE and LPS treatments showed cytotoxicity except the 100 µg/mL KTE treatment. Cytotoxicity was either due to mitochondrial stress or necrotic cell death. Only treatment with 100 µg/mL LPS showed significant results for both a reduction in mitochondrial dehydrogenase activity and increased LDH presence in the media. However, it is likely that through further

repeats that this would be seen for the 50 mM treatment. Collection of this data allowed for the selection of KTE and the highest non-toxic LPS treatments which could be used for a 24-hour exposure period for the measurement of TNF-α concentration.

Unfortunately, when the first TNF-α ELISA experiment was carried out using the HeLa cells, negative TNF-α concentrations were obtained. This indicated that the issues were not HEPG2 specific. Therefore, as a positive result using metformin had been previously obtained by our laboratory (unpublished results) by using a longer exposure period this was trialled. HeLa cells exposed to metformin and LPS for five days showed positive TNF-α concentrations. The need for a longer exposure period fits within evidence presented in the literature which suggests that sTNFRs are present in the complete media [104].

Next, the HSP60 protein expression in HeLa cells exposed to high glucose, KTE and LPS concentrations was carried out to determine if modulation of HSP60 was occurring. This protein is known to be involved in inflammation. Unfortunately, again, non-significant results were obtained for these tests.

LPS exposed cells were tested using western blotting to check whether LPS was able to modulate HSP60 under small exposure periods. A 24-hour exposure of 100 ng/mL LPS showed a significant 1.4-fold increase in HSP60 production compared to the control. There was a non-significant increase seen in the 100 µg/mL treatment which showed a 2.1-fold increase in the same exposure period. This response indicated that the issues obtained in the TNF-α ELISA experiments was likely due to the sTNFRs as the LPS was working as intended in smaller exposure periods.

The concentrations and brand of commercial KTE tested in this study have not been tested previously in the literature. The dose-response curve, MTT and LDH assays show novel results for HEPG2, and HeLa cells exposed to KTE. The 1 µg/mL, 10 µg/mL, and 1000 µg/mL KTE concentrations demonstrated significant reduction in mitochondrial dehydrogenase activity over a 48-hour exposure period. It would be very interesting to test these concentrations on non-cancerous cell lines in order to see whether this response is due to general cytotoxicity or whether the response seen is due to anti-cancer activity from the KTE.

Also, application of KTE including tea extracts made from different commercial tea brands or from freshly gathered kawakawa tea leaves (with appropriate Māori consultation and tikanga protocols in place) could be carried out using cell lines from tissues which are closely related to diabetes such as human intestinal epithelial cells (Caco-2) which are derived from colon carcinoma [106] or human monocytes (THP-1) which were derived from acute childhood monocytic leukaemia [107]. Alongside this, testing multiple batches of kawakawa tea pure would allow for the identification of any differences in activity between batches which may be affected by the kawakawa bush the leaves were collected from, location they were collected from, or differences due to season.

Future research could be undertaken to investigate the presence of sTNFRs in the complete media of HEPG2 and HeLa cells. The evidence from this study forms the hypothesis that sTNFRs are present in the conditioned media from HEPG2 and HeLa cells. However, no testing was undertaken to check for their presence. Therefore, future investigation using soluble TNF-α receptor 1 (sTNFR1) and soluble TNF-α receptor 2 (sTNFR2) ELISA kits should be carried out. If sTNFRs are present in the conditioned media following experiments could use of a different ELISA kit which employs the use of a different capture antibody to reduce interference from sTNFRs. Further TNF-α experiments could also investigate the intracellular levels following the same treatments used in this study. This could be achieved using a TNF-α western blot. Understanding the up- or down-regulation of TNF-α intracellularly could provide useful information when comparing to the extracellular levels. This would show how the cell is responding to the treatments and how much TNF-α is being exported into the extracellular space.

If an accurate picture could be painted regarding the modulation of TNF-α in response to KTE then investigation into the pathway being modulated could occur. Investigation into the presence of ROS, concentrations of NF-κB or what occurs when TLR4 is inhibited could all narrow down the mechanism of action. Alternatively, the use of transcriptomics could give a full understanding of the modulation of cellular processes and provide insight into changes that may be occurring that might be missed if singular process is investigated at a time.

A final direction this study could be taken in is investigating the anti-inflammatory effect of digested tea extract. In this study the whole tea extract was used for testing rather than

singular components such as diayangambin as the molecules making up the plant extract are likely to have synergistic effects when taken together. Also, testing the tea as a whole is representative of how the plant is typically consumed. However, in the body the tea would be digested in the stomach before any tissues of interest would be exposed to the tea components. Therefore, further research studying artificial digestion or *in vivo* testing of the tea would also be of interest with 3D bioprints [111] or using an animal model such as db/db mice with appropriate ethical approvals [112].

Investigating the use of kawakawa tea as an anti-inflammatory agent for diabetes could have beneficial impacts in NZ. As discussed in **Chapter 1.3** there is currently issues regarding the pakeha focus of our health care [7]. The use of kawakawa tea as a way to manage or prevent the onset of T2D could bring a sense of Tino Rangatiratanga (sovereignty over oneself), Mana Motuhake (self-determination), and whanau (family) back into health care, thus, tailoring the care to the communities which bear the brunt of T2D prevalence in NZ [7].

Appendices

Appendix A: Supporting figures for Chapter 5.

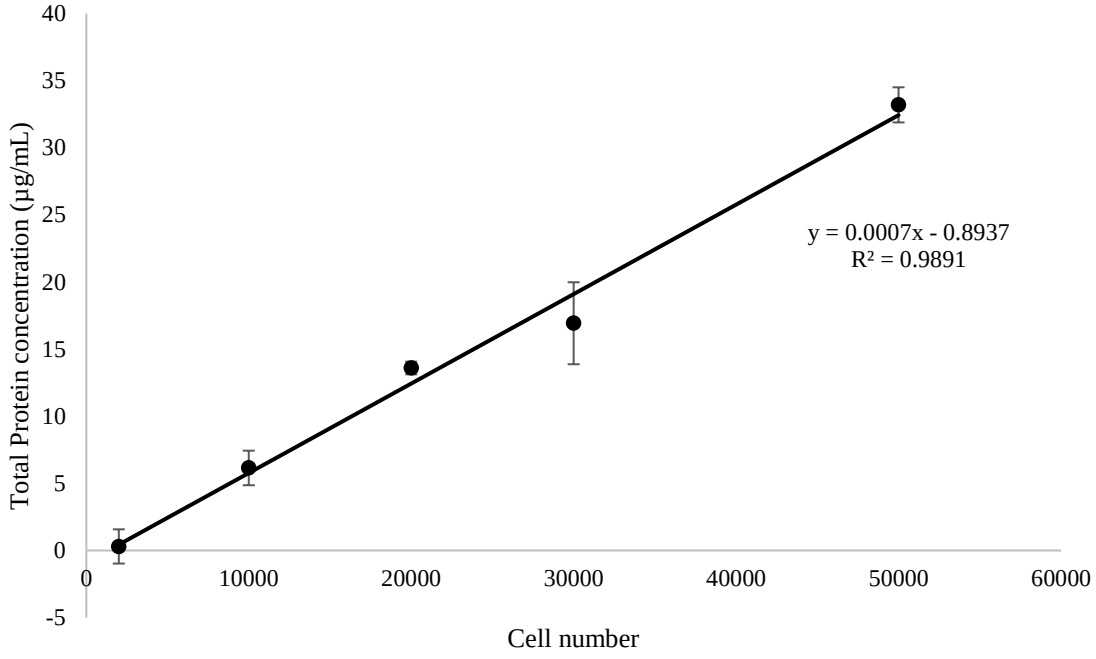

Figure A.1 HEPG2 standard curve for total protein concentrations for known cell numbers. Error bars showing S.E.M, n=3 in duplicate

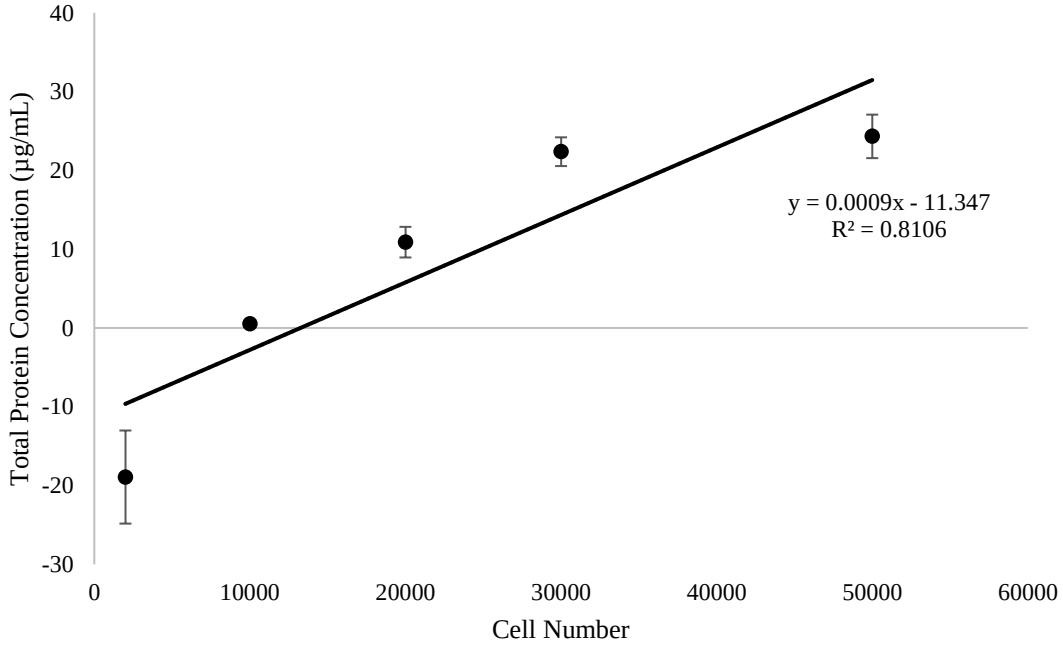

Figure A.2 HeLa standard curve for total protein concentrations for known cell numbers. Error bars showing S.E.M, n=3 in duplicate.

Appendix B: Supporting Figures for Chapter 6

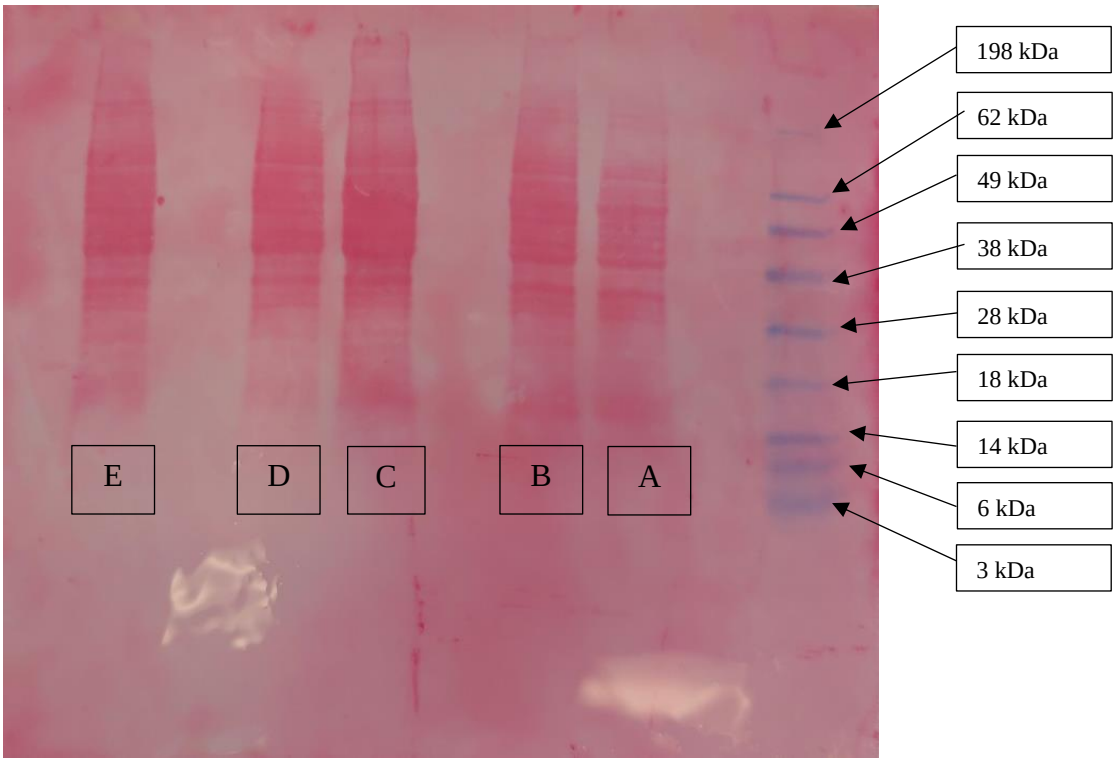

Figure B.1. Ponceau staining for HSP60 expression for treatments. A = Control, B = 50 mM Glucose, C =1 µg/mL KTE, D= 10 µg/mL KTE, E = 100 µg/mL KTE.

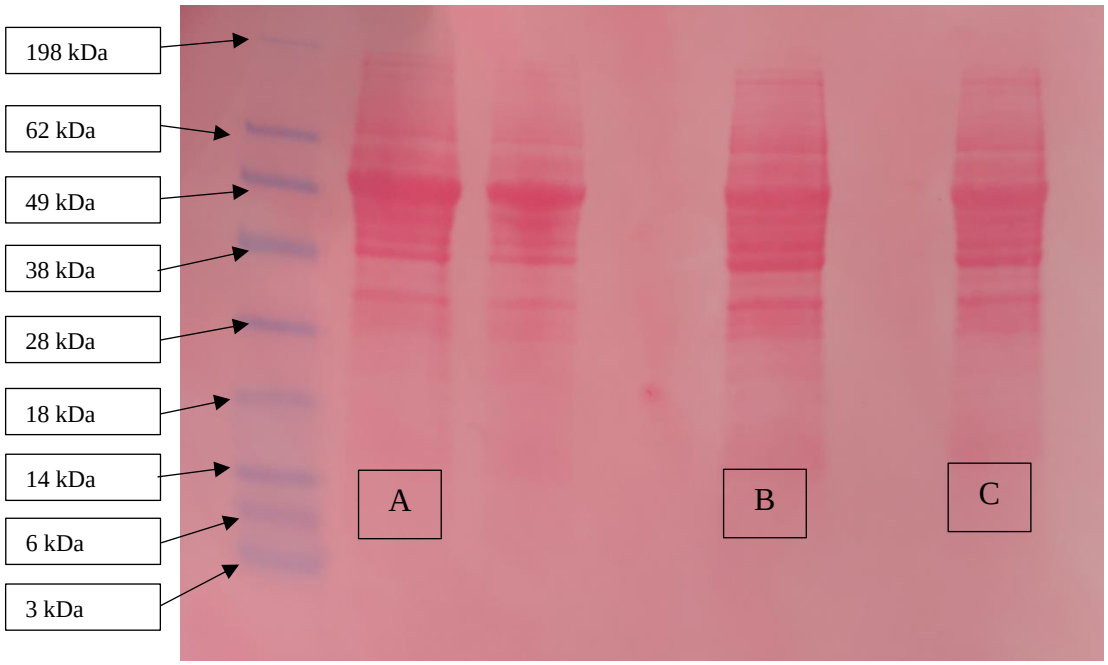

Figure B.2. HSP60 expression for treatments. A = Control, B =100 ng/mL LPS, C =100 µg/mL LPS, unlabelled band was incorrectly loaded and has been discounted from these results.

References

[1] Eknoyan, G., & Nagy, J. (2005). A history of diabetes mellitus or how a disease of the kidneys evolved into a kidney disease. *Advances in Chronic Kidney Disease, 12*(2), 223-229. doi: 10.1053/j.ackd.2005.01.002.

[2] Song, R. (2016). Mechanism of Metformin: A Tale of Two Sites. *Diabetes Care, 39*(2), 187-189. doi: 10.2337/dci15-0013.

[3] Banting, F. G., Best, C., Collip, J., & Macleod, J. (1922). The preparation of pancreatic extracts containing insulin. *Trans. R. Soc. Can., 16*, 27-29.

[4] Mekala, K. C., & Bertoni, A. G. (2020). Chapter 4 - Epidemiology of diabetes mellitus. In G. Orlando, L. Piemonti, C. Ricordi, R. J. Stratta & R. W. G. Gruessner (Eds.), *Transplantation, Bioengineering, and Regeneration of the Endocrine Pancreas* (pp. 49-58). Academic Press.

[5] Atlas, I. D. (2019). *IDF Diabetes Atlas*. Retrieved 13/07/2020, 2020, from https://diabetesatlas.org/data/en/country/142/nz.html.

[6] American Diabetes Association. (2014). Diagnosis and Classification of Diabetes Mellitus. *Diabetes Care, 37*(Supplement_1), S81-S90. doi: 10.2337/dc14-s081.

[7] Atlantis, E., Joshy, G., Williams, M., & Simmons, D. (2017). Diabetes Among Māori and Other Ethnic Groups in New Zealand. In S. Dagogo-Jack (Ed.), *Diabetes Mellitus in Developing Countries and Underserved Communities* (pp. 165-190). Cham: Springer International Publishing.

[8] Kopp, W. (2019). How Western Diet And Lifestyle Drive The Pandemic Of Obesity And Civilization Diseases . *Diabetes, Metabolic Syndrome and Obesity: Targets and Therapy, Volume 12*, 2221-2236. doi: 10.2147/dmso.s216791.

[9] Koia, J. H., & Shepherd, P. (2020). The Potential of Anti-Diabetic Rākau Rongoā (Māori Herbal Medicine) to Treat Type 2 Diabetes Mellitus (T2DM) Mate Huka: A Review. *Frontiers in Pharmacology, 11*. doi: 10.3389/fphar.2020.00935.

[10] Kharroubi, A. T. (2015). Diabetes mellitus: The epidemic of the century. *World Journal of Diabetes, 6*(6), 850. doi: 10.4239/wjd.v6.i6.850.

[11] Röder, P. V., Wu, B., Liu, Y., & Han, W. (2016). Pancreatic regulation of glucose homeostasis. *Experimental & Molecular Medicine, 48*(3), e219-e219. doi: 10.1038/emm.2016.6.

[12] Wilcox, G. (2005). Insulin and insulin resistance. *The Clinical biochemist. Reviews, 26*(2), 19-39.

[13] Skelin Klemen, M., Dolenšek, J., Slak Rupnik, M., & Stožer, A. (2017). The triggering pathway to insulin secretion: Functional similarities and differences between the human and the mouse β cells and their translational relevance. *Islets, 9*(6), 109-139. doi: 10.1080/19382014.2017.1342022.

[14] Boucher, J., Kleinridders, A., & Kahn, C. R. (2014). Insulin Receptor Signaling in Normal and Insulin-Resistant States. *Cold Spring Harbor Perspectives in Biology, 6*(1), a009191-a009191. doi: 10.1101/cshperspect.a009191.

[15] Watanabe, M., Hayasaki, H., Tamayama, T., & Shimada, M. (1998). Histologic distribution of insulin and glucagon receptors. *Brazilian Journal of Medical and Biological Research, 31*(2), 243-256. doi: 10.1590/s0100-879x1998000200008.

[16] Thorens, B., & Mueckler, M. (2010). Glucose transporters in the 21st Century. *American journal of physiology. Endocrinology and metabolism, 298*(2), E141-E145. doi: 10.1152/ajpendo.00712.2009.

[17] Hædersdal, S., Lund, A., Knop, F. K., & Vilsbøll, T. (2018). The Role of Glucagon in the Pathophysiology and Treatment of Type 2 Diabetes. *Mayo Clinic Proceedings, 93*(2), 217-239. doi: 10.1016/j.mayocp.2017.12.003.

[18] Briant, L., Salehi, A., Vergari, E., Zhang, Q., & Rorsman, P. (2016). Glucagon secretion from pancreatic α-cells. *Upsala Journal of Medical Sciences, 121*(2), 113-119. doi: 10.3109/03009734.2016.1156789.

[19] Hatting, M., Tavares, C. D. J., Sharabi, K., Rines, A. K., & Puigserver, P. (2018). Insulin regulation of gluconeogenesis. *Annals of the New York Academy of Sciences, 1411*(1), 21-35. doi: 10.1111/nyas.13435.

[20] Atkinson, M. A., Eisenbarth, G. S., & Michels, A. W. (2014). Type 1 diabetes. *The Lancet, 383*(9911), 69-82. doi: 10.1016/s0140-6736(13)60591-7.

[21] Weyer, C., Bogardus, C., Mott, D. M., & Pratley, R. E. (1999). The natural history of insulin secretory dysfunction and insulin resistance in the pathogenesis of type 2 diabetes mellitus. *Journal of Clinical Investigation, 104*(6), 787-794. doi: 10.1172/jci7231.

[22] Sirdah, M. M., & Reading, N. S. (2020). Genetic predisposition in type 2 diabetes: A promising approach toward a personalized management of diabetes. *Clinical Genetics*. doi: 10.1111/cge.13772.

[23] Buniello A, M. J., Cerezo M, Harris LW, Hayhurst J, Malangone C, McMahon A, Morales J, Mountjoy E, Sollis E, Suveges D, Vrousgou O, Whetzel PL, Amode R, Guillen JA, Riat HS, Trevanion SJ, Hall P, Junkins H, Flicek P, Burdett T, Hindorff LA, Cunningham F and Parkinson H. (Compiler) (2019). *The NHGRI-EBI GWAS Catalog of published genome-wide association studies, targeted arrays and summary statistics*: Nucleic Acids Research. Accessed 2019 from https://www.ebi.ac.uk/gwas/docs/about.

[24] Godoy-Matos, A. F. (2014). The role of glucagon on type 2 diabetes at a glance. *Diabetology & Metabolic Syndrome, 6*(1), 91. doi: 10.1186/1758-5996-6-91.

[25] Taylor, R. (2008). Pathogenesis of type 2 diabetes: tracing the reverse route from cure to cause. *Diabetologia, 51*(10), 1781-1789. doi: 10.1007/s00125-008-1116-7.

[26] Hruby, A., & Hu, F. B. (2015). The Epidemiology of Obesity: A Big Picture. *PharmacoEconomics, 33*(7), 673-689. doi: 10.1007/s40273-014-0243-x.

[27] Schwartz, M. W., Seeley, R. J., Zeltser, L. M., Drewnowski, A., Ravussin, E., Redman, L. M., & Leibel, R. L. (2017). Obesity Pathogenesis: An Endocrine Society Scientific Statement. *Endocrine Reviews, 38*(4), 267-296. doi: 10.1210/er.2017-00111.

[28] Shoelson, S. E., Lee, J., & Goldfine, A. B. (2006). Inflammation and insulin resistance. *The Journal of clinical investigation, 116*(7), 1793-1801. doi: 10.1172/JCI29069.

[29] Izquierdo, A. G., Crujeiras, A. B., Casanueva, F. F., & Carreira, M. C. (2019). Leptin, Obesity, and Leptin Resistance: Where Are We 25 Years Later? *Nutrients, 11*(11), 2704. doi: 10.3390/nu11112704.

[30] Chawla, A., Chawla, R., & Jaggi, S. (2016). Microvasular and macrovascular complications in diabetes mellitus: Distinct or continuum? *Indian journal of endocrinology and metabolism, 20*(4), 546-551. doi: 10.4103/2230-8210.183480.

[31] Volpe, C. M. O., Villar-Delfino, P. H., Dos Anjos, P. M. F., & Nogueira-Machado, J. A. (2018). Cellular death, reactive oxygen species (ROS) and diabetic complications. *Cell Death & Disease, 9*(2). doi: 10.1038/s41419-017-0135-z.

[32] Rhee, S. Y., & Kim, Y. S. (2018). The Role of Advanced Glycation End Products in Diabetic Vascular Complications. *Diabetes & Metabolism Journal, 42*(3), 188. doi: 10.4093/dmj.2017.0105.

[33] Schalkwijk, C. G., & Stehouwer, C. D. A. (2020). Methylglyoxal, a Highly Reactive Dicarbonyl Compound, in Diabetes, Its Vascular Complications, and Other Age-Related Diseases. *Physiol Rev, 100*(1), 407-461. doi: 10.1152/physrev.00001.2019.

[34] Chen, L., Deng, H., Cui, H., Fang, J., Zuo, Z., Deng, J., Li, Y., Wang, X., & Zhao, L. (2018). Inflammatory responses and inflammation-associated diseases in organs. *Oncotarget, 9*(6), 7204-7218. doi: 10.18632/oncotarget.23208.

[35] Tian, J., Guo, X., Liu, X. M., Liu, L., Weng, Q. F., Dong, S. J., Knowlton, A. A., Yuan, W. J., & Lin, L. (2013). Extracellular HSP60 induces inflammation through activating and up-regulating TLRs in cardiomyocytes. *Cardiovasc Res, 98*(3), 391-401. doi: 10.1093/cvr/cvt047.

[36] Zhang, W., & Liu, H. T. (2002). MAPK signal pathways in the regulation of cell proliferation in mammalian cells. *Cell Research, 12*(1), 9-18. doi: 10.1038/sj.cr.7290105.

[37] Rawlings, J. S. (2004). The JAK/STAT signaling pathway. *Journal of Cell Science, 117*(8), 1281-1283. doi: 10.1242/jcs.00963.

[38] Liu, T., Zhang, L., Joo, D., & Sun, S.-C. (2017). NF-κB signaling in inflammation. *Signal Transduction and Targeted Therapy, 2*(1), 17023. doi: 10.1038/sigtrans.2017.23.

[39] Hotamisligil, G., Shargill, N., & Spiegelman, B. (1993). Adipose expression of tumor necrosis factor-alpha: direct role in obesity-linked insulin resistance. *Science, 259*(5091), 87-91. doi: 10.1126/science.7678183.

[40] Ouchi, N., Parker, J. L., Lugus, J. J., & Walsh, K. (2011). Adipokines in inflammation and metabolic disease. *Nature Reviews Immunology, 11*(2), 85-97. doi: 10.1038/nri2921.

[41] Wellen, K. E., & Hotamisligil, G. S. (2005). Inflammation, stress, and diabetes. *Journal of Clinical Investigation, 115*(5), 1111-1119. doi: 10.1172/jci25102.

[42] Kern, P. A., Saghizadeh, M., Ong, J. M., Bosch, R. J., Deem, R., & Simsolo, R. B. (1995). The expression of tumor necrosis factor in human adipose tissue. Regulation by obesity, weight loss, and relationship to lipoprotein lipase. *Journal of Clinical Investigation, 95*(5), 2111-2119. doi: 10.1172/jci117899.

[43] Senn, J. J., Klover, P. J., Nowak, I. A., Zimmers, T. A., Koniaris, L. G., Furlanetto, R. W., & Mooney, R. A. (2003). Suppressor of cytokine signaling-3 (SOCS-3), a potential mediator of interleukin-6-dependent insulin resistance in hepatocytes. *J Biol Chem, 278*(16), 13740-6. doi: 10.1074/jbc.M210689200.

[44] Brownlee, M. (2001). Biochemistry and molecular cell biology of diabetic complications. *Nature, 414*(6865), 813-820. doi: 10.1038/414813a.

[45] Giacco, F., & Brownlee, M. (2010). Oxidative stress and diabetic complications. *Circulation research, 107*(9), 1058-1070. doi: 10.1161/CIRCRESAHA.110.223545.

[46] Brownlee, M. (2005). The Pathobiology of Diabetic Complications. *A Unifying Mechanism, 54*(6), 1615-1625. doi: 10.2337/diabetes.54.6.1615.

[47] Lorenzi, M. (2007). The polyol pathway as a mechanism for diabetic retinopathy: attractive, elusive, and resilient. *Experimental diabetes research, 2007*, 61038-61038. doi: 10.1155/2007/61038.

[48] Giardino, I., Edelstein, D., & Brownlee, M. (1994). Nonenzymatic glycosylation in vitro and in bovine endothelial cells alters basic fibroblast growth factor activity. A model for intracellular glycosylation in diabetes. *J Clin Invest, 94*(1), 110-7. doi: 10.1172/jci117296.

[49] Noh, H., & King, G. L. (2007). The role of protein kinase C activation in diabetic nephropathy. *Kidney International, 72*, S49-S53. doi: https://doi.org/10.1038/sj.ki.5002386.

[50] Liemburg-Apers, D. C., Willems, P. H. G. M., Koopman, W. J. H., & Grefte, S. (2015). Interactions between mitochondrial reactive oxygen species and cellular glucose metabolism. *Archives of Toxicology, 89*(8), 1209-1226. doi: 10.1007/s00204-015-1520-y.

[51] Murphy, M. P. (2009). How mitochondria produce reactive oxygen species. *The Biochemical journal, 417*(1), 1-13. doi: 10.1042/BJ20081386.

[52] Burel, C., Mezger, V., Pinto, M., Rallu, M., Trigon, S., & Morange, M. (1992). Mammalian heat shock protein families. Expression and functions. *Experientia, 48*(7), 629-634. doi: 10.1007/BF02118307.

[53] Ritossa, F. (1996). Discovery of the heat shock response. *Cell stress & chaperones, 1*(2), 97-98. doi: 10.1379/1466-1268(1996)001<0097:dothsr>2.3.co;2.

[54] Benjamin, I. J., & McMillan, D. R. (1998). Stress (Heat Shock) Proteins. *Circulation Research, 83*(2), 117-132. doi: doi:10.1161/01.RES.83.2.117.

[55] Ranford, J. C., Coates, A. R., & Henderson, B. (2000). Chaperonins are cell-signalling proteins: the unfolding biology of molecular chaperones. *Expert Rev Mol Med, 2*(8), 1-17. doi: 10.1017/s1462399400002015.

[56] Ranford, J. C., & Henderson, B. (2002). Chaperonins in disease: mechanisms, models, and treatments. *Molecular pathology : MP, 55*(4), 209-213. doi: 10.1136/mp.55.4.209.

[57] Hoter, A., Rizk, S., & Naim, H. Y. (2020). Heat Shock Protein 60 in Hepatocellular Carcinoma: Insights and Perspectives. *Frontiers in Molecular Biosciences, 7*(60). doi: 10.3389/fmolb.2020.00060.

[58] Caruso Bavisotto, C., Alberti, G., Vitale, A. M., Paladino, L., Campanella, C., Rappa, F., Gorska, M., Conway De Macario, E., Cappello, F., Macario, A. J. L., & Marino Gammazza, A. (2020). Hsp60 Post-translational Modifications: Functional and Pathological Consequences. *Frontiers in Molecular Biosciences, 7*. doi: 10.3389/fmolb.2020.00095.

[59] Cappello, F., Conway de Macario, E., Marasà, L., Zummo, G., & Macario, A. J. L. (2008). Hsp60 expression, new locations, functions, and perspectives for cancer diagnosis and therapy. *Cancer Biology & Therapy, 7*(6), 801-809. doi: 10.4161/cbt.7.6.6281.

[60] Duan, Y., Tang, H., Mitchell-silbaugh, K., Fang, X., Han, Z., & Ouyang, K. (2020). Heat Shock Protein 60 in Cardiovascular Physiology and Diseases. *Frontiers in Molecular Biosciences, 7*(73). doi: 10.3389/fmolb.2020.00073.

[61] Soltys, B. J., & Gupta, R. S. (1997). Cell surface localization of the 60 kDa heat shock chaperonin protein (hsp60) in mammalian cells. *Cell Biol Int, 21*(5), 315-20. doi: 10.1006/cbir.1997.0144.

[62] Cechetto, J. D., Soltys, B. J., & Gupta, R. S. (2000). Localization of Mitochondrial 60-kD Heat Shock Chaperonin Protein (Hsp60) in Pituitary Growth Hormone Secretory Granules and Pancreatic Zymogen Granules. *Journal of Histochemistry & Cytochemistry, 48*(1), 45-56. doi: 10.1177/002215540004800105.

[63] Chen, W., Wang, J., Shao, C., Liu, S., Yu, Y., Wang, Q., & Cao, X. (2006). Efficient induction of antitumor T cell immunity by exosomes derived from heat-shocked lymphoma cells. *Eur J Immunol, 36*(6), 1598-607. doi: 10.1002/eji.200535501.

[64] Lewthwaite, J., Owen, N., Coates, A., Henderson, B., & Steptoe, A. (2002). Circulating human heat shock protein 60 in the plasma of British civil servants: relationship to physiological and psychosocial stress. *Circulation, 106*(2), 196-201.

[65] KALSI, A., SINGH, S., TANEJA, N., KUKAL, S., & MANI, S. (2017). Current treatments for Type 2 diabetes, their side effects and possible complementary treatments. *International Journal, 10*(3).

[66] White, J. R. (2014). A Brief History of the Development of Diabetes Medications. *Diabetes Spectrum, 27*(2), 82-86. doi: 10.2337/diaspect.27.2.82.

[67] Marín-Peñalver, J. J., Martín-Timón, I., Sevillano-Collantes, C., & Del Cañizo-Gómez, F. J. (2016). Update on the treatment of type 2 diabetes mellitus. *World journal of diabetes, 7*(17), 354-395. doi: 10.4239/wjd.v7.i17.354.

[68] Messina, G., Palmieri, F., Monda, V., Messina, A., Dalia, C., & De Luca, V. (2015). Exercise causes muscle GLUT4 translocation in an insulin. *Biol Med. S, 3*, 007.

[69] Mgbeahuruike, E. E., Yrjönen, T., Vuorela, H., & Holm, Y. (2017). Bioactive compounds from medicinal plants: Focus on Piper species. *South African Journal of Botany, 112*, 54-69. doi: https://doi.org/10.1016/j.sajb.2017.05.007.

[70] De León, E. J., Olmedo, D. A., Solís, P. N., Gupta, M. P., & Terencio, M. C. (2002). Diayangambin exerts immunosuppressive and anti-inflammatory effects in vitro and in vivo. *Planta Med, 68*(12), 1128-31. doi: 10.1055/s-2002-36355.

[71] Butts, C. A., Van Klink, J. W., Joyce, N. I., Paturi, G., Hedderley, D. I., Martell, S., & Harvey, D. (2019). Composition and safety evaluation of tea from New Zealand kawakawa (Piper excelsum). *Journal of Ethnopharmacology, 232*, 110-118. doi: 10.1016/j.jep.2018.12.029.

[72] Rossi, P.-G., Bao, L., Luciani, A., Panighi, J., Desjobert, J.-M., Costa, J., Casanova, J., Bolla, J.-M., & Berti, L. (2007). (E)-Methylisoeugenol and Elemicin: Antibacterial Components of Daucus carota L. Essential Oil against Campylobacter jejuni. *Journal of Agricultural and Food Chemistry, 55*(18), 7332-7336. doi: 10.1021/jf070674u.

[73] de Cássia da Silveira E Sá, R., Andrade, L. N., Dos Reis Barreto de Oliveira, R., & de Sousa, D. P. (2014). A review on anti-inflammatory activity of phenylpropanoids found in essential oils. *Molecules (Basel, Switzerland), 19*(2), 1459-1480. doi: 10.3390/molecules19021459.

[74] Xu, H. (2018). *Anti-inflammatory and Anti0cancer Effects of Kawakawa (Macropiper excelsum) Leaves.* Masters thesis, The University of Auckland.

[75] Ricciotti, E., & FitzGerald, G. A. (2011). Prostaglandins and inflammation. *Arteriosclerosis, thrombosis, and vascular biology, 31*(5), 986-1000. doi: 10.1161/ATVBAHA.110.207449.

[76] Dawidowicz, A. L., & Dybowski, M. P. (2013). Simple and rapid determination of myristicin in human serum. *Forensic toxicology, 31*(1), 119-123. doi: 10.1007/s11419-012-0151-8.

[77] Lee, J. Y., & Park, W. (2011). Anti-inflammatory effect of myristicin on RAW 264.7 macrophages stimulated with polyinosinic-polycytidylic acid. *Molecules (Basel, Switzerland), 16*(8), 7132-7142. doi: 10.3390/molecules16087132.

[78] Borghi, S. M., Carvalho, T. T., Staurengo-Ferrari, L., Hohmann, M. S., Pinge-Filho, P., Casagrande, R., & Verri, W. A., Jr. (2013). Vitexin inhibits inflammatory pain in mice by targeting TRPV1, oxidative stress, and cytokines. *J Nat Prod, 76*(6), 1141-9. doi: 10.1021/np400222v.

[79] Newland, J. (2016). *In vitro cell culture to study microglial inflammation.* thesis, Waikato University, Hamilton.

[80] Wei, Y., Wang, Y., Zang, A., Shang, Y., Song, Z., Wang, Z., Wang, Y., & Yang, H. (2018). Inducible T-cell co-stimulators regulate the proliferation and invasion of human hepatocellular carcinoma HepG2 cells. *Biological Research, 51*(1). doi: 10.1186/s40659-017-0150-7.

[81] Chen, P.-C., Peng, J.-R., Huang, L., Li, W.-X., Wang, W.-Z., Cui, Z.-Q.-Q., Han, H., Gong, L., Xiang, D.-P., Qiao, S.-S., Yu, X., Wei, Y.-H., Ma, L.-P., Li, N., Zhu, J.-Y., & Leng, X.-S. (2013). Overexpression of human telomerase reverse transcriptase promotes the motility and invasiveness of HepG2 cells in vitro. *Oncology Reports, 30*(3), 1157-1164. doi: 10.3892/or.2013.2563.

[82] Collection, A. T. C. (2015). *FAQ's*. Retrieved 09/04/2021, 2021, from https://www.atcc.org/Global/FAQs/B/0/Difficulties%20with%20adherent%20cells%20to%20dissociate%20or%20trypsinize.aspx.

[83] Saraste, A., & Pulkki, K. (2000). Morphologic and biochemical hallmarks of apoptosis. *Cardiovascular Research, 45*(3), 528-537. doi: 10.1016/s0008-6363(99)00384-3.

[84] Kumar, P., Nagarajan, A., & Uchil, P. D. (2018). Analysis of Cell Viability by the MTT Assay. *Cold Spring Harb Protoc, 2018*(6). doi: 10.1101/pdb.prot095505.

[85] Kumar, P., Nagarajan, A., & Uchil, P. D. (2018). Analysis of Cell Viability by the Lactate Dehydrogenase Assay. *Cold Spring Harb Protoc, 2018*(6). doi: 10.1101/pdb.prot095497.

[86] Häcker, G. (2000). The morphology of apoptosis. *Cell and Tissue Research, 301*(1), 5-17. doi: 10.1007/s004410000193.

[87] Shoemaker, M., Cohen, I., & Campbell, M. (2004). Reduction of MTT by aqueous herbal extracts in the absence of cells. *Journal of Ethnopharmacology, 93*(2-3), 381-384. doi: 10.1016/j.jep.2004.04.011.

[88] Sharifi, A. M., Hoda, F. E., & Noor, A. M. (2010). Studying the effect of LPS on cytotoxicity and apoptosis in PC12 neuronal cells: Role of Bax, Bcl-2, and Caspase-3 protein expression. *Toxicology Mechanisms and Methods, 20*(6), 316-320. doi: 10.3109/15376516.2010.486420.

[89] Collection, A. T. C. (2021). *PC-12 (ATCC® CRL-1721™)*. Retrieved 06/05/2021, 2021, from https://www.atcc.org/products/all/CRL-1721.aspx.

[90] Liu, W., Qi, Y., Liu, L., Tang, Y., Wei, J., & Zhou, L. (2016). Suppression of tumor cell proliferation by quinine via the inhibition of the tumor necrosis factor receptor-associated factor 6-AKT interaction. *Molecular Medicine Reports, 14*(3), 2171-2179. doi: 10.3892/mmr.2016.5492.

[91] Hao, H., Xu, F., Hao, J., He, Y.-Q., Zhou, X.-Y., Dai, H., Wu, L.-Q., & Liu, F.-R. (2015). Lipoxin A4 Suppresses Lipopolysaccharide-Induced Hela Cell Proliferation and Migration via NF-κB Pathway. *Inflammation, 38*(1), 400-408. doi: 10.1007/s10753-014-0044-6.

[92] Harwood, S. M., Allen, D. A., Raftery, M. J., & Yaqoob, M. M. (2007). High glucose initiates calpain-induced necrosis before apoptosis in LLC-PK1 cells. *Kidney International, 71*(7), 655-663. doi: 10.1038/sj.ki.5002106.

[93] Allen, D. A., Harwood, S. M., Varagunam, M., Raftery, M. J., & Yaqoob, M. M. (2003). High glucose ‐ induced oxidative stress causes apoptosis in proximal tubular epithelial cells and is mediated by multiple caspases. *The FASEB Journal, 17*(8), 1-21. doi: 10.1096/fj.02-0130fje.

[94] Martin, L. J. (2010). Mitochondrial and Cell Death Mechanisms in Neurodegenerative Diseases. *Pharmaceuticals, 3*(4), 839-915. doi: 10.3390/ph3040839.

[95] Leng, S. X., McElhaney, J. E., Walston, J. D., Xie, D., Fedarko, N. S., & Kuchel, G. A. (2008). ELISA and Multiplex Technologies for Cytokine Measurement in Inflammation and Aging Research. *The Journals of Gerontology Series A: Biological Sciences and Medical Sciences, 63*(8), 879-884. doi: 10.1093/gerona/63.8.879.

[96] Gao, F., Jian, L., Zafar, M. I., Du, W., Cai, Q., Shafqat, R. A., & Lu, F. (2015). 4-Hydroxyisoleucine improves insulin resistance in HepG2 cells by decreasing TNF-α and regulating the expression of insulin signal transduction proteins. *Mol Med Rep, 12*(5), 6555-6560. doi: 10.3892/mmr.2015.4298.

[97] Kanmani, P., & Kim, H. (2018). Protective effects of lactic acid bacteria against TLR4 induced inflammatory response in hepatoma HepG2 cells through modulation of toll-like receptor negative regulators of mitogen-activated protein kinase and NF-κB signaling. *Frontiers in immunology, 9*. doi: https://doi.org/10.3389/fimmu.2018.01537.

[98] Zhao, R., Zhang, T., Ma, B., & Li, X. (2017). Antitumor activity of Portulaca oleracea L. polysaccharide on HeLa cells through inducing TLR4/NF-κB signaling. *Nutrition and cancer, 69*(1), 131-139.

[99] Mukaka, M. M. (2012). Statistics corner: A guide to appropriate use of correlation coefficient in medical research. *Malawi medical journal : the journal of Medical Association of Malawi, 24*(3), 69-71.

[100] Gutsmann, T., Haberer, N., Carroll, S. F., Seydel, U., & Wiese, A. (2001). Interaction between lipopolysaccharide (LPS), LPS-binding protein (LBP), and planar membranes. *Biol Chem, 382*(3), 425-34. doi: 10.1515/bc.2001.052.

[101] Kato, A., Ogasawara, T., Homma, T., Saito, H., & Matsumoto, K. (2004). Lipopolysaccharide-Binding Protein Critically Regulates Lipopolysaccharide-Induced IFN-β Signaling Pathway in Human Monocytes. *The Journal of Immunology, 172*(10), 6185-6194. doi: 10.4049/jimmunol.172.10.6185.

[102] Jiang, N., Xie, F., Guo, Q., Li, M.-Q., Xiao, J., & Sui, L. (2017). Toll-like receptor 4 promotes proliferation and apoptosis resistance in human papillomavirus–related cervical cancer cells through the Toll-like receptor 4/nuclear factor-κB pathway. *Tumor Biology, 39*(6), 101042831771058. doi: 10.1177/1010428317710586.

[103] Hsiao, C.-C., Chen, P.-H., Cheng, C.-I., Tsai, M.-S., Chang, C.-Y., Lu, S.-C., Hsieh, M.-C., Lin, Y.-C., Lee, P.-H., & Kao, Y.-H. (2015). Toll-like receptor-4 is a target for suppression of proliferation and chemoresistance in HepG2 hepatoblastoma cells. *Cancer Letters, 368*(1), 144-152. doi: 10.1016/j.canlet.2015.08.004.

[104] Moreau, E., Philippé, J., Couvent, S., & Leroux-Roels, G. (1996). Interference of soluble TNF-alpha receptors in immunological detection of tumor necrosis factor-alpha. *Clinical Chemistry, 42*(9), 1450-1453. doi: 10.1093/clinchem/42.9.1450.

[105] Weldenegodguad, M., Popov, R., Pokharel, K., Ammosov, I., Ming, Y., Ivanova, Z., & Kantanen, J. (2019). Whole-Genome Sequencing of Three Native Cattle Breeds Originating From the Northernmost Cattle Farming Regions. *Frontiers in Genetics, 9*(728). doi: 10.3389/fgene.2018.00728.

[106] Habich, C., Kempe, K., Van Der Zee, R., Rümenapf, R., Akiyama, H., Kolb, H., & Burkart, V. (2005). Heat Shock Protein 60: Specific Binding of Lipopolysaccharide. *The Journal of Immunology, 174*(3), 1298-1305. doi: 10.4049/jimmunol.174.3.1298.

[107] Hall, L., & Martinus, R. D. (2013). Hyperglycaemia and oxidative stress upregulate HSP60 & HSP70 expression in HeLa cells. *SpringerPlus, 2*(1), 431. doi: 10.1186/2193-1801-2-431.

[108] Neris, R. L. S., Kaur, A., & Gomes, A. V. (2020). Incorrect Molecular Weights due to inaccurate Prestained Protein Molecular Weight Markers that are used for Gel Electrophoresis and Western Blotting. *bioRxiv*, 2020.04.03.023465. doi: 10.1101/2020.04.03.023465.

[109] Abcam. (2021). *Anti-Hsp60 antibody [2E1/53] (ab5479)*. Retrieved 11/06/2021, 2021, from https://www.abcam.com/hsp60-antibody-2e153-ab5479.html.

[110] Kanta, J. (2015). Collagen matrix as a tool in studying fibroblastic cell behavior. *Cell Adhesion & Migration, 9*(4), 308-316. doi: 10.1080/19336918.2015.1005469.

[111] Madden, L., Nguyen, T., Garcia, S., Shah, V., Le, A., Peier, A., Visconti, R., Parker, E., Presnell, S., Nguyen, D., & Retting, K. (2018). Bioprinted 3D Primary Human Intestinal Tissues Model Aspects of Native Physiology and ADME/Tox Functions. *2*. doi: 10.1016/j.isci.2018.03.015.

[112] Burke, S. J., Batdorf, H. M., Burk, D. H., Noland, R. C., Eder, A. E., Boulos, M. S., Karlstad, M. D., & Jason Collier, J. (2017). db/db Mice Exhibit Features of Human Type 2 Diabetes That Are Not Present in Weight-Matched C57BL/6J Mice Fed a Western Diet. *Journal of Diabetes Research, 2017*, 1-17. doi: 10.1155/2017/8503754.